Control of Organ Size and Shape During the Differential Development of Wing and Haltere in *Drosophila*

विद्या वाचस्पति की

उपाधि की अपेक्षाओं की आंशिक पूति में प्रस्तुत शोध प्रबंध

A Thesis
Submitted in Partial Fulfillment of Requirements for the Award of Degree of ***Doctor of Philosophy***

द्वारा / By

दलि सी / DILSHA C

पंजीकरण सं. / Registration No.: २०१७३५१७/ 20173517

शोध प्रबंध पर्यवेक्षक / Thesis Supervisor:

प्रोफ. ल. स. शशिधरा / Prof. LS Shashidhara

भारतीय विज्ञान शिक्षा एवं अनुसंधान संस्थान पुणे

Indian Institute of Science, Education, and Research, Pune

२०२३ / 2023

DEDICATION

To my Pappa, Mamma and Grandparents. Without your selfless love and endless support, I would not have completed my journey. I will never be able to repay your love and kindness. At least I owe you this.

CERTIFICATE

This is to certify that the work incorporated in the thesis entitled "Control of Organ Size and Shape during the Differential Development of Wing and Haltere in *Drosophila*", Submitted by **DILSHA C** was carried out by the candidate, under my supervision. The work presented here or any part of it has not been included in any other thesis submitted previously for the award of any degree or diploma from any other University or institution.

Date: 16 October 2023 (Prof. LS Shashidhara)

DECLARATION

Name of Student: Dilsha C

Reg. No.: 20173517

Thesis Supervisor(s): Prof. LS Shashidhara

Department: Biology

Date of joining program: 01 August, 2017

Date of Pre-Synopsis Seminar: 17 January 2022

Title of Thesis: Control of Organ Size and Shape during the Differential Development of Wing and Haltere in *Drosophila*

I declare that this written submission represents my idea in my own words and where others' ideas have been included; I have adequately cited and referenced the original sources. I declare that I have acknowledged collaborative work and discussions wherever such work has been included. I also declare that I have adhered to all principles of academic honesty and integrity and have not misrepresented or fabricated or falsified any idea/data/fact/source in my submission. I understand that violation of the above will be cause for disciplinary action by the Institute and can also evoke penal action from the sources which have thus not been properly cited or from whom proper permission has not been taken when needed.

The work reported in this thesis is the original work done by me under the guidance of

Prof. LS Shashidhara

Date: 16 October 2023

Signature of the student

Acknowledgements

I would like to express my heartfelt gratitude to my supervisor, Prof. LS Shashidhara, for his invaluable guidance and support throughout my academic journey. Working in his laboratory has been a privilege and an enriching experience. His influence has been the most instrumental in grooming my career. I deeply appreciate his trust in me, allowing me to design and conduct my own experiments and his unwavering belief in my abilities throughout this period. His patience, passion for multiple arenas of knowledge, and our insightful conversations have left a profound and lasting imprint on me. I am truly fortunate to have had such an inspiring mentor who shared his expertise and encouraged me to explore my potential.

I extend my heartfelt gratitude to our esteemed collaborator, Prof. Mandar Inamdar from IIT Mumbai, whose enthusiastic support, numerous insightful discussions, and invaluable contributions to the computational aspects presented in this study.

I sincerely thank my Research Advisory Committee (RAC) members, Dr. Richa Rikhy and Dr. Girish Ratnaparkhi from IISER, Pune, for their invaluable support. Their dedication to academic discussions and constructive criticism has been a tremendous asset throughout my research journey. I am grateful for their unwavering availability for academic discourse and assistance with various aspects of my work. The inputs provided during RAC meetings have been useful in shaping the direction of my research, and I am truly appreciative of their guidance.

I want to express my heartfelt gratitude to Dr Girish Deshpande for the academic suggestions and career-related discussions that have guided me throughout my entire Ph.D. journey. Thank you, Dr. Deshpande, for sharing your motivation and enthusiasm for science with me.

I would like to thank Mrugank, Aneesha, Sumedha, Neel and Salima- who served as interns in our lab during the course of this project. I am deeply appreciative of the contributions you have made. It has been a pleasure and a unique experience to be working with each one of you. Thank you for being an essential part of our team.

I want to express my heartfelt appreciation to the wonderful members of our lab, namely Pooja, Soumen, Sanket and Madhumita. Our lab was not just a place of work, but a space filled with camaraderie and vibrant discussions encompassing both scientific topics and a wide array of subjects. I extend special thanks to Pooja for her invaluable assistance with

orders and for being there this whole time. I thank Aditi for her aid in conducting meticulous dissections for the RNA Seq. I thank MK lab members- Shruti and Gomathi along with the vibrant FFA members. Each of you has contributed significantly to the positive atmosphere and collaborative spirit within our lab, making it a truly enjoyable and productive environment. Your contributions have been instrumental, and I am grateful for the friendship and expertise you have shared during our time together. I extend my heartfelt thanks to Bipasha from the RR lab for introducing me to the laser ablation technique.

I would like to express my heartfelt gratitude to the IISER management for generously providing access to exceptional research facilities on campus and to the Council of Scientific & Industrial Research (CSIR) for their vital funding support throughout my research journey. I am deeply thankful to the microscopy facility for their seamless access to state-of-the-art microscopes, and I extend my appreciation to Vijay and Dr Santhosh for their training and unwavering technical assistance during my experiments. Furthermore, I would like to acknowledge the indispensable support from the academic and biology office members at IISER, with particular thanks to Sayalee, Tushar, Mahesh, Mrinaliani, Piyush, and Kalpesh for their instrumental help in navigating the paperwork, reagent ordering and administrative procedures. I would like to thank Snehal and Yashwant for taking care of the fly stocks and managing the fly food. My gratitude extends to all the esteemed faculty members of the biology department for their technical guidance, provision of reagents, and valuable recommendations during my project. Special thanks are also due to Ashoka University for their funding support and to NCBS Bangalore for providing a comfortable and green environment during the preparation of my thesis and manuscript draft.

I am genuinely thankful for my 2017 PhD batchmates and friends who have been my companions on this journey. Thank you, Rajeshwari, Firdousi, Sandra, and Shirsa, for being there for insightful discussions, fun and unwavering support; and to Teju, Prachi, Mayuresh, Shruti, Arjun, and Saurabh for the enriching discussions and unforgettable adventures that made our journey together truly remarkable.

In addition, I would like to acknowledge the support of my family, especially my siblings Shalu and Tinkvu, whose encouragement and understanding sustained me throughout this journey. This journey wouldn’t have been the same without the constant support of Aatata, cousins and my both families. Your belief in me and prayers gave me the strength to persevere, and I am indebted to you all.

CONTENTS

List of Abbreviations

ap	Apterous
AP	Anterior Posterior
APF	After puparium formation
Atro	Atrophin
a/bECM	Apical/ Basal Extracellular matrix
BM	Basement membrane
$d_{0\text{-}1}$	displacements
dmlf	*Drosophila* myeloid leukemia factor
DP cells	Disc-proper cells
DPP	Decapentaplegic
DV	Dorso-Ventral
ECM	Extracellular Matrix
Ex	Expanded
G4	GAL4
Gug	Grunge
H, W (in figures)	Haltere and wing, respectively
IIS	insulin/IGF-1
MMP's	Matrix metalloproteinases
N	Notch
PM	Peripodial membrane
Pten	Phosphatase And Tensin Homolog
Sd	Scalloped
T2	Second Thoracic segment
T3	Third Thoracic segment
Ubx	Ultrabithorax
vg	Vestigial
Vkg	Viking
v_o	initial velocity
Wg	Wingless
YAP	yes-associated protein
Yki	Yorkie

ABSTRACT

ABSTRACT

Diverse organ shapes and sizes arise from the complex interplay between cellular properties, mechanical forces, and gene regulation. *Drosophila* wing- a flat structure and the globular haltere are two homologous flight appendages emerging from a similar group of progenitor cells. The activity of a single Hox transcription factor, Ultrabithorax (Ubx), governs the development of these two distinct organs- wing and haltere with different cell and organ morphologies. Studying the differential development of wing and haltere presents a unique paradigm for understanding the complexities of organogenesis and how Hox genes modulate different signalling pathways and cellular processes, thereby influencing morphogenesis to mould different cell and organ shapes.

Our studies on differential development of wing and haltere shapes suggest that the localisation and abundance of actomyosin complexes, apical cell contractility, properties of extracellular matrix, and cell size and shape, which is a result of various cell intrinsic and extrinsic forces, can influence the flat vs. globular geometry of these two organs. Our data indicate that the columnar cells of the wing and haltere discs are mechanically different. Loss of Ubx function led to reversed cellular features and increased actomyosin accumulation in haltere discs, mimicking wing cell-like characteristics at the cellular and organ levels. We observed that RNAi-mediated downregulation of *Atrophin* (also known as Grunge) or *Pten*, in the background of downregulated *expanded* (resulting in elevated Yorkie (Yki), gives significant overgrowth in halteres. These mutants also induced a change in the cell dimensions, increase in cell apical contractility and actomyosin levels in halteres. The mutant adult halteres exhibited increased capitellum, size, flatter morphology, ECM remodelling, and changes in cellular architecture, leading to a partial haltere to wing homeotic transformation. We also observed deformations in the three-dimensional architecture of the mutant halteres during early pupal morphogenesis, indicating the role of the above-mentioned factors in force generation and in driving differential morphogenesis, leading to different organ shapes. When combined with computational modelling, these approaches now permit us to understand the relative contributions of cell size and shape changes and various inter- and intra-cellular forces to the overall change in the tissue shape. The study provides insights into the cellular mechanisms underlying the differential development and conferring the shape of the wing and haltere. Taken together, our study enhances our understanding of how small changes in cellular physical properties, gene expression and cell-cell, cell-ECM interactions modulated by Ubx can lead to the development of distinct structures.

CHAPTER 1

Introduction

Introduction

Specific morphology and dimension of various organs are vital for their functionality and, in turn, for the survival of the organism. The size and shape of organs are influenced by the shape, size, and physical properties of their constituent cells. The shape of individual cells and their arrangement within tissues contribute to tissue architecture and mechanical properties. The precise spatiotemporal regulation of cell size, shape and their organization to generate diverse and reproducible organ shapes and sizes has been the focus of recent research in developmental biology. The cells in the tissue undergo various cellular processes like cell division, apoptosis, and complex morphogenesis, and thus, their shapes are dynamic. Epithelial cells exhibit remarkable plasticity and are capable of adopting various shapes, arrangements, and structural features to fulfil organ-specific functions. This plasticity is facilitated by the dynamic interplay between intracellular signalling pathways, spatiotemporal patterning of cytoskeletal regulators, cell-cell connections, and interactions with the extracellular matrix. Epithelial tissues undergo extreme topological changes like folding and flattening during organogenesis and embryonic development (Nelson & Gleghorn, 2012; Tozluoğlu & Mao, 2020; Zartman & Shvartsman, 2010). These dynamic changes are crucial for transforming a flat two-dimensional (2D) epithelium into a three-dimensional (3D) structure. The plasticity, organisation, and properties of epithelial tissues influence organ morphogenesis and contribute to the diversity of organ shapes and functions observed in living organisms. Recent studies have shown that morphogenesis and tissue mechanics can conversely feed back into cell-fate decisions and regulate developmental programs. They report that the physical properties and mechanical forces within developing tissues can actively impact the determination of cell fate, with changes in tissue mechanics influencing transcription, cell differentiation and lineage commitment (Chan et al., 2017; Gjorevski & Nelson, 2010; Mammoto et al., 2012; Roffay et al., 2021).

The conserved Hippo pathway plays a multifaceted role in regulating cell proliferation, cell size, shape, and tissue growth in organisms, including mammals and *Drosophila.* The Hippo pathway has emerged as a major signalling network which integrates biochemical and mechanical signals for gene regulation (Detailed in Section 1.3). For instance, studies in *Drosophila* show that specific mutations in capping proteins, which resulted in F-actin accumulation, lead to the upregulation of *Yorkie* (*Yki*; Yap in mammals) target genes and

tissue outgrowth in imaginal discs (Fernández et al., 2011; Sansores-Garcia et al., 2011; Singh et al., 2015). These findings underscore the importance of the interplay between tissue morphogenesis and mechanical cues in understanding organ development and cell fate specification.

Studies on the differential development of homologous structures such as the *Drosophila* wing (large and flatter) and haltere (smaller and globular shaped) open powerful opportunities to investigate the mechanisms underlying organ-specific size and shape. The *Drosophila* wing is an extensively studied organ. The developmental pathways and signalling networks involved in wing development are fairly understood. The Hox gene *Ultrabithorax* (*Ubx*), which is only present in the haltere, is known to regulate/modulate these developmental pathways at multiple levels of wing development to specify haltere fate. In the sections that follow, I will brief about the Hox gene and its role in the specification of halteres. I further elaborate on our understanding of organ size and shape determination, with emphasis on the differential wing and haltere fate specification at various stages of development. Finally, I outline the specific objectives of the study and provide an account of the studies performed to address those objectives.

1.1 Hox Genes

Hox genes or Homeotic genes encode a group of transcription factors that encode a highly conserved DNA-binding homeodomain. Homeodomain is a 60 amino acid-long DNA binding domain highly conserved across all metazoan species. These genes were first discovered in fruit flies- *Drosophila melanogaster* but are evolutionarily conserved across a wide range of species, including humans.

The HOX proteins, function as key regulators during embryonic development and maintain their expression during postnatal life. They play indispensable roles in determining the body plan and segmental identity of organisms during development. Hox genes provide positional information and control the identity of body segments. They do so by binding to the DNA and regulating the expression of downstream target genes involved in the development of specific body structures, such as limbs, organs, and sensory organs.

Homeotic genes are organised into clusters on the chromosomes and are expressed in a sequential and spatially specific manner along the anterior-posterior (AP) axis of the

developing embryo. This expression pattern correlates with the regions of the body where the genes exert their effects along the body axis, a phenomenon known as Spatial collinearity. This means that the genes located at the 3' end of the Hox gene cluster are expressed earlier and in more anterior regions, while genes located at the 5' end are expressed later and in more posterior regions (Hughes & Kaufman, 2002; J. Durston et al., 2012; Michael Akam, 1995) (Fig 1.1).

Spatial collinearity is evident in both fruit flies and vertebrates, such as mice and humans. In *Drosophila*, the Antennapedia complex (ANT-C) and Bithorax complex (BX-C) are Hox gene clusters that determine body segment identity. In the BX-C cluster, genes like *Antennapedia* (Antp), *Ultrabithorax* (*Ubx*), *abdominal-A* (*abd*-A), and *Abdominal-B* (*Abd-B*) are sequentially expressed in posterior segments. Similarly, vertebrates possess four Hox gene clusters: HoxA, HoxB, HoxC, and HoxD (J. Durston et al., 2012; Michael Akam, 1995). These clusters contain multiple Hox genes, and their expression follows spatial collinearity. In the HoxD cluster, genes located at the 3' end, such as Hoxd1 and Hoxd3, are expressed in anterior regions, while genes at the 5' end, like Hoxd11 and Hoxd13, are expressed in more posterior regions, including developing limbs (Fig 1.1).

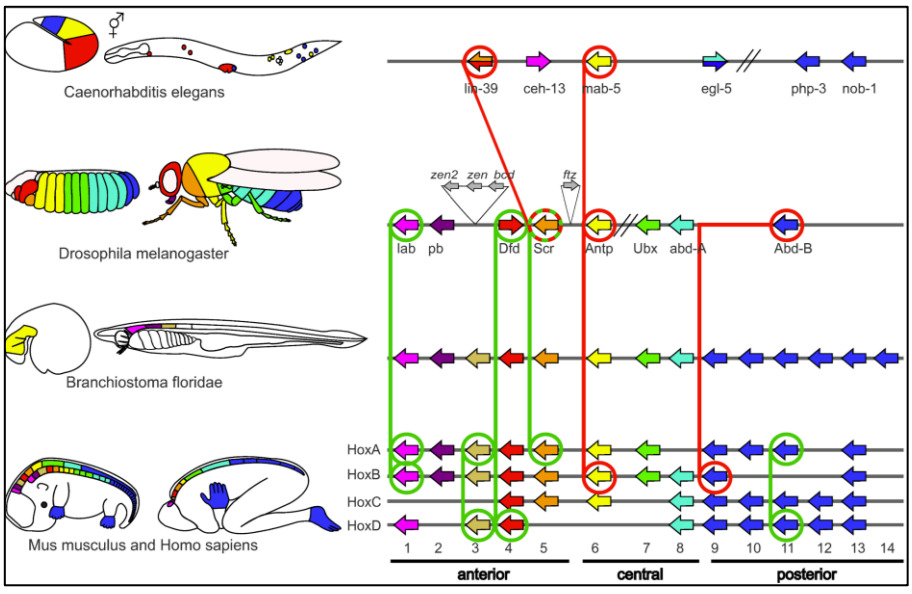

Figure 1.1. Hox gene organisation and expression in different organisms**.** The left side depicts the known expression patterns for the Hox-genes in four model organisms. The right side illustrates the corresponding chromosomal organisation of the Hox-genes. Coloured

arrows represent individual Hox-genes. Expression of Hox genes along the A/P axis of the adult or embryo matches the order of the genes along the chromosome, displaying spatial collinearity. (Adapted from Hueber et al., 2010).

Mutations or alterations in homeotic genes can lead to dramatic changes in the body plan, resulting in the transformation of one body segment into another. For example, in fruit flies, a mutation in the Antennapedia complex can cause the development of legs in place of antennae (Schneuwly et al., 1987). Similarly, in humans, mutations in certain homeotic genes have been linked to developmental disorders and congenital malformations (Goodman & Scambler, 2001).

1.2 Ultrabithorax (Ubx)

There is a direct correlation between the evolution of Hox genes to evolution of diversity along the antero-posterior axis in the animal kingdom reviewed in (Hughes & Kaufman, 2002; Pearson et al., 2005). In *Drosophila*, there are 8 Hox genes expressed along the anterior-posterior axis. Insects display huge diversity in their wings, with most species possessing two pairs: forewings and hindwings. Ubx plays a pivotal role in regulating the morphology of these "hindwing" structures. Ubx is consistently expressed in the hindwings of various insect species, and its function in generating diverse hindwing morphologies has been studied using model organisms such as *Drosophila* (fruit flies), *Apis Mellifera* (honey bees), *Tribolium castaneum* (Beetles), *Bombyx mori* (Silkworm) and *Precis coenia* (Butterfly). Hox genes regulate the morphology of serially homologous structures within a species and the homologous structures of different species (Carroll, 1995).

Drosophila Ubx is extensively studied and has been shown to regulate the development of the third thoracic segment (T3). The *Drosophila* Hox genes are organised into two complexes: the Antennapedia complex (ANT-C) and the Bithorax complex (BX-C). Ubx is located in the BX-C on the third chromosome, and its expression starts as early as embryonic stages. The flight appendages in *Drosophila*, the wing and haltere, are present on the second (T2) and third thoracic (T3) segments, respectively. The wing is considered to be a Hox-free state- meaning there is no Hox gene that is indispensable for the normal development of wings. The halteres, on the other hand, are specified by the Hox protein Ultrabithorax (Ubx) by the suppression of wing development pathways in the T3 segment (Carroll et al., 1995, Tomoyasu, 2017).

Loss of Ubx function in developing halteres induces haltere-to-wing transformations (Lewis, 1978), whereas ectopic expression of *Ubx* in developing wing discs leads to wing-to-haltere transformations (Cabrera et al., 1985; Castelli-Gair et al., 1990; White & Akam, 1985; White & Wilcox, 1985). The differential development of wings and halteres constitutes an excellent genetic system to study cell fate determination at different levels, such as growth, cell shape, size and its biochemical and physiological properties. They also represent the evolutionary trend that has established the differences between serial homologues such as fore and hind wings in insects, wings and legs in birds and fore and hind limbs in mammals.

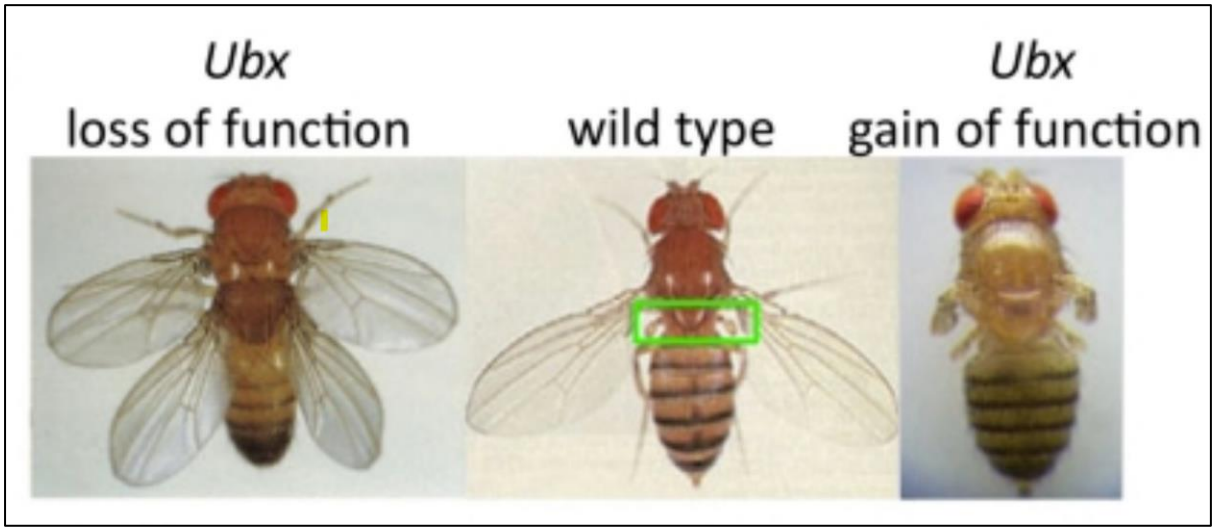

Fig1.2 Homeotic transformations of wing and haltere in *Drosophila.* Ubx is necessary and sufficient to specify the identity of the T3 segment and haltere fate. Loss of function of *Ubx* from T3 segment results in the homeotic transformation of haltere to wings with duplication of thorax. Conversely, gain of function of *Ubx* in the T2 segment transforms wings to rudimentary halteres. (Adapted from Slattery et al., 2011).

1.3 The *Drosophila* Wing and haltere

Drosophila wing and haltere are homologous flight appendages emerging from a near-identical group of progenitor cells. While wings provide lift when moving in the air, halteres function as a balancing organ during the flight. The wing is a two-layered (dorsal and ventral) flat structure with veins and interveins. Cells are squamous, hence flatter and the two layers-dorsal and ventral, are closely zippered in wings. The cells in the wing epithelia are larger, secrete a thin layer of cuticle and contain one trichome (hair-like structures) per cell (Fig 1.3). Thus, as the wing cells are larger and flatter, the trichomes are sparsely arranged. In contrast,

the haltere is bulbous or has a knob-like structure. The dorsal and ventral compartments do not physically oppose each other: cells, too, are more bulbous or cuboidal in nature and bear multiple trichomes per cell, and thus, are densely arranged (Fig 1.3) (Roch & Akam, 2000).

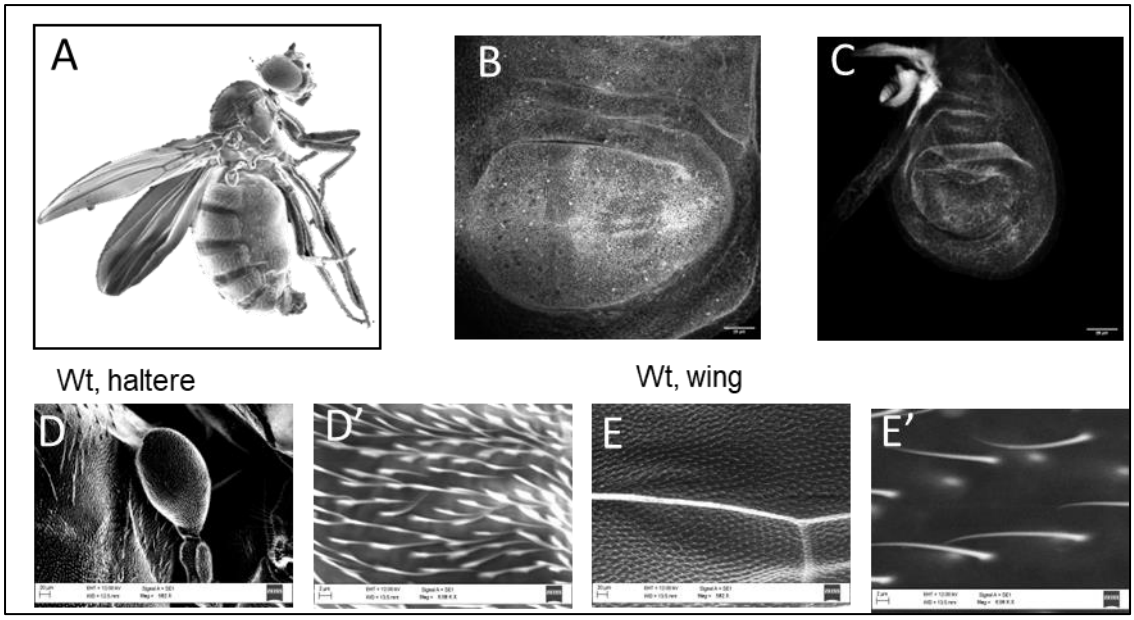

Figure 1.3 A. An SEM image of *Drosophila* showing wing and haltere. B, C Wing and haltere third instar imaginal discs stained with actin (grey), respectively. Scale bar, 25µm. D, E SEM image of wildtype haltere. D', E' A higher magnification of the representative area is shown in the bottom panel to visualise the trichome density and arrangement. Note the difference in trichome density between D'(haltere) and E' (wing).

1.4 Ubx-mediated Haltere Specification

During development, wing and haltere primordial cells are specified in the embryo. Later, during larval stages, these cells organise themselves as one single continuous epithelium sheet termed an imaginal disc, eventually giving rise to the respective adult appendages. Different sections of the wing imaginal disc develop into dorsal and ventral wing blades, hinge and vein regions, and specialised sensory bristles of the margin. The two-wing imaginal discs in T2 correspond to two wings in the adult. The more proximal part of each of the two wing imaginal discs specifies the dorsal thorax of the adult body. The dorsal thorax, thus, develops from two independent modules, which fuse laterally, making one single continuous thorax from all sides. Wing development is controlled by two major patterning events along its anterior-posterior (A/P) and dorso-ventral (D/V) axis to specify wing per se

while patterning events along the proximo-distal axis specify hinges and the dorsal thorax of the adult body (Fig. 2) (Beira & Paro, 2016; Hariharan, 2015). Haltere development follows a similar path, although the primordium itself is made up of fewer cells compared to the wing primordium. Ubx regulates several genes and pathways at multiple levels of their hierarchy. Many studies in the past have identified several targets of Ubx and their function to regulate growth control (at the level of cell number) and patterning in haltere imaginal discs (detailed in the next section). Ubx-mediated modulation of patterning events eventually results in the growth and differentiation of haltere discs into structurally and, thereby, functionally, into different structures as compared to wings (Makhijani et al., 2007; Roch & Akam, 2000; Singh et al., 2015). However, the Ubx-mediated regulation of cell size and shape, which, in turn, contributes to haltere shape, is relatively less explored.

1.5 Ubx modulates wing development pathways to specify haltere fate

1.5.1 Antero-Posterior patterning

In the larval discs, *Engrailed* (*En*)-expressing cells constitute the posterior compartment. It induces the expression of the short-range signalling molecule Hedgehog (Hh), which diffuses to the anterior compartment to activate Patched (Ptc), Smoothened (Smo), Cubitus interruptus (Ci), Knot (Kn) and Decapentaplegic (Dpp). The posterior compartment itself does not respond to Hh signalling as En represses its receptor Ptc and is also the sole mediator, Ci. The role of Dpp is central to wing development; it acts as a long-range morphogen and activates several important wing patterning genes, such as spalt (Sal) and optomotor blind (Omb). Proper positioning of cells receiving varied levels of Dpp is essential for cell proliferation in the wing disc (Rogulja & Irvine, 2005, Aza-Blanc, 1999; Brook et al., 1996; Ingham & McMahon, 2001; Ruiz-Losada et al., 2018). In haltere discs, while expression patterns of En, Hh, Ptc and Ci are unaltered, expression of Dpp and other downstream genes are modulated by Ubx (Mohit et al., 2006). Not only is dpp downregulated in haltere discs at the transcript level, its receptor Thickveins (Tkv) is up regulated in the A/P boundary, making Dpp protein to be internalised in the cells it is made. Additionally, Dally, which is required for Dpp to diffuse away from the A/P boundary, is specifically down regulated in the posterior compartment of the haltere discs (Crickmore & Mann, 2006, 2007; de Navas et al., 2006; Makhijani et al., 2007). This may result in an asymmetric distribution of Dpp between anterior and posterior compartments. Indeed, in haltere discs, the anterior compartment is

larger than the posterior compartment (3:1 ratio in size), while in wing discs, the two are of the same size (1:1 ratio in size). As expected, downstream components of the Dpp pathway, such as Dad, Spalt major, DSRF and Kn, are also repressed in the haltere discs (Galant et al., 2002; Hersh & Carroll, 2005; Mohit et al., 2006; Weatherbee et al., 1998a). Interestingly, in addition to *dpp, tkv* and *kn* are also directly repressed by Ubx suggesting that Ubx acts at multiple levels of a given signalling pathway to specify haltere fate, which supports the possibility that Ubx functions more like a micromanager (Akam, 1998).

1.5.2 Dorso-ventral patterning

Similar to the A/P boundary, the D/V boundary functions as the organising centre for proper patterning and growth of the wing discs along the D/V axis (Diaz-Benjumea, 1993). The selector gene, apterous (ap), specifies the dorsal compartment in the wing discs, which cell-autonomously activates Serrate (Ser) and Fringe (Fng). These two proteins, whose expression is restricted to the dorsal compartment, potentiate Notch (N) to respond to signals coming from the ventral compartment (in the form of Delta (Dl)) only at the D/V boundary. N specifies the D/V boundary as an organiser along the D/V axis (reviewed in (Brook et al., 1996; Ruiz-Losada et al., 2018)). Notch further activates Wingless (Wg), Cut (Ct) and boundary enhancer of Vestigial (Vg). Wg functions as a morphogen activating Vein (Vn), Achaete (Ac), Distal-less (Dll) and Vg in non-DV cells in a concentration-dependent manner. The vg gene is a pro-wing gene. The expression of this gene is very tightly regulated since any ectopic expression of this gene leads to ectopic wings (Kim et al., 1996). Vn is a ligand for the EGFR pathway, which, together with Dll, specifies the wing margin (Schnepp et al., 1996). Ac is required to specify sensory organs of the margin (reviewed in Calleja et al., 2002). In haltere discs, Ubx modulates D/V patterning differently than the way it regulates A/P patterning events. While Ap, N, Ser and D/V boundary–specific Vg are unaltered, expression of Wg is repressed, but only in the posterior compartment. However, further downstream (of Wg), Ac, Vn, Dll and non-D/V Vg are completely repressed in both anterior and posterior compartments. Repression of Wg expression in the posterior compartment could be either direct and/or through the repression of N activity. While it is not clear how Ubx represses targets of Wg in the anterior compartment of haltere discs, genetic mosaic experiments suggest a non-cell autonomous role of Ubx in repressing wing identity and specifying haltere identity (Shashidhara et al., 1999). As vg is a pro-wing gene, its downregulation is an important factor for haltere specification. In wing discs, Vg is activated

by both N (in the D/V boundary) and Wg (in non-D/V cells) pathways. Ubx appears to inhibit nuclear localisation of Armadillo (Arm) in the anterior compartment (Wg itself is completely repressed in the posterior compartment), in addition to repressing events downstream of N and also directly suppressing non-D/V expression of vg. All these indicate that D/V signalling is also modulated at multiple levels of the hierarchy of gene regulation. Perhaps, such a mechanism could be a common theme in the evolution of body plan.

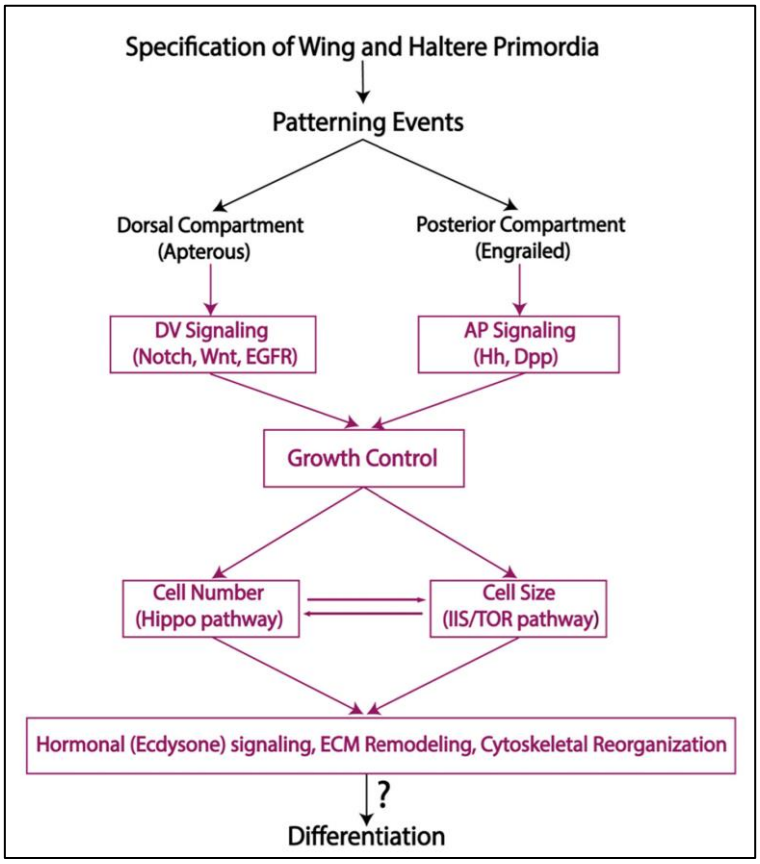

Figure 1.4 Major developmental events that occur after specification of the wing and haltere primordia, finally lead to the development of respective organs in the adult fly. At the embryonic stage, Wg and Dpp pathways specify the appendage primordia. The primordia retain compartmental identifies as defined by the expression of Apterous (for dorsal) and Engrailed (for posterior). At the larval stages, the wing and haltere imaginal discs are patterned by the Hedgehog (Hh) signaling pathway for the anterior-posterior compartment, whereas the Notch, Wingless (Wnt) and EGFR pathways pattern the dorso-ventral region. The Hippo and Insulin/TOR pathways control the growth of the discs by influencing cell number and cell size. Patterning and growth events are followed by hormonal signaling, ECM remodelling and cytoskeletal reorganization during the pupal stages to shape the organ

in the adult fly. Ubx modulates each of these developmental and growth events (from embryo to pupal stages) to repress the wing fate and specify the haltere fate in the third thoracic (T3) segment (shown in magenta). However, knowledge about its role in the terminal differentiation program still remains largely unknown (Khan et al., 2020).

1.6 Ubx-mediated organ shape and size determination

1.6.1 Ubx control of cell number and cell size.

In Drosophila, EGFR signal transduction via the RAS/MAPK kinase cascade has been implicated in many aspects of pattern formation as well as in the control of tissue growth, cell proliferation, and apoptosis (Crossman et al., 2018; Pallavi & Shashidhara, 2003, Shilo, 2005). Ubx-mediated regulation of the EGFR pathway is important in specifying the haltere fate as overexpression of the positive components of this pathway, such as EGFR and Vn in halteres, causes significant haltere to wing transformation. Interestingly, many of the components of the EGFR pathway, such as *egfr, vn, pointed*, and *yan*, are direct targets of Ubx (Khan et al., 2023).

In a simplified perspective, organ size is determined by the size and shape of its component cells. However, they may not be additive, as an increase in cell number can be compensated partly be decreasing cell size and vice versa (Neufeld et al., 1998). The Hippo/Yorkie (Yki) pathway is implicated in organ size control and tissue homeostasis, which it accomplishes by integrating signals within the cell, cell-cell interactions and mechanical cues. It regulates growth by promoting cell proliferation, cell growth and inhibiting apoptosis (Irvine & Harvey, 2015). Many of its components are thought to be differentially regulated between wing and haltere, and some are direct target of Ubx (refer Chapter 3). We will use this opportunity to introduce the hippo pathway, its major components and targets.

Hippo pathway in organ size control:

The Hippo pathway is a crucial determinant of organ size in both Drosophila and mammals (reviewed in Zheng & Pan, 2019). Though one of the newly discovered members of the family of signalling pathways, the Hippo pathway is ancient in terms of metazoan evolution.

The pathway components were initially identified as tumour suppressors in *Drosophila melanogaster* through mutant screening experiments (Pan, 2010). It is implicated in organ size control and tissue homeostasis by integrating signals from within the cell, amongst cells by cell-cell interactions and from the mechanical cues experienced by the cells or tissues. The Hippo pathway controls growth by promoting cell growth and proliferation, and inhibiting apoptosis. For simplicity, the hippo signalling cascade can be divided into three parts: central core kinases, downstream transcriptional regulatory proteins, and multiple upstream regulatory proteins. The core kinase includes the NDR family kinase Warts (Wts) (Justice et al., 1995; Xu et al., 1995), the Hippo kinase (Hpo) (Jia et al., 2003; Udan et al., 2003) along with the scaffolding proteins Salvador (Sav) (Tapon et al., 2002) and Mob as Tumor suppressor (Mats) (Lai et al., 2005). Interestingly, all core kinase pathway components were found to play pivotal roles in maintaining the delicate equilibrium between cell proliferation and apoptosis, crucial for determining tissue and organ size.

Yki and YAP-TAZ's (in mammals) role in organ development is highly context-dependent and varies across different tissue types (LeBlanc et al., 2021). It regulates the gene expression by cooperating with its binding partners such as Scalloped, Mad and homothorax. When the Hippo signalling is ON, the phosphorylation events prevent the downstream effector Yki/YAP from entering the nucleus. Conversely, when the kinases are inactive, or the hippo pathway is OFF, Yki is not phosphorylated, and it can enter into the nucleus and bind to its binding partners to activate genes promoting proliferation such as Myc, bantam micro-RNA, Cyclin E. The core Hippo-Warts kinase cassette is activated by the Crumbs-Expanded (Crb-Ex) and Merlin-Kibra (Mer-Kib) protein complexes at apical cell-cell junctions (Zheng & Pan, 2019). Expression of these upstream apical regulators is negatively regulated by Hippo signalling. Furthermore, Wts activity is inhibited by E-cadherin-associated proteins, such as Ajuba (Jub), and by Dachsous-cadherin-associated proteins, such as Dachs, Mib or Riq. The multitude of studies from the past two decades points out that the Hippo pathway and Yap/Yki act as a signalling nexus and integrates several other growth regulatory and patterning pathways such as Insulin, EGFR and Wnt/Wg signalling (reviewed in Gokhale & Shingleton, 2015). It integrates growth regulatory pathways, cellular mechanical properties, growth and pattern formation, systemic hormonal signals and the final differentiated state of the organ.

Growth is also influenced by environmental factors such as the nutritional status of the organism (reviewed in Shingleton, 2010). The Insulin-like (IIS/ Akt) pathway plays an important role in sensing the nutrition status and regulating growth, primarily by regulating cell size (reviewed in Gokhale & Shingleton, 2015). Ubx downregulates the function of both the the Yki and IIS/Akt pathways. Interestingly, while upregulation, individually, of Yki and IIS/Akt pathways in developing haltere have only marginal phenotypes, their combined upregulation shows dramatic haltere to wing phenotypes, both in size and shape of the organ (Singh et al., 2015). Cells appear to be larger and also flatter, making the transformed haltere a flattened structure like a wing. Thus, it appears that the cross-talk between Hippo-Yki and IIS/Akt pathways is key in maintaining an inverse relationship between cell size and shape (Straßburger et al., 2012). Further investigation is needed to understand the precise mechanism, perhaps at the levels of cytoskeletal organisation, by which cell size is determined (reviewed in Diaz de la Loza & Thompson, 2017; Sánchez-Herrero, 2013).

1.6.2 Control of extracellular matrix and hormonal components

Ubx regulates the haltere shape by preventing the formation of flat wings by inhibiting the cell shape changes and adhesion of dorsal and ventral wing blades. Integrins, which are required for this opposition of two blades, are not regulated by Ubx, instead Ubx has employed an interesting mechanism to achieve the bulbous shape of the haltere (De Las Heras et al., 2018, Diaz-de-la-Loza et al., 2018). At a time when basal components of the extracellular matrix (ECM), such as Viking, are degraded in wing discs due to high levels of Matrix metalloprotease 1 (Mmp1) expression in early pupal stages, Ubx-mediated inhibition of Mmp1 in haltere discs maintains a gap between dorsal and ventral layers. This gap is subsequently filled by hemolymph, thus permanently preventing close opposition of the two layers in developing halteres (De las Heras et al., 2018; Pastor-Pareja & Xu, 2011). Additional control of organ size may be mediated by growth hormones such as Ecdysone. Recently, we have observed, by ChIP-seq and RNA-seq, that many positive regulators of the Ecdysone pathway are down regulated in haltere discs, while negative regulators are upregulated (Khan et al., 2023).

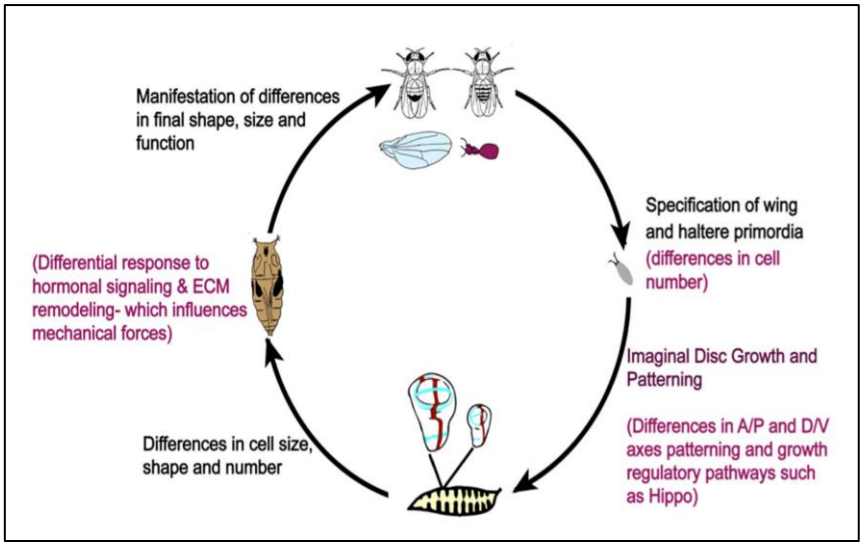

Figure 1.5 Life cycle of *Drosophila* indicating key steps in the development of wing and halteres (Khan et al., 2020). Events/traits regulated by Ubx in developing haltere are shown in magenta. Ubx regulates haltere development throughout the life cycle. It regulates cell number of the primordium in the embryo. Ubx regulates patterning events (gene expression patterns) that results in differential cell number, size and shape later during pupal development. Ubx also regulates certain events in the pupa, such as clearance of ECM, hormonal signalling etc to bring about final differences between size and shape between adult wing and haltere.

1.7 Wing and Haltere morphogenesis

Drosophila wing and haltere imaginal discs have very similar overall morphology until the third instar larval stage (L3). A third instar wing and haltere discs can be physically subdivided into areas of pouch, hinge and notum. Their characteristic folds and three-dimensional architecture separate them. The cells of the respective pouch region give rise to the adult wing blade and haltere capitellum; hence, our work focuses on the pouch cells' characteristics in these discs at various stages of their development. Both the wing and haltere discs consist of a single layer of pseudostratified columnar epithelium, also referred to as disc proper (DP), and a squamous epithelium located apically to the DP, which forms the peripodial membrane. The pouch has a characteristic curvature resembling a “dome,” where the DV boundary cells pass through the tip of the dome in wing discs (Fig 2.1).

At the start of metamorphosis, the wing disc everts through its peripodial membrane. The pouch region expands to form the wing blade, dorsal and ventral surfaces appose, and the constituent epithelial cells change from columnar to cuboidal cell shape. Columnar to cuboidal cell shape change results in a decreased cell height, correlated with a lateral localisation of Myosin II and increased cell apical area by 7-9h after puparium formation (APF). This correlates with the apical and basal extracellular matrix (ECM) degradation mediated by matrix metalloproteinases (MMPs) (Fig 1.6). Subsequently, various morphogenesis and differentiation events occur, forming the adult wing (De las Heras et al., 2018; Diaz-de-la-Loza et al., 2018).

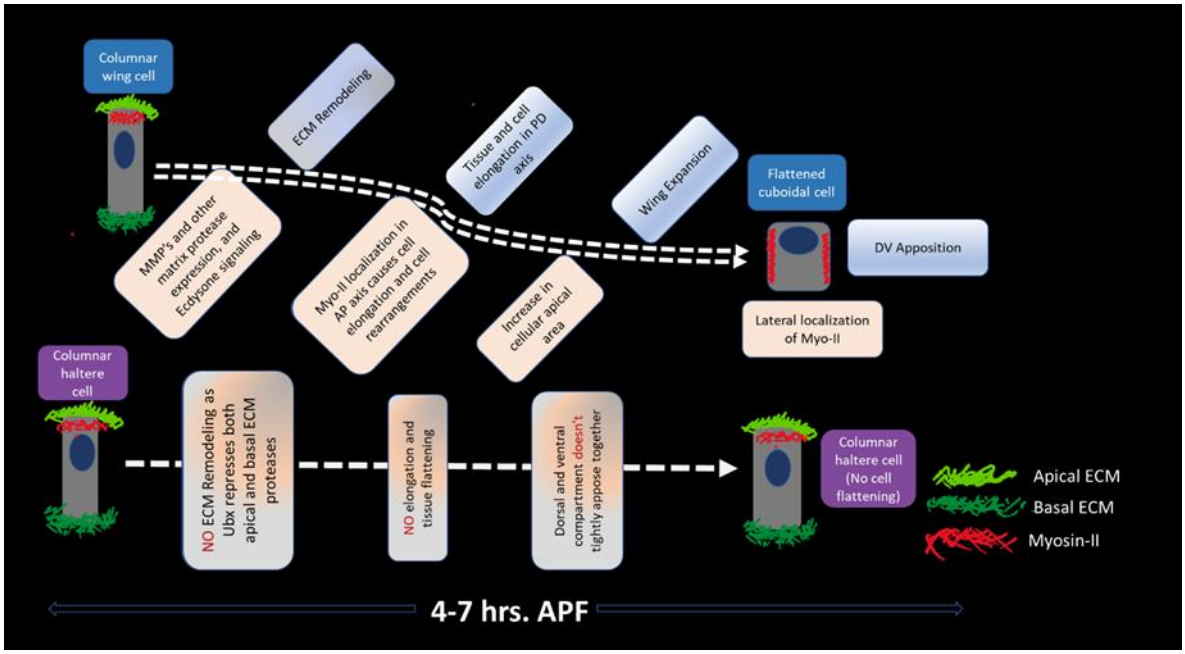

Figure 1.6 Summary of events in early wing (top)and haltere (bottom) disc morphogenesis. The ECM remodelling, lateral localisation of myosin, cell shape transition from columnar to cuboidal drives tissue expansion and DV apposition in the wing. Ubx represses the ECM remodelling in the haltere disc, therefore, there is no cell shape change, tissue expansion or DV apposition.

In contrast, the haltere discs maintain columnar cell shapes and resist ECM degradation due to the presence of Ubx. Ubx represses the activity of MMPs and other proteases like stubble (Sb) in the haltere disc, thereby retaining the ECM. As a result, haltere epithelia fail to

elongate, and the DV layers do not appose together, resulting in their characteristic globular shape (De las Heras et al., 2018; Diaz-de-la-Loza et al., 2018). The precise identity of targets of Ubx and developmental pathways modulated by Ubx in mediating such differences between wing and haltere are less understood. In this study, we would like to understand the mechanism/s by which Ubx regulates cell shape and size in determining the globular shape of halteres.

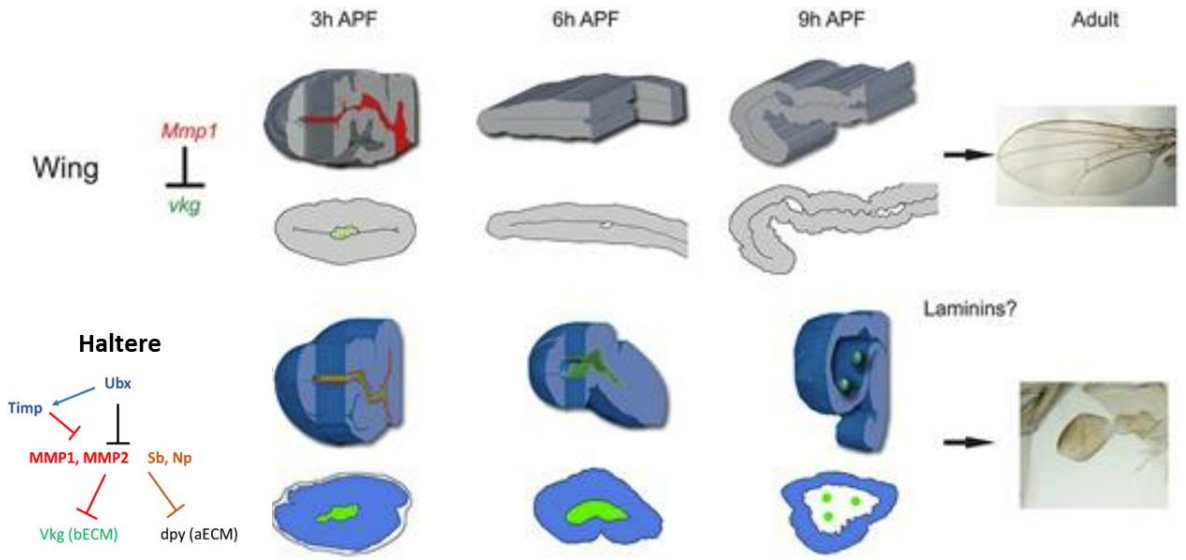

Figure 1.7 Ubx inhibits apical and basal extracellular matrix remodelling in haltere discs. This prevents disc expansion and dorsal-ventral layer apposition that happens in the wing disc at 3hrAPF. Modified from (De las Heras et al., 2018).

Specific Objectives of the study

1. To study the mechanical properties of epithelial cells of the *Drosophila* wing and haltere imaginal discs.

2. To understand the role of cellular mechanics, ECM, and molecular signalling in the determination of wing vs. haltere morphology

3. Identification of molecular targets of Ubx in the specification of haltere size and shape

4. Modelling cell and organ deformations, incorporating our findings to validate and understand the differential morphology of wings and halteres.

Summary of results:

With the recent advances in microscopy techniques, quantitative imaging and analysis, we re-investigated the cellular biophysical properties of wing and haltere discs at the third instar larval stage (L3). The wing and haltere discs analysed at the third instar larval stage, revealed that wing cells were more elongated and had a narrower apical surface compared to haltere cells. Actin and myosin levels, which play a crucial role in regulating cell tension and contractility, were also found to be apically higher in wing disc cells. Laser ablation experiments indicated increased cell contractility in wing discs compared to haltere discs. Additionally, the study examined the effect of Ubx downregulation in haltere discs, resulting in the reversal of cellular features observed in wild-type haltere discs. Furthermore, we investigated the changes in the cellular biophysical properties and 3D tissue architecture in some of the mutants of major growth regulatory pathways, which, when knocked down using RNAi lines in haltere, gave varying degrees of homeotic transformation. The mutants displayed alterations in cell morphology, increased actomyosin accumulation, and heightened cell junctional tension. When combined with computational modelling, these approaches now permit us to understand the relative contributions of cell size and shape changes and various inter- and intra-cellular forces to the overall change in the tissue shape. The study provides insights into the cellular mechanisms underlying the differential development and shape of the wing and haltere organs.

CHAPTER 2

Comparative Study of Mechanical Properties of Epithelial Cells in *Drosophila* Wing and Haltere Imaginal Discs

Comparative study of mechanical properties of epithelial cells in *Drosophila* wing and haltere imaginal discs

2.1 Introduction

Epithelial tissues and their cellular dynamics play a crucial role in shaping the morphology and architecture of organs during the development. A balance between cytoskeletal mechanics driven by the actomyosin network, cell-cell adhesion, and cell-ECM interactions exert influence over individual cell geometry, along with contributing to the tissue-level dynamics (Díaz-de-la-Loza & Stramer, 2024; Kozyrina et al., 2020; Luciano et al., 2022; Miao & Blankenship, 2020). These are often mediated by altering the relative contractility within cells achieved by polarised localisation and accumulation of cytoskeletal components such as actomyosin complexes. Hence, mechanics are key in enabling the complex folding and tissue bending of the epithelia during morphogenesis. However, the precise mechanisms and coordination of these factors in sculpting organs remain unclear. In this chapter, the differences between the cellular mechanical properties of *the Drosophila* wing and haltere imaginal discs are investigated. Understanding the cellular features and differences between these two discs can help us understand the factors and developmental processes that drive their distinct morphologies and functions.

During the first and second instar larval stages, the disc proper cells of wing and haltere imaginal discs are cuboidal. However, the lateral thickness of the cells increases (doubles in wing discs) between 65 AEL (mid second instar) and 120 AEL (end of larval development), rendering the cells columnar (Harmansa et al., 2023). Thus, the *Drosophila* wing and haltere imaginal discs are composed of pseudostratified columnar epithelia at the third instar larval (L3) stage Until the third instar larval stages, the properties of the cells of the wing and haltere epithelia and their spatial arrangements were considered to be very similar (Makhijani et al., 2007; Roch & Akam, 2000; Singh et al., 2015). The wing and haltere morphologies become progressively distinct from the early puparium formation. They also play pivotal roles in shaping the disc structures and ultimately determining the unique morphological and functional features of the adult wing and halteres. Recent studies have shown that, unlike halteres, wing discs undergo columnar to cuboidal cell shape transition and ECM

remodelling, aiding in tight apposition of dorsal and ventral layers at early hours of puparium formation (APF). Presence of the hox protein Ubx in halteres prevents ECM degradation by repressing MMPs and other proteases, such as Stubble protease (Sb) and Notopleural (Np), necessary for the matrix remodelling (De las Heras et al., 2018; Diaz-de-la-Loza et al., 2020). This retention of cell shape and ECM is thought to be one of the major factors preventing dorso-ventral apposition in halteres and, thereby, maintaining the globular geometry. However, degrading the basal ECM (bECM) by expressing MMP1 only resulted in a mild flattening, prompting the need for the identification of more factors in the haltere (De las Heras et al., 2018).

With the recent advances in microscopy techniques, quantitative imaging, and analysis, we re-investigated the cellular biophysical properties of wing and haltere discs at the third instar larval stage(L3). The aim is to understand the differential cell shape and the three-dimensional morphology change mediated by Ubx in the halteres at early stages, leading to the differential development of the two organs. Moreover, this could also pave the way towards identifying more factors that influence organ size and shape in the context of the *Drosophila* wing and haltere. The wing and haltere discs were analysed at the third instar larval stage. We observe that the wing cells were more elongated and had a narrower apical surface compared to haltere cells. Actin and myosin levels, which play a crucial role in regulating cell tension and contractility, were also found to be higher in wing discs. Laser ablation experiments indicated increased cell contractility in wing discs compared to the haltere discs.

2.2 Results

2.2.1 Third-instar larval wing disc cells are more elongated than the haltere disc cells.

Drosophila wing and haltere imaginal discs have very similar overall morphology until the third instar larval stage (L3). Third instar wing and haltere discs can be physically subdivided into areas of pouch, hinge and notum. They are separated by their characteristic folds and three-dimensional architecture. The cells of the respective pouch region give rise to the adult wing blade and haltere capitellum; hence, our study majorly focuses on the characteristics of the pouch cells in these discs at various stages of their development. Both the wing and haltere discs consist of a single layer of pseudostratified columnar epithelium (as the nuclei are not in the same plane), also referred to as disc proper (DP), and a squamous epithelium located apically to the DP, which forms the peripodial membrane (Figure 2.1). While the imaginal discs are often regarded as simple epithelial cell sheets, they possess complex morphologies, cell shape and type heterogeneities and variations in organisational patterns. The pouch has a characteristic curvature resembling a “dome,” where the DV boundary cells pass through the centre of the dome in wing discs (Fig 2.1 C, D).

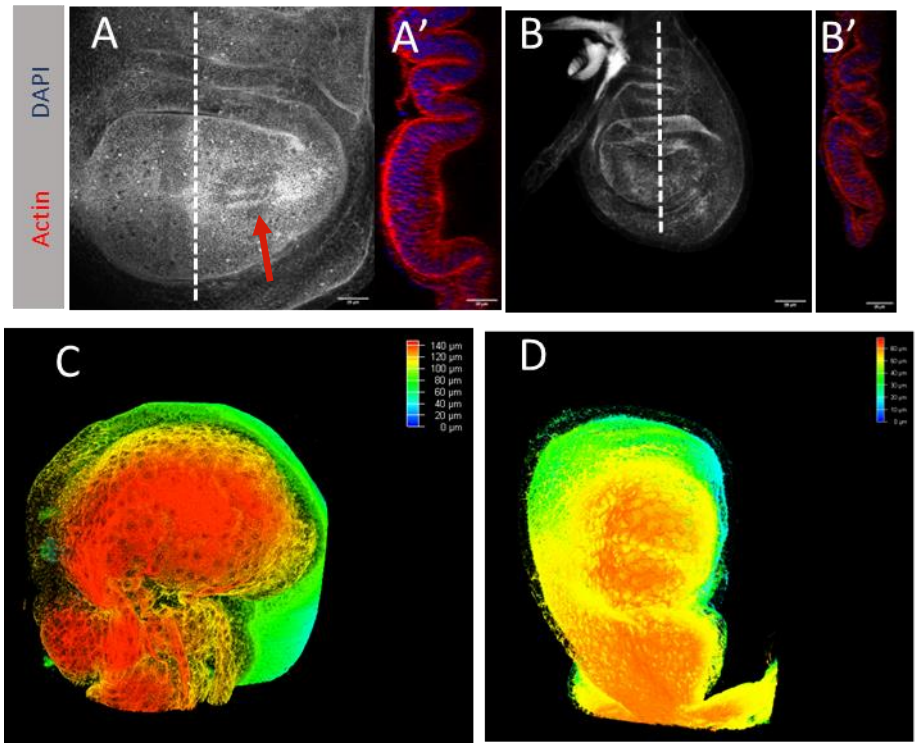

Figure 2.1 A, B Maximum intensity projection of third instar wing and haltere disc stained for Actin, respectively. The red arrow shows the DV boundary cells in the wings. A', B' Lateral cross-section along the dashed white line shows the organisation of DP cells in the pouch of the wing (A') and haltere disc (B'). Scale bar, 25 μm. C 3D reconstruction of a wing disc, pseudo-colouring is based on the depth coding done with LAS X 3D software. Note the complex overall topology and the dome-like structure of the wing pouch. D 3D reconstruction of the haltere disc.

In order to understand the differential cell size, shape and tissue architecture acquired by wing and haltere discs in the early hours of puparium formation, we studied the quantifiable cellular properties of the wing and haltere discs at L3. To visualise the pseudostratified columnar DP cells, the third instar wing and haltere discs were stained with Rhodamine Phalloidin. Although concentrated at the apical belt of the cells, the phalloidin staining was present along the entire length of the columnar cells. This was further confirmed by the co-visualisation of F-actin and a basal membrane marker Viking GFP (Collagen IV α2-subunit, component of basal ECM) (Figure 2.2).

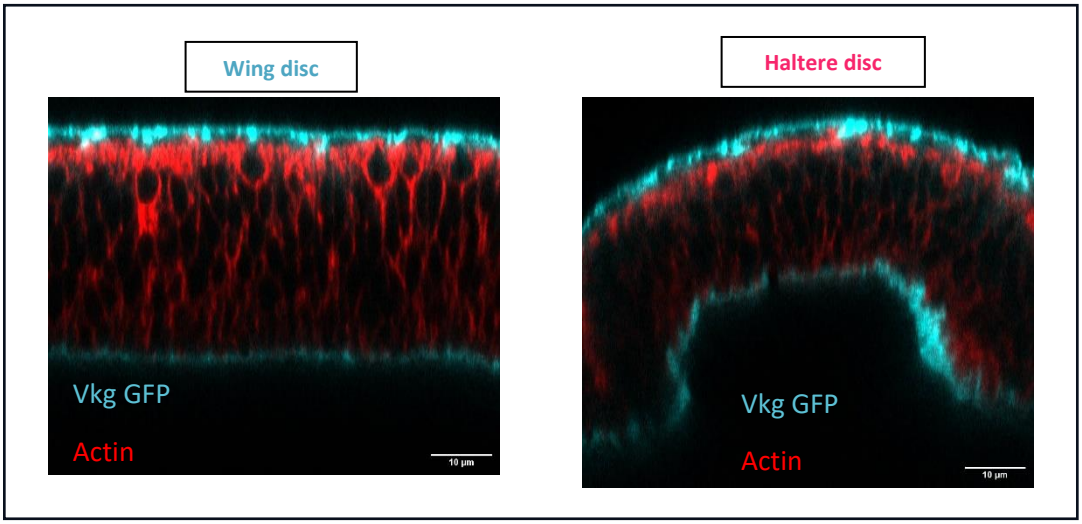

Figure 2.2 Wing and haltere discs stained for F- Actin and GFP to improve Vkg GFP signal. Note the pseudostratified columnar cells present in both the wing and haltere discs. Scale bar, 10 µm.

Interestingly, we observed that the relative thickness or the lateral cell height of the wing and haltere discs were different. Hence, we measured the lateral cell height of the DP cells stained for actin. The discs were carefully mounted with appropriate spacers (double-sided tape) between the slide and the coverslip to avoid accidental flattening of the discs. The discs with a flattened appearance or a straightened dome of the pouch were discarded from the analysis. The cell heights were measured manually using ImageJ-Fiji from the acquired disc cross-sections parallel to the DV axis. While the wing disc cells were 40 microns in length on average, the haltere discs were much shorter and averaged close to 30 microns. Hence, our results suggest that the columnar cells of the wing discs are more elongated than the haltere cells at the third-instar larval stage (Fig 2.3).

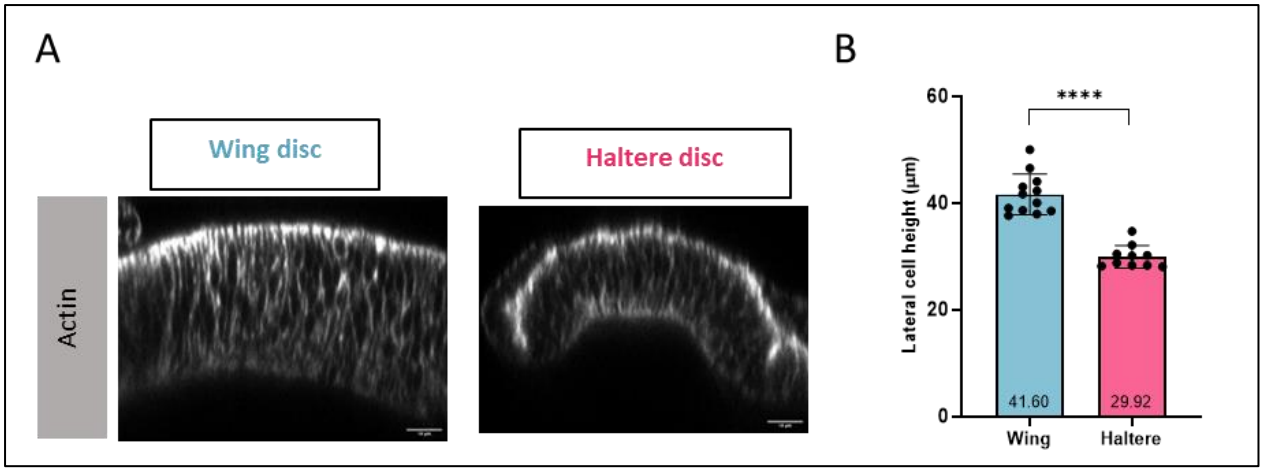

Figure 2.3 Third instar larval wing disc cells are more elongated than the haltere disc cells. A. Cross section of wing and haltere pouch cells showing the lateral cell height. Scale bar, 10 µm. B. Quantification of the lateral cell height. The mean, s.d and individual data points are presented, Student's t-test n= 12 and 10 discs for wing and haltere, respectively.

2.2.2 Wing disc cells are more apically constricted compared to the haltere disc cells at L3

We further compared the cell apical surface areas between the wing and haltere discs using DE-cadherin as a marker to visualise the cell apical membranes. We performed cell segmentation on acquired confocal images using Tissue Analyzer (Aigouy et al., 2016) and found that the cells of the wing discs are more constricted at the apical surface compared to the haltere discs (Fig 2.4).

We also tried to approximate the volume of the pseudostratified columnar cells between the wing and haltere. Since the precise estimation of the volume of pseudostratified columnar cells is difficult, we approximated the volume by multiplying a known area with the lateral cell height and dividing it by the number of nuclei. Our preliminary data suggest that the volume of the wing and haltere cells are comparable (Figure 2.5D).

Overall, our results suggest that wing disc cells are elongated and apically narrower compared to the halteres discs at the L3 stage of development.

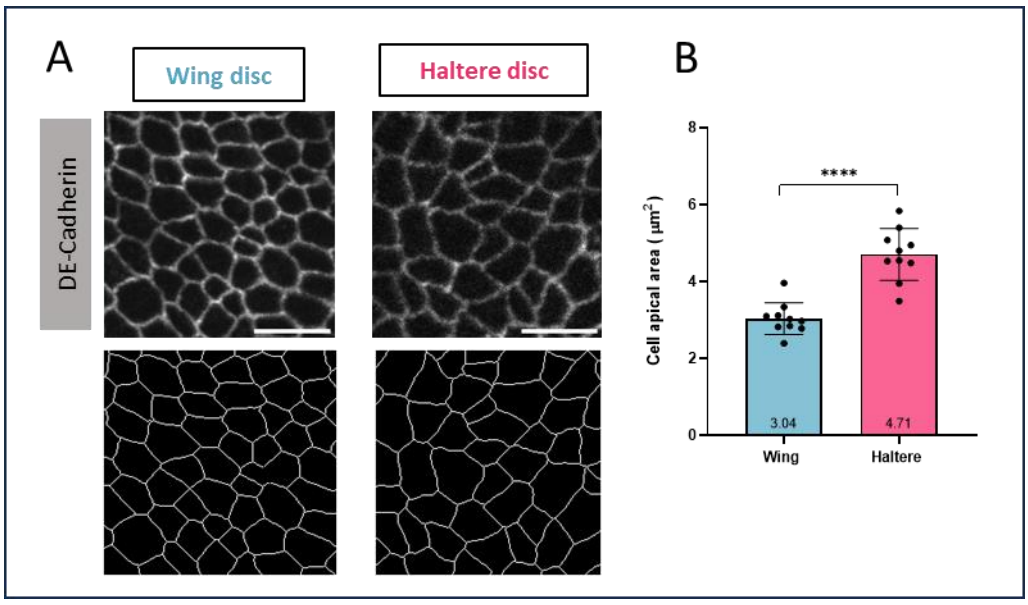

Figure 2.4 A. Apical projection of wing and haltere disc cells expressing DE-Cadherin, below panel, shows the segmented cell boundaries. Scale bar, 5 μm B. Quantification of cell apical area. The mean, s.d and individual data points are plotted. n=10 discs, Student's t-test.

2.2.3 Higher levels of Actin and Myosin II in wing disc cells compared to the haltere disc cells

The epithelial cell shapes are determined by the balance of the cell's internal and external forces. Actin and myosin, key components of the cytoskeleton, play pivotal roles in controlling cell size and shape by orchestrating dynamic changes in the cellular architecture. Since we observed differences in the cellular shape and size between the L3 wing and haltere discs, we investigated the actin and Myosin II abundance at the apical cortex of these two tissues. We stained the wing and haltere imaginal discs with Rhodamine Phalloidin. Although actin was distributed throughout the length of the DP cells, it was noticeably concentrated in the discs' apical belts. We quantified the mean fluorescence intensity between the two discs and observed an increase in the actin intensity at the apical cortex of the wing compared to the haltere cells (Fig 2.3 A, 2.5A).

Similarly, we measured the MyosinII levels using the light regulatory chain Spaghetti squash/ (sqh) using a GFP tagged transgene (sqh GFP) line GFP line (referred to hereafter as Myosin or Myosin II). The Myosin was densely localised in the peripodial cells and apical cortex of DP cells. However, the wing disc cells showed higher levels of myosin in the apical belt of DP than the haltere cells at L3 (Fig 2.5 B, C). Cellular contractile force primarily arises from the collective interactions of type II myosin motors and actin filaments. An increase in actomyosin abundance is correlated with higher tension/contractility and surface constriction. This can, in turn, determine the curvature and three-dimensional shape of the tissues for instance, tissue folding and tube formation during gastrulation and vertebral neural (Martin & Goldstein, 2014).

We also observed a significant enrichment of phalloidin in the apical belt of cultured wing discs at 3hrAPF compared to the corresponding haltere discs (Fig 2.5E, F). However, although there was a slight reduction of myosin intensity at 3hr APF in halteres compared to wings, the difference is not statistically significant (data not shown).

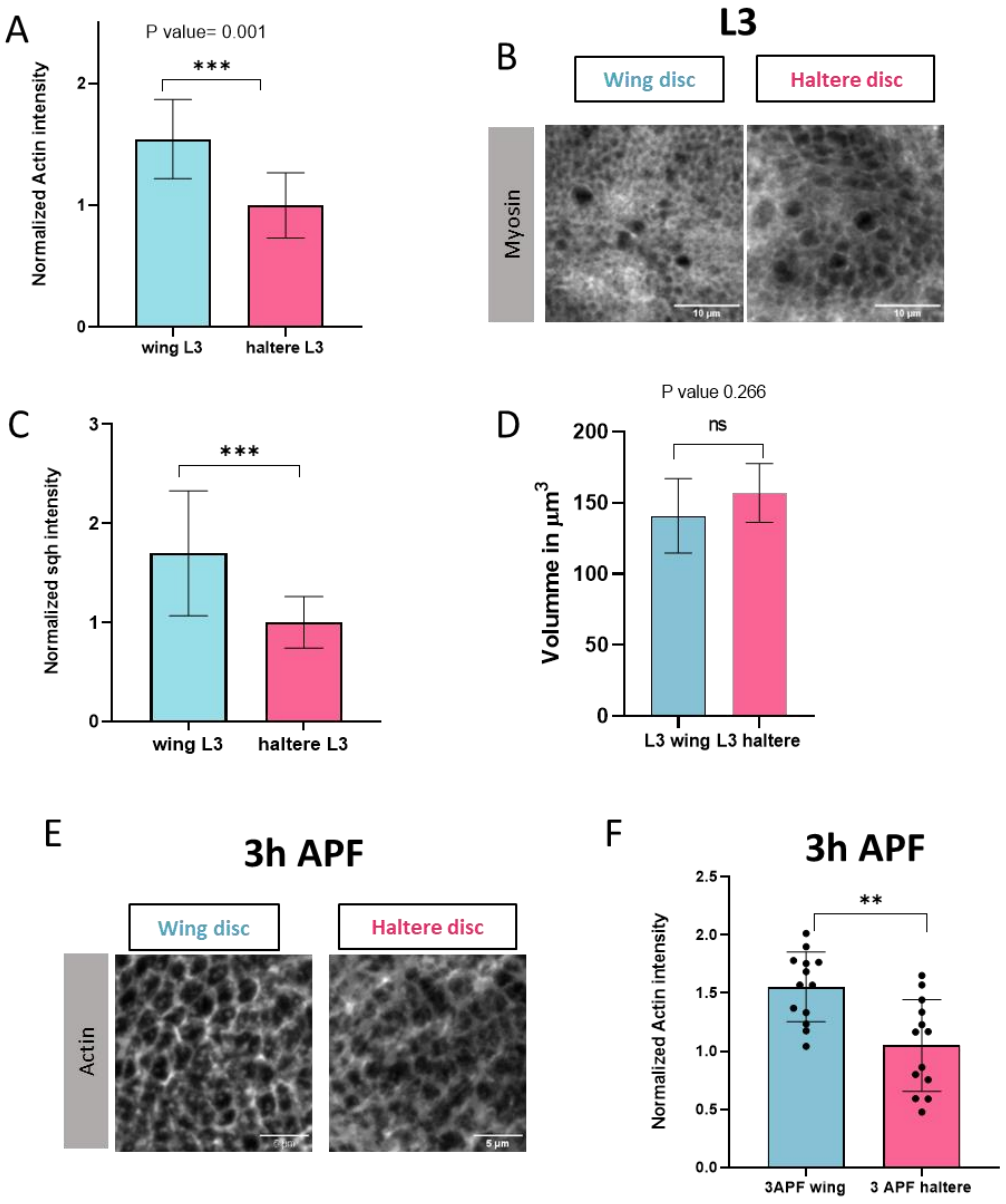

Figure 2.5 A. Quantification of apical actin intensity in the third instar wing and haltere discs. Normalised actin intensity is plotted, n=11 discs each. B. Sum of slices apical intensity Z-projection of wing and haltere cells stained for anti-squash myosin at L3. Scale bar,10 µm. C. Quantification of apical myosin fluorescence intensity at the L3 stage. n=11 discs each, average and s.d are presented, Student's t-test. D. Bar Plot showing the volume approximation between L3 wing and haltere discs n=5 discs. E. Sum of apical Z-projection showing apical actin from the wing and haltere at 3hAPF. Wing discs have higher levels of actin accumulation compared to the halteres at 3h APF, Scale bar, 5 µm. F. Quantification of apical actin fluorescence intensity, mean fluorescence intensities are normalised with the intensity of haltere discs (in A, C and F). Errors bars depict the s.d, n=13 discs.

2.2.4 Wing disc cells display higher levels of apical contractility than haltere cells

The actomyosin network plays a crucial role in regulating cell tension and contractility, which is essential for various cellular processes, such as cell adhesion, migration, and tissue morphogenesis. We investigated potential differences in the cell apical junctional tension between wing and haltere cells at L3 (Farhadifar et al., 2007; Sui et al., 2018). To achieve this, we conducted laser ablation on the apical pouch region of the wing and haltere discs expressing *endo-DE cadherin* GFP. A high-power two-photon laser was used to physically break the apical membrane cortex and measure the recoil or vertex displacement of the cells. A higher recoil or vertex displacement indicates an increased tension under the same experimental conditions. Our results demonstrated a significant increase in the relative vertex displacement and initial recoil velocity of wing disc cells in comparison to haltere cells, indicating a higher contractility in wing discs (Fig 2.6).

Taken together, our data indicate that wing discs are more elongated and apically constricted, and may have higher contractility compared to the haltere discs at L3.

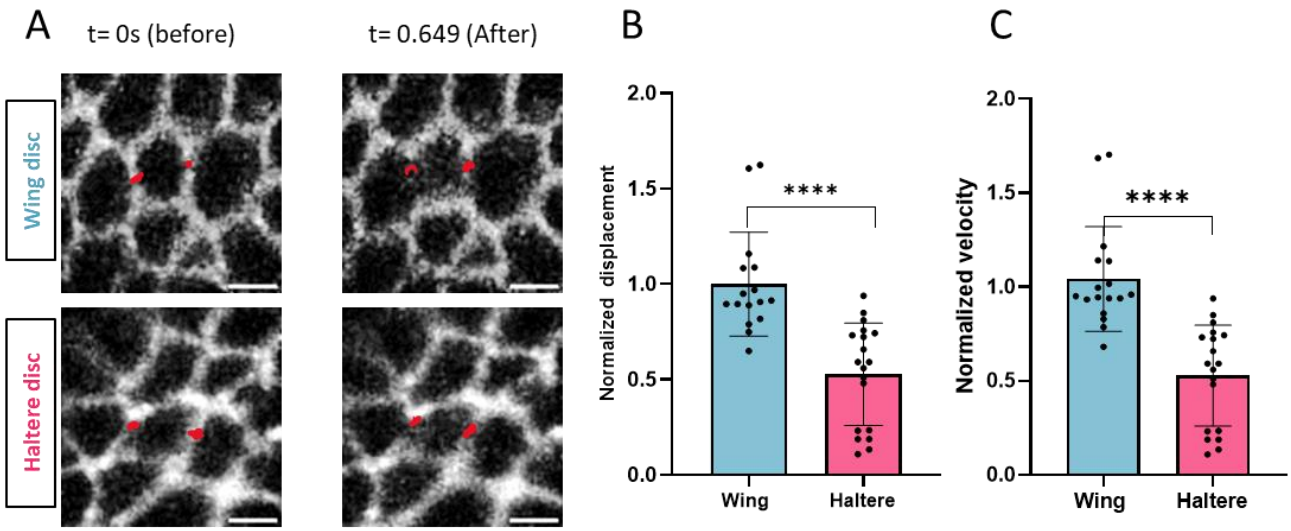

Figure 2.6 A. Wing and haltere disc cells expressing E cadherin GFP to mark the apical membrane, before (t=0 s) and after (t=0.649s) the ablation. The ablated cell bonds are marked with red dots. Scale bar, 2µm B, C. Normalised mean displacement and initial recoil velocity are plotted; n=17 and 20 cuts for wing and haltere discs, respectively, Mann Whitney test.

2.3 Discussion

The activity of a single Hox transcription factor, Ultrabithorax (Ubx), governs the development of two distinct organs with different cell morphologies. Studying the differential development of wing and haltere presents a unique paradigm for understanding the complexities of organogenesis and how Hox genes micromanage different signalling pathways and cellular processes and influence morphogenesis to mould different cell and organ shapes.

During development, wing and haltere primordial cells are specified in the embryonic stages. Subsequently, in the larval stages, these cells organise themselves as one single continuous epithelium sheet- the imaginal disc. The morphology of these two discs is strikingly similar, sharing common regions such as the pouch, hinge and notum. The constituent cells, characterised by pseudostratified columnar epithelial cells, and their spatial arrangements were also once thought to be indistinguishable. While numerous studies have delved into the role of Ubx in finely modulating various patterning and growth regulatory pathways, its role in altering the cellular biophysical properties are less studied. This aspect is crucial for understanding the pronounced differences that arise between these two organs during the later stages of their development.

Our study sheds light, for the first time, on the differences in cell properties between the wing and haltere third instar imaginal discs during *Drosophila* development. The comparative analysis of the wing and haltere discs at the larval stage revealed that the columnar cells of the wing were more elongated and had a narrower apical surface compared to the haltere cells. These morphological differences were accompanied by higher levels of actin and myosin in wing discs, indicating an increased cell contractility. Laser ablation experiments further supported the higher contractility of wing cells compared to the haltere cells. These experiments provide a new insight into the relationship between the mechanical properties of cells and, the cellular shape and size to the outcome as organs (Fig 2.7). However, a direct implication of the observed differences in the final shape of the organ is yet to be uncovered.

The wing and haltere disc shapes start to diverge from each other by the early hours of Puparium formation. The wing discs undergo specific cell shape changes and ECM remodelling, leading to the formation of a flat structure. In contrast, the haltere discs exhibit restrained ECM degradation, cell shape changes and tissue expansion due to the presence of Ubx (De las Heras et al., 2018; Diaz-de-la-Loza et al., 2018, 2020). We hypothesise that the

above-mentioned differences might act as initial constraints for differences that arise in their eversion properties and early morphogenesis. As alterations in cell contractility/tension can drive two-dimensional (2D) and three-dimensional (3D) shape deformations. Nonetheless, more extensive studies are required to strengthen this claim further. Towards this, we have utilised partial haltere to wing homeotic mutants identified in this study (Chapter 3&4) apart from Ubx^{RNAi}, and vertex modelling (detailed in Chapter 5) to enhance our understanding.

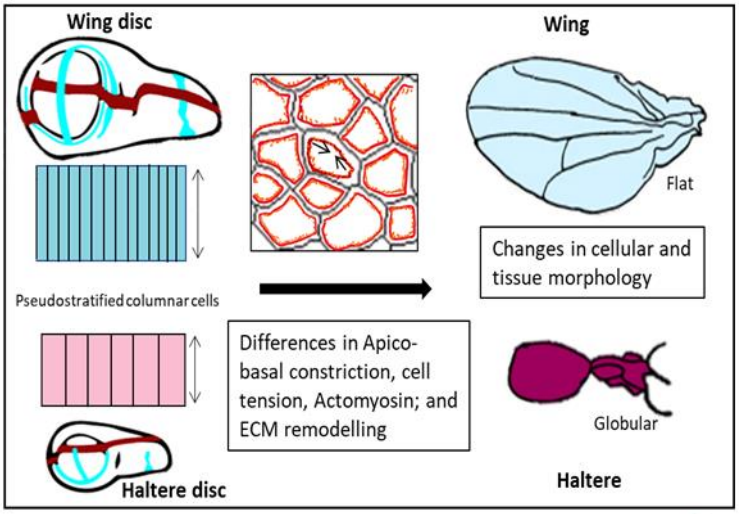

Figure 2.7 Provides a schematic overview highlighting the distinctions between the wing and haltere structures during the third instar larval and adult stages.

CHAPTER 3

Identification of Molecular Targets of Ubx in Haltere Size and Shape Specification

Identification of Molecular Targets of Ubx in Haltere Size and Shape Specification

3.1 Introduction

The development of precise organ size and shape is a fundamental aspect of organismal development, and it is tightly regulated by various signalling pathways. The size of an organ is specified as a function of a complex interplay between positive and negative regulators of growth. Many negative regulators of growth are activated as a feedback response to elevated levels of positive regulators of growth; most of them function in a context-specific manner. Alterations in cell contractility/tension can affect cell division and proliferation, and tissue structure, which ultimately influences organ size and shape in three dimensions. A complex integration of these factors is necessary for the development of precise organ shape and sizes. In the previous chapter, we observed inherent differences in the cellular mechanical properties between the wing and haltere disc cells. Ubx re-specifies the haltere from its default wing fate, encompassing both size and shape, partly through alterations in cell number and morphology. The adult wing epithelial cells exhibit larger and more flattened, squamous cells in contrast to the smaller, cuboidal-shaped cells of haltere epithelia (Roch & Akam, 2000). This variance in cell shape might have an implication in attaining the unique three-dimensional morphology of the organ. However, the downstream targets of Ubx in dictating the cell and organ size and shape is relatively less understood.

The Hippo pathway appears to be one of the critical targets of Ubx. Alterations in its components, such as the overexpression of Yorkie (Yki), a positive regulator of growth, or the downregulation of Expanded (Ex), a negative regulator of growth, lead to the development of overgrown halteres. Ubx downregulates the function of the Yki (upregulates Hippo) pathway (Singh et al., 2015). Interestingly, while upregulation, individually, of Yki and IIS/Akt pathways in developing haltere have only marginal phenotypes, their combined upregulation shows dramatic haltere to wing phenotypes, both in size and shape of the organ (Singh et al., 2015). Cells appear to be larger and also flatter, making the transformed haltere relatively flatter. These changes demonstrate their role in determining cell size, trichome characteristics, and arrangement, all of which are essential parameters in shaping organ

morphology. In this project, we aimed to identify specific molecular players that are capable of inducing more intense phenotypes affecting both cell and organ shape and size in halteres. These targets can be used to gain insights into the cellular biophysical properties governing the differential organ shapes between wing and haltere.

To identify molecular players that could be potential targets of Ubx in resisting cell and organ shape and size in halteres, we conducted a screen for enhancers using the UAS GAL4 system (Brand and Perrimon, 1993) and VDRC RNAi lines (as shown in Figure 1). A previous genome-wide screen conducted in our lab has identified around 904 genes as potential growth suppressors. These genes, when downregulated in the background of moderately elevated levels of Yki, resulted in neoplastic growth, disrupting the fine balance between cell size and cell number (Groth et al., 2020). However, the effect of these genetic backgrounds on the cellular morphology of halteres was unaddressed. As the presence of the Hox gene, Ubx is generally thought to resist major deviations from the haltere fate. We utilised ChIP (of Yki and Ubx) and transcriptome data generated in this study, as well as previously published data, to shortlist potential growth regulators. Following the identification of genes exhibiting substantial and consistent overgrowth effects in the haltere imaginal disc as a result of this initial screen (tumour model), we subsequently developed an additional screening approach to assess their impact on adult morphology, specifically looking for homeotic transformation in terms of organ size, trichome arrangement and shape (or flattening) in the haltere. We observed that when either *Atrophin* or *Pten*, is downregulated in haltere discs in the background of reduced *Expanded* (increased Yki activity), leads to overgrowth and flattening of the haltere, resulting in a partial haltere to wing homeotic transformation. This is in the background of intact Ubx expression, thereby providing us with genetic tools to study events downstream of Ubx that regulate cell size and shape.

3.2 Results

3.2.1 Comparison of Yki and Ubx ChIP Targets

The Hippo pathway regulates the precise control of cell proliferation and apoptosis, essential for determining the final size, shape, and patterning of various organs, including the *Drosophila* wing and halteres. Overexpression of Yki or downregulation of Hippo pathway upstream kinases is known to cause overgrowth due to increased cell proliferation and reduced cell death in both wing and haltere discs (Hariharan, 2015; Irvine & Harvey, 2015; Singh et al., 2015). This underlines the role of Yki and Hippo pathway in maintaining the tissue proportionality in these discs. Moreover, Yki and many of its upstream and downstream targets are thought to be differentially regulated between the developing wing and haltere discs(Singh et al., 2015). We observed that ChIP seq data of Ubx (Khan et al., 2023) from L3 haltere discs and the only available Yki-ChIP (Oh et al., 2013) from wing discs share many common target genes. There were approximately 3900 putative targets for Yki, and 1546 targets of Ubx were identified. Out of which, they share 438 genes as targets. We performed a STRING analysis on these common targets. Various genes related to multiple growth regulatory and patterning pathways were enriched (Fig 3.1). Furthermore, genes associated with extracellular matrix, basal membrane components (such as MMP2, Stubble protease (Sb) and dlp), PcG PRC1 complex, and several other related terms were enriched. It is also interesting to note that upstream and downstream regulators of Yki, such as ex, wts and Kibra, are putative direct targets of Ubx. Similarly, pathways and genes such as dpp, N, and vg, which are modulated by Ubx to specify haltere fate, are also plausible direct targets of Yki.

Additional note: Expanded (Ex) and Gug/Atrophin are targets of both Ubx and Yki.

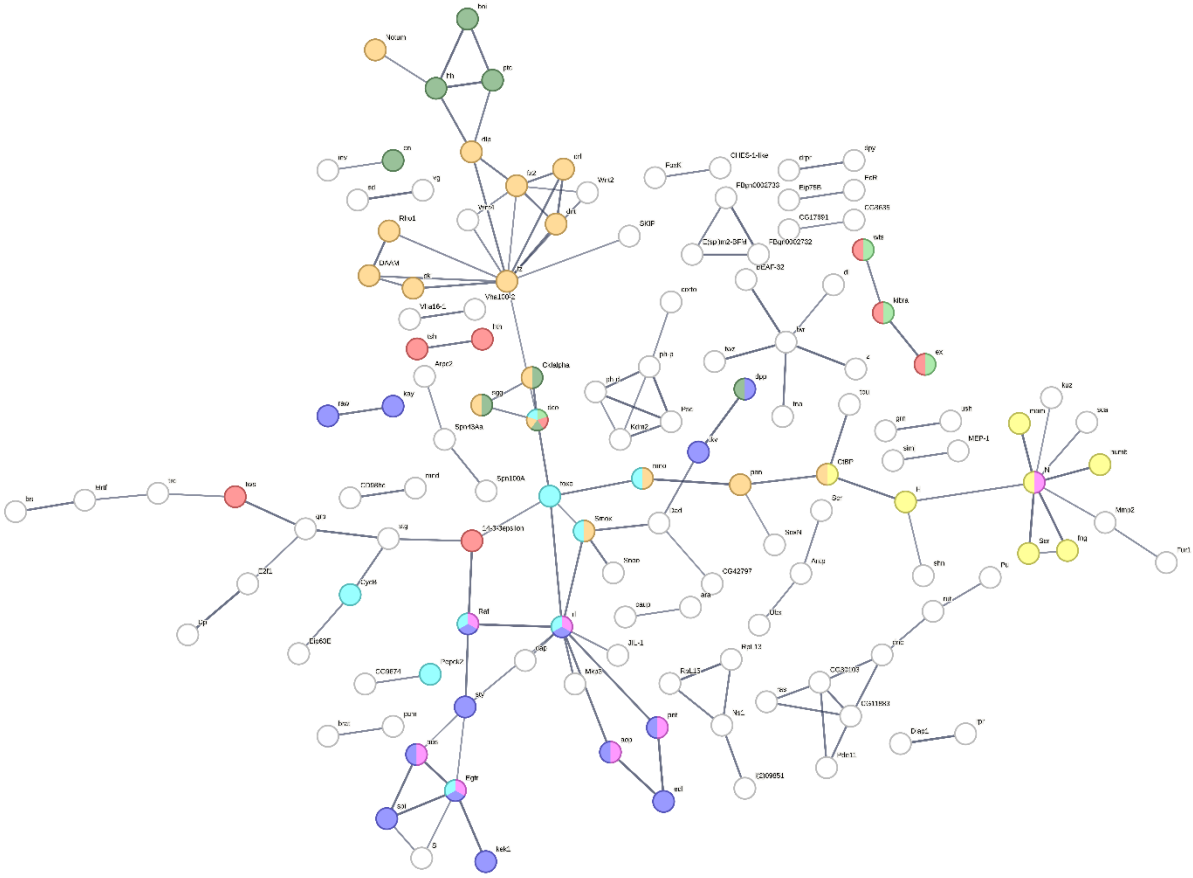

KEGG Pathways

pathway	description	count in network	strength	false discovery rate
dme04320	Dorso-ventral axis formation	8 of 27	0.98	0.00024
dme04330	Notch signaling pathway	7 of 24	0.97	0.00079
dme04392	Hippo signaling pathway - multiple species	4 of 15	0.94	0.0318
dme04013	MAPK signaling pathway - fly	19 of 89	0.84	5.90e-08
dme04391	Hippo signaling pathway - fly	11 of 51	0.84	8.92e-05
dme04341	Hedgehog signaling pathway - fly	8 of 37	0.84	0.0011
dme04310	Wnt signaling pathway	19 of 102	0.78	2.16e-07
dme04068	FoxO signaling pathway	10 of 64	0.7	0.0013
dme04350	TGF-beta signaling pathway	6 of 39	0.7	0.0318
dme04214	Apoptosis - fly	8 of 62	0.62	0.0191

Figure 3.1 shows the STRING analysis performed on potential common direct targets of Ubx in halteres (Khan et al., 2023) and Yki in third instar wing disc (Oh et al., 2013). The panel below displays the enriched KEGG pathways, which are colour-coded to correspond with the network above.

3.2.2 Screening for growth regulatory genes in the wing and haltere imaginal discs

Overexpression of Yki in the wing and haltere imaginal discs is known to cause hyperplasia, mainly due to the increase in the cell number. We also observed an increase in the third instar haltere disc size upon moderately elevated Yki. The tissue was overgrown with no signs of apicobasal polarity disruption, consistent with previous studies with Yki overexpressing wing discs (Groth et al., 2020).

A previous genome-wide screen in our lab identified around 904 genes, which, when downregulated in the background of moderately-elevated levels of Yki, gives overgrown wing discs showing their potential growth suppressor activities (Groth et al., 2020). This growth was neoplastic, and the balance between cell size and shape was disrupted. The expression of Yki in these lines was controlled spatially using the *apterous* GAL4 to drive the expression only in the dorsal compartment and temporally by using the temperature-sensitive Gal80 driver. We re-screened a subset of these previously identified "Yki positive" genes (those that are also potential direct targets of Ubx) using the same crossing scheme to identify genes that are important for the size and the globular shape of the halteres. The details of the crosses and mating schemes are described in (Groth et al., 2020) and in the methods section (Fig 3.2).

When excessive overgrowth is triggered in imaginal discs of *Drosophila*, they fail to undergo puparium formation. As a result, the larval phase in their life cycle gets prolonged by several days, leading to the 'Giant larvae' phenotype and prepupal lethality. All the tested lines in this screen showed a giant larval phenotype and did not proceed to the pupal stages. The wing and haltere imaginal discs are visible with an appropriate microscope in intact larvae due to the presence of UAS GFP with the GAL4 driver, and this has been used as a way of primary selection (Fig 3.3 A). These larvae were then dissected to visualise the respective wing and haltere disc sizes and morphology. Initially, we used the overall area and the length of the haltere disc (AP axis) as a crude way to gauge the growth in the wing and haltere discs compared to the controls (Fig. 3.3 B, C). However, the overgrown discs, particularly the wing discs, were highly folded, rendering the measurements of disc area less reliable and time consuming for a qualitative large screen. We observed that the wing disc has overgrown approximately 167% upon Yki expression compared to the GAL4 control wing, while halteres have only shown an ~135% increase in growth upon Yki expression. However, upon

pushing the system further to induce growth, as in the case of UAS *Yki; Pten* ^{RNAi} larvae, halteres show a dramatic overgrowth of around 323% compared to the controls, while wings show a 298% increase.

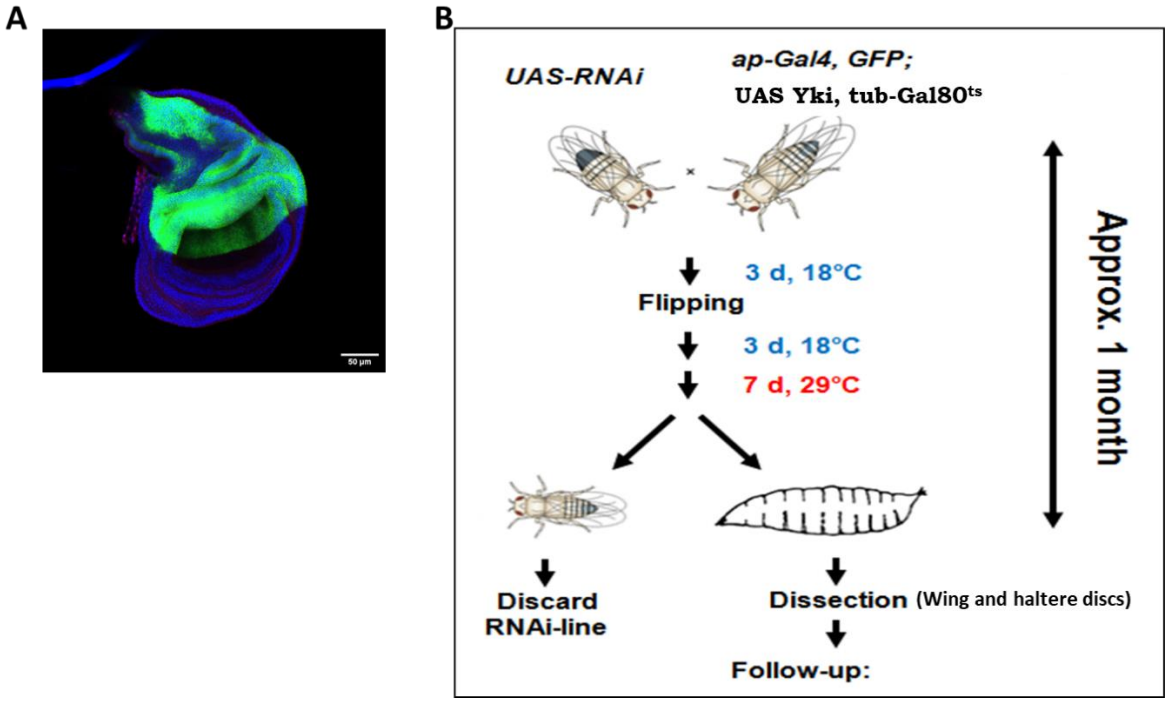

Figure 3.2 A. Wing disc expressing UAS GFP in the dorsal compartment under the control of *apterous*-GAL4 driver, blue is nuclei stained with DAPI. B. Schematic representing the screen workflow, adapted from (Groth et al., 2020), the wing and haltere discs were further assessed for their morphology after dissection.

113 out of 131 RNAi lines consistently showed an overgrowth in both wing and haltere discs. Among the remaining 18 lines, *glutamate synthase (NADH), Lachesin (Lac), SOD,* and *dMLF* did not induce significant overgrowth in the haltere discs (Fig 3.3C). The size of the haltere discs was comparable to Yki halteres and were considered "screen negatives"; others were inconsistent in giving the phenotypes and hence were not considered. The screen positives include Pten (also used as a positive control during the screen), hippo, expanded and novel growth regulators such as Atrophin/Grunge, hale, and fred. Some of these genes were

tested to see whether they were capable of inducing growth without cooperating with Yki. We found that depletion of these genes alone (including *Pten*, *ex* and *Atro*) did not produce massive overgrowth (Fig 3.3 A, B).

However, their effect on the adult haltere morphology could not be studied, as these gene combinations (driven with *ap* GAL4) were lethal and did not advance to pupal stages.

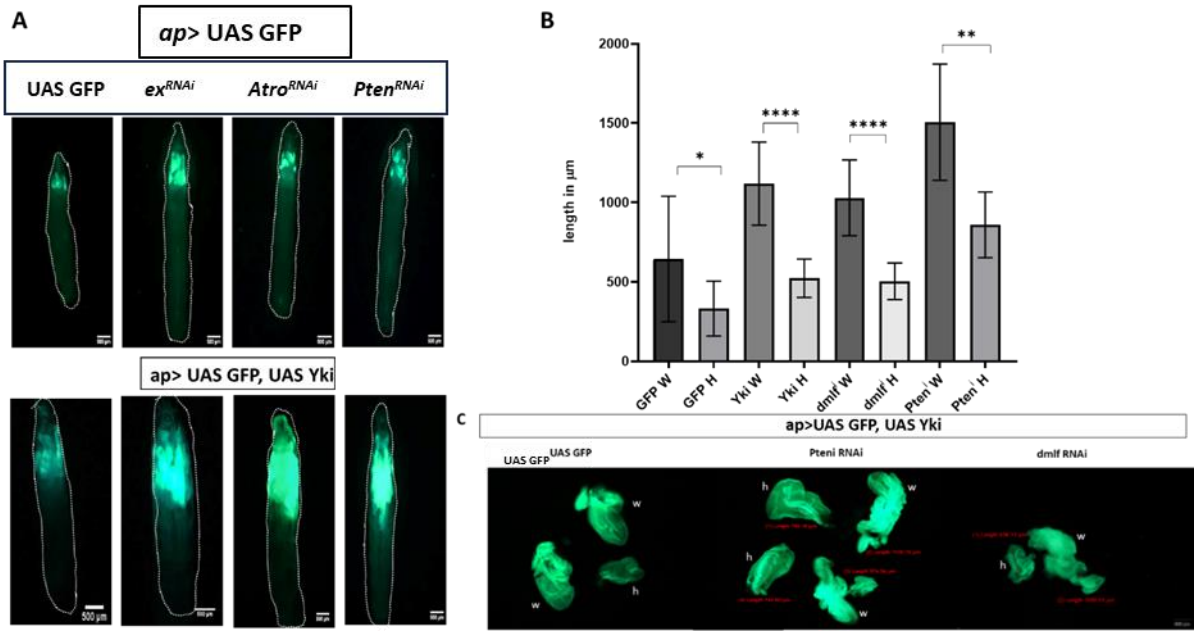

Figure 3.3 A. Wing and haltere disc overgrowth visualised in intact larvae co-expressing UAS-GFP with the indicated transgenes to permit visualisation of the imaginal under the GFP fluorescence microscope. The top panel shows growth in the larvae with the indicated genotype without cooperation with the Yki. The bottom panel shows the larvae with (left to right) Yki expression alone, Yki expression combined with *Ex* ^{RNAi}, *Atro* ^{RNAi} and *Pten* ^{RNAi} (the positive control). B. Quantification of the length of the wing and haltere discs in microns. Note that dmlf is a screen negative and has a length comparable to Yki expressing halteres, and their size difference is not significant (see panel C). n≥24 discs. C. Image showing w-wing and h-haltere discs with respective genotypes expressing GPF. Scale bar, 200 µm.

3.2.3 Secondary screening for genes shaping adult haltere growth and morphology

To see the effect of the aforementioned genes responsible for haltere disc overgrowth on the subsequent development of adult halteres and their morphology, we conducted a secondary screening. In this phase, we employed haltere pouch-specific *Ubx* GAL4 driver within a UAS Yki-sensitised background. *Ubx*-GAL4 is also a null allele of Ubx and is expressed in the anterior compartment of halteres. As expected, Yki upregulation on its own did not yield any notable growth or morphology defects. We subjected the genes identified from the previous section, other overlapping genes between our transcriptome analysis of Yki wing and haltere (refer to Annexure for more details), and Ubx and Yki ChIP to assess their influence on the haltere size and shape.

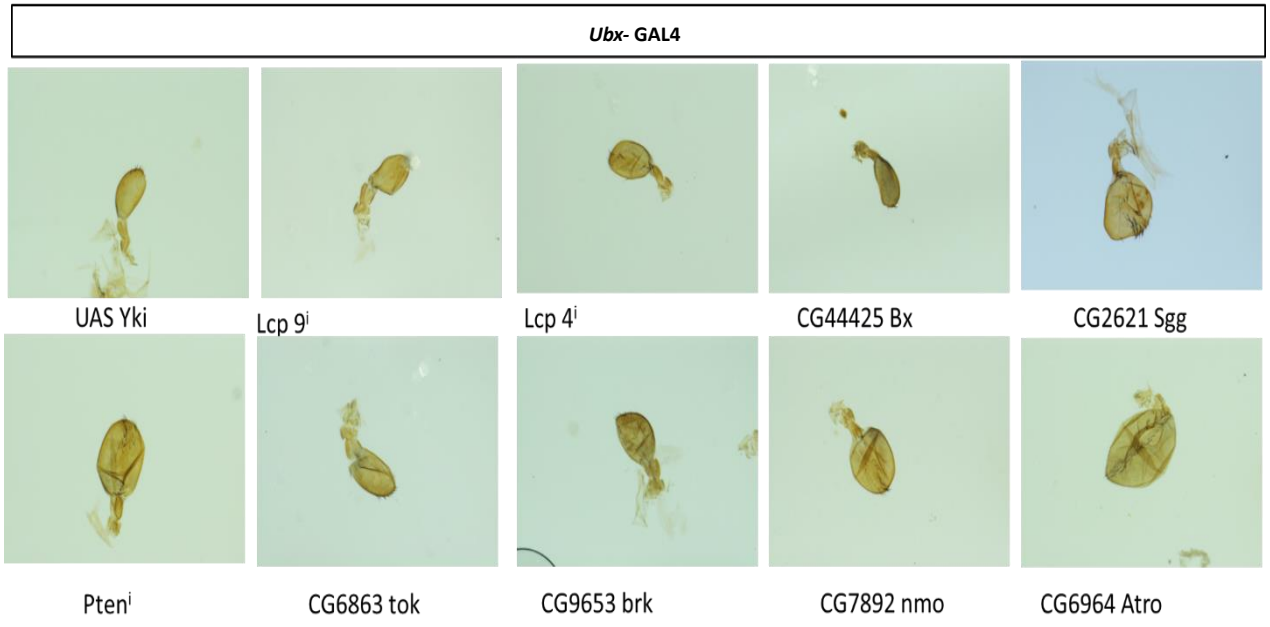

Figure 3.4 Panel shows some genes screened for haltere growth and shape. The UAS *RNAi* lines were driven using the *Ubx*-GAL4 driver in the presence of UAS *Yki*.

The screen was targeted to identify genes or a combination of genes, capable of haltere to wing homeotic transformations at the level of organ size, shape, trichome arrangement and marginal bristles. A few genes, when downregulated in the background of elevated Yki levels

resulted in a general increase in the capitellum size (see Fig 3.4). However, despite this enlargement, the overall shape of the haltere remained globular. Particularly notable were the genes *Atrophin* (or Grunge), *Expanded*, and *Pten*, which induced more intense growth cooperating with Yki. Their capitellum size was significantly larger, and they also had wing marginal hairs (Fig 3.4). The size of the capitellum was used as a measure of growth in the haltere. In the absence of UAS *Yki*, the downregulation of these genes alone gave rise to smaller halteres compared to that with *Yki* upregulation (see Fig 3.5). In the case of *Atro* downregulation alone, halteres showed thick bristles along the DV margin (Fig 3.5).

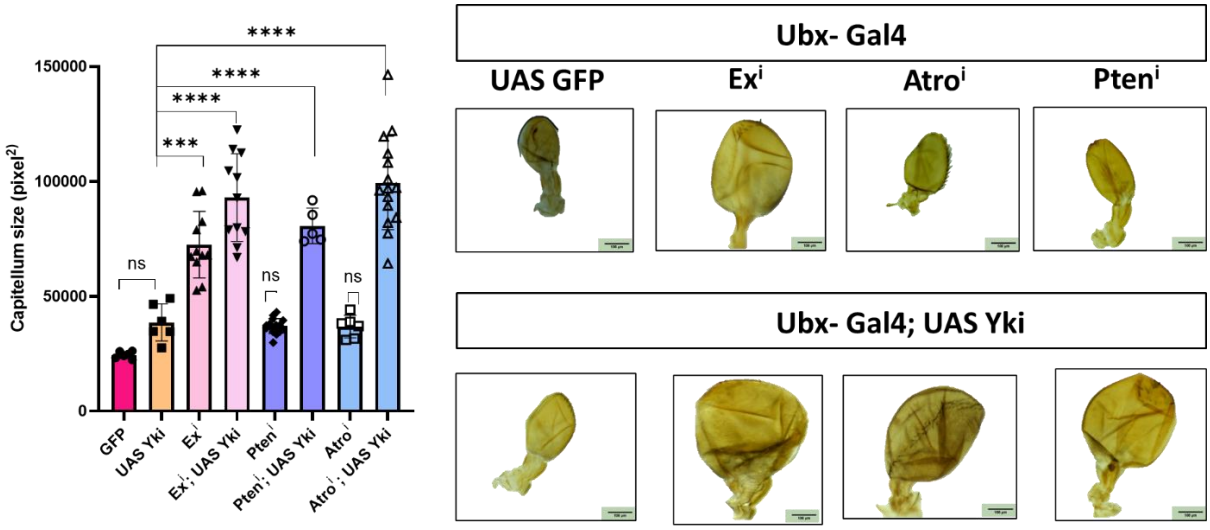

Figure 3.5 (Left)- Graph shows the quantification of haltere capitellum size across the different mutant combinations- with or without cooperating with Yki, mean, SD and individual values are plotted, n≥6. (Right)- Overgrown halteres with the indicated RNAi (top) and in a Yki overexpressing background (bottom), Scale bar, 100 μm. Note that except for expanded, there was no significant growth was seen in the halteres when the respective *RNAi*s were alone.

A previous report suggests that the downregulation of Expanded (Ex) induced more pronounced growth compared to over-expressing Yki (Singh et al., 2015), which we confirmed again. We then examined the effect of downregulating *Atrophin* and *ex* or *Pten* and *ex*. $Atro^{RNAi}$; ex^{RNAi} and $Pten^{RNAi}$; ex^{RNAi} (referred to as $Atro^{i}$; Ex^{i} and $Pten^{i}$; Ex^{i})

combinations led to a further increase of at least 50% in the adult haltere capitellum size. Moreover, these mutant halteres were significantly larger (at least four folds) compared to the wild type. Interestingly, *Atro*^{i}*; Ex*^{i} halteres showed flatter "wing-like" halteres. In contrast, the halteres of flies with *Pten*^{i}*; Ex*^{i} were notably larger; they retained a distinct fluid-filled and bulbous appearance reminiscent of an enlarged haltere, complete with the presence of wing marginal hairs in both scenarios (Fig 3.6 A, C). For comparison, the flies expressing *Ubx*^{RNAi} under the control of *Ubx*-GAL4 is shown in Fig 3.6. Note the flattened "winglets" in the T3 segment.

3.2.4 Characterisation of the *Atro*^{RNAi}*; ex*^{RNAi} and *Pten*^{RNAi}*; ex*^{RNAi} halteres

The presence of trichomes (hair-like structures) on the surface of both wings and halteres serves as an indicator of the cell size, arrangement and polarity that ultimately contributes to their distinct structures (Singh et al., 2015). While adult wings consist of squamous cells, each containing a single hair or trichome per cell, haltere cells are comparatively smaller, more cuboidal, and possess multiple hairs per cell. Scanning electron micrographs revealed that the arrangement of hairs in the halteres, wherein *Atro*^{RNAi}*; ex*^{RNAi} or *Pten*^{RNAi}*; ex*^{RNAi} were downregulated, was sparser when compared to the control halteres. To further confirm this, we did a quantitative analysis of trichome density by counting the number of trichomes within a defined area at various locations on the wing blade and haltere capitellum. A noticeable decrease of 50% in trichome density was observed in both the mutant combinations (Fig 3.6 D), suggesting partial haltere to wing transformations.

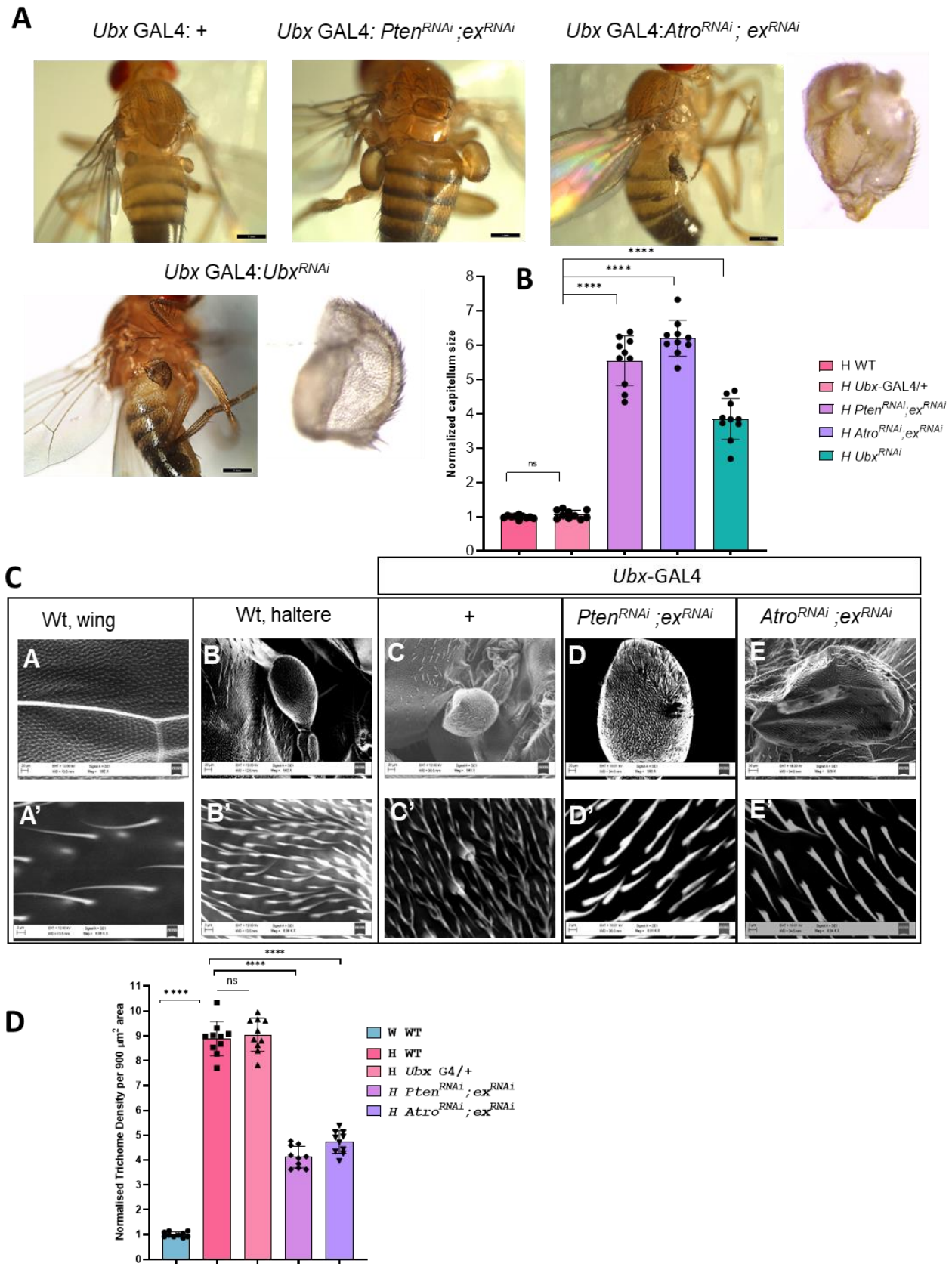
A
Ubx GAL4: +
Ubx GAL4: Pten^RNAi ;ex^RNAi
Ubx GAL4:Atro^RNAi ; ex^RNAi
Ubx GAL4:Ubx^RNAi
B
Normalized capitellum size
ns
****
H WT
H Ubx-GAL4/+
H Pten^RNAi;ex^RNAi
H Atro^RNAi;ex^RNAi
H Ubx^RNAi
C
Ubx-GAL4
Wt, wing
Wt, haltere
+
Pten^RNAi ;ex^RNAi
Atro^RNAi ;ex^RNAi
A
A'
B
B'
C
C'
D
D'
E
E'
D
Normalised Trichome Density per 900 µm² area
W WT
H WT
H Ubx G4/+
H Pten^RNAi;ex^RNAi
H Atro^RNAi;ex^RNAi

Figure 3.6 A. flies with overgrown halteres. B. quantification of adult haltere capitellum size normalised with the wild-type haltere, n≥10. C. Scanning electron microscope (SEM) images of halteres with the indicated genotypes, except A&A', is a representative wing. The top panel shows the overall size and morphology of the organs. A higher magnification of representative area is shown in the bottom panel to visualise the trichome density and arrangement. Please note that the $Atro^{RNAi}$; ex^{RNAi} halteres are larger and flatter. D. Quantification of trichome density in a 30 X 30 micron^2 area. Normalisation was done with the number of trichomes in the wings, n=10. B &D. Average, s.d and individual data points are plotted. Scale bars: 1mm (A), 20 and 2 μm for the upper and lower panels, respectively, for (C).

3.3 Discussion

Ubx is known to regulate various growth regulatory pathways at multiple tiers of its cascade to specify the identity of halteres. Thus, except for alterations in Ubx, halteres are highly resistant to reverting to a wing fate through single-gene mutations. For instance, misexpression of genes that are part of major signalling pathways, such as the Dpp and Wg pathway, only gave a marginal increase in the haltere size, indicating the tight regulation of cell size, cell number and the organ shape (Mohit et al., 2006). This is crucial for the organism as the haltere's knob-like shape and its size are vital for its function in aiding flight.

The Hippo pathway is important for the development of properly sized and shaped organs in metazoans, including the *Drosophila* wing and haltere. The transcriptional co-activator of Hippo pathway, Yki, is known to cause overgrowth by increasing cell proliferation and inhibiting apoptosis. Yki ChIP (Oh et al, 2013) seq data from the wing disc suggest that many critical growth regulators such as wg, Akt, foxo, Insulin receptor (InR), and Egfr are part of the Yki targets. Hence, It is obvious to assume that Ubx would modulate the Hippo pathway and Yki target genes in the halteres. A comparison of Yki and Ubx ChIP targets further strengthens this claim, as they share 438 common targets, including *Atro, Ex, dpp, N, Egfr* and pro wing gene *Vg*, to list a few. Previous studies from our group and others suggest that many components of the Hippo pathway are differentially regulated between the wing and haltere. A small degree of haltere-to-wing transformation at the level of trichomes, organ size and bristles were observed in flies over-expressing or down-regulating some of the positive and negative components of the hippo pathway, respectively. Thus, Ubx may modulate the Hippo pathway during the development of haltere to confer correct organ size and shape, which is also crucial for the function of the organ.

We aimed to identify genes involved in determining the size and globular shape of the halteres downstream of Ubx. We rescreened genes identified as negative regulators of growth in a previous genome-wide screen conducted by our group in a Yki-sensitised background (Groth et al., 2020). The inferences from the Ubx and Yki ChIP seq and the RNA sequencing of Yki expressing halteres generated in this study (see Appendix) were used in part to shortlist the candidates for the two-screens carried out.

We identified gene combinations *Pten RNAi; Ex RNAi*, and $Atro^{RNAi}$*;* ex^{RNAi} to give the largest halteres tested in this study. $Pten^{RNAi}$*;* ex^{RNAi} flies exhibited larger but bulbous halteres with wing marginal hairs and sparser trichome arrangement. Interestingly, approximately 30-40 %

of flies with $Atro^{RNAi}$; ex^{RNAi}, displayed larger, flatter- "wing-like" halteres with marginal bristles and decreased trichome density. The halteres from $Atro^{RNAi}$; ex^{RNAi} animals also showed areas of partial apposition and small blistered phenotypes. The tight zippering between the dorsal and ventral blades in the wings renders its flat geometry. In contrast, the lack of apposition between the D and V layers, ultimately filled by fluid (hemolymph), confers the globular or knob-like shape of the haltere. The reduced trichome density observed in the $Atro^{RNAi}$; ex^{RNAi}, and $Pten^{RNAi}$; ex^{RNAi} halteres may suggest an increase in cell size or a change in trichome arrangement, indicating a homeotic transformation. Hippo pathway regulators such as Yki and Ex are known to regulate growth via increasing cell proliferation, thereby the cell number(Irvine & Harvey, 2015). *Pten* downregulation is known to increase cell growth and cell area (Gao et al., 2000). Hence, these pronounced phenotypes could potentially arise from surpassing both the cell size and number constraints.

Combined with the two screens and the RNA-seq and ChIP seq, we identified putative regulators of growth and organ shape in halteres, whose precise role and mechanism are yet to be uncovered. Thus, Atrophin, Pten and Expanded seem to be good candidates for further analysis (Chapter 4). Given the insights gained from the previous chapter (Chapter 2), it would be interesting to explore their function in regulating cellular properties and three-dimensional tissue structure and decipher the underlying factors driving the formation of these morphologies (Chapter 4). This, in turn, can enhance our comprehension of how the wing and haltere achieve their contrasting flat and globular morphologies.

In our screens, we noticed that when Yki was overexpressed, the growth in haltere discs appeared less proportional compared to wing discs. However, when we pushed the system further by simultaneously downregulating Pten or Atro along with Yki, the halteres exhibited a more significant increase in size relative to their respective control discs. This suggests a potential disruption in the balance between cell size and cell number. It is worth emphasising that organ size is intricately linked to both cell size and cell number, and there exists a feedback mechanism that regulates this balance precisely. While the presence of Ubx confers greater resistance to alterations in haltere size and shape, surpassing the thresholds of cell size and number constraints might partially override Ubx's influence. In contrast, wing discs are free of hox regulations and, thus, may arguably exhibit relatively less resistance to growth alterations under the conditions examined in this study.

CHAPTER 4

Cellular Mechanics and Molecular Signalling in the determination of Wing vs. Haltere Morphology

Cellular mechanics and molecular signalling in the determination of wing vs. haltere morphology

4.1 Introduction

The determination of organ and, cell size and shape involves the integration of various intrinsic and extrinsic factors. It is evident that there is no single universal mechanism governing organ size and shape control. Instead, a multitude of signalling pathways, genes and mechanical cues influence this event. In the previous chapter (Chapter 2), we established differences between actomyosin abundance, cell contractility and the overall cell size and shape of cells between wing and haltere discs at L3. These distinctions indicate differences in the mechanical properties of cells in these two structures. Mechanical forces are integral to the processes that determine the size, shape, and organisation of organs during development. Understanding these forces and their interactions with molecular signalling pathways in sculpting tissues and organs is important.

Recent studies show that morphogenesis and tissue mechanics can conversely feed back into cell-fate decisions and regulate developmental programs. They report that the physical properties and mechanical forces within developing tissues can actively impact the determination of cell fate, with changes in tissue mechanics influencing transcription, cell differentiation and lineage commitment (Chan et al., 2017; Gjorevski & Nelson, 2010; Mammoto et al., 2012; Roffay et al., 2021). The Hippo pathway responds to and communicates the cellular mechanical cues through its upstream regulators and co-activator Yki. Higher cytoskeletal tension promotes Yki's localisation into the nucleus, thereby transcriptional activity and growth. Specific mutations in capping proteins, which resulted in F-actin accumulation, lead to the upregulation of Yki target genes and tissue outgrowth in imaginal discs (Fernandez-Gonzalez et al., 2009; Sansores-Garcia et al., 2011) Components of various signalling pathways appear to be cooperating with Yki in specifying tissue growth and morphology. This is evident from the mutants of the Hippo, Insulin, and EGFR pathways in haltere (Fig 3.6), as they demonstrate their involvement in specifying cell size, trichome morphology and arrangement. In this chapter, we will explore potential alterations in cellular mechanical properties and extracellular matrix (ECM) dynamics, if any, in the mutants identified in Chapter 3.

In order to extend our findings regarding the cell morphology and mechanical properties determining the wing vs. haltere morphology, we studied the cellular properties of Ubx^{RNAi} haltere discs. We observed an increase in cell height, apical contractility and actomyosin abundance, suggesting their role in the overall organ shape and size. We further tested this utilising the targets identified in Chapter 3. We observed that the downregulation of Atrophin (Grunge), Pten, and Expanded enhanced the haltere growth during the screening. The genetic combinations of $Atro^{RNAi}$; ex^{RNAi} (showed organ flattening) *and* $Pten^{RNAi}$; ex^{RNAi} showed partial haltere to wing homeotic transformation in terms of their size, shape and trichome arrangements. In this chapter, we further investigated the role of cell size, shape, actin, myosin and cell junctional tension in attaining these differential organ shapes. We observed significant deviation in the cellular biophysical properties of these mutants compared to the control halteres.

A brief description of Pten, Atrophin and Expanded:

PTEN:

PTEN (Phosphatase and tensin homolog) acts as a tumour suppressor and possesses both lipid and protein phosphatase activities, playing a key role in maintaining cellular homeostasis (Chen et al., 2018). In *Drosophila*, studies have highlighted the significance of PTEN in multiple processes, such as cell proliferation, growth control, and tissue development. It is a negative regulator of the IIS/Akt pathway (Gao et al., 2000; Goberdhan et al., 1999). Loss of PTEN function has been shown to result in increased cell proliferation, cell size and aberrant tissue growth. Pten is also shown to be involved in regulating cytoskeletal and junctional rearrangements. In the pupal epithelium, it was suggested that PTEN-dependent reduction of MyoII contractility in the newly formed junction plays a role in regulating its elongation and stability (Bardet et al., 2013).

Atrophin/Grunge:

The Atrophin/grunge (Atro/Gug) is a transcriptional co-repressor involved in multiple developmental processes, such as cell proliferation, tissue differentiation, and patterning (L. Wang & Tsai, 2008; Yeung et al., 2017). It represses its wide range of targets by recruiting histone deacetylases (L. Wang et al., 2006, 2008). Loss of Atro results in planar polarity, segmentation, and eye, leg, and wing developmental defects in *Drosophila*. Notably, Atro loss of function clones induces cell-autonomous expression of EGFR targets and results in

the formation of extra vein tissues and an increase in bristle density in the wings (Charroux et al., 2006; Erkner et al., 2002). Thus, Atro seems to antagonise the EGFR pathway in the wings. Atro interacts with GAGA factor- Trithorax-like (Trl) and has also been shown to regulate DPP and Notch signaling in larval imaginal discs partly via Thickveins (tkv) and Fringe (Yeung et al., 2017). The precise mode of action of Atro is yet to be uncovered.

Expanded:

The FERM domain-containing protein, Expanded, is one of the upstream components of the Hippo pathway. It promotes the activity of the Hippo pathway and is also known to physically interact with Yorkie (Yki). It adheres to cell subapical junctions and its activity is regulated by Crumbs and Fat (Bennett & Harvey, 2006; Fulford et al., 2019, 2023; Ling et al., 2010; Ribeiro et al., 2014; Silva et al., 2006; Singh et al., 2015; X. Wang et al., 2019). The Ex is also activated as a negative feedback mechanism to the growth-promoting activity of Yki. The loss of expanded causes overgrowth mainly due to the increase in cell number rather than cell size (Singh et al., 2015). In the wing and haltere imaginal discs, loss of expanded gives rise to more prominent phenotypes compared to other Hippo pathway regulators (chapter 3 and Singh et al., 2015). Previous reports show that loss of Ex caused F-actin accumulation, indicating its role in actin dynamics (Fernández et al., 2011).

Note: Atrophin and Expanded are targets of both Ubx and Yki (inferred from ChIP data, Chapter 3).

4.2 Results

4.2.1 Ubx modulates cellular size, shape and contractility in the developing halteres

The presence of Ultrabithorax (Ubx) is crucial in differentially developing haltere from the default wing fate. The loss of Ubx function in developing halteres leads to the complete homeotic transformation of haltere to the wing, along with the duplication of the thorax, resulting in the four-winged fly. The extent of the transformation depends upon the timing of Ubx expression, meaning the early downregulation of Ubx results in the formation of large, flat appendages resembling small wings, while late downregulation produces smaller, globular appendages (De las Heras et al., 2018). However, the impact of Ubx downregulation on cell size and shape at the L3 stage remained unknown.

We have observed inherent differences between the seemingly similar-looking wing and haltere disc cells (Chapter 3). To see the effect of Ubx downregulation on the cellular morphology of the haltere discs, we studied Ubx^{RNAi} flies driven by *Ubx*-GAL4. The adult flies in which Ubx is downregulated had halteres transformed into small flat 'winglets' (Fig 3.6). Ubx^{RNAi} haltere discs were bigger compared to the control discs. These cells were more elongated and apically constricted, resembling the cellular characteristics observed in the wild-type wing disc (Fig 4.1, 4.3, 4.4). They exhibited an increase in Actomyosin accumulation and enhanced cell contractility in the apical region of the disc proper (DP) cells.

Overall, our findings indicate a reversal of the cellular features when Ubx is downregulated, which otherwise are different between the wing and haltere. The observed alterations in cellular morphology suggest that wing and haltere transformations involve cell shape changes brought by changing force mechanics in the individual cells by Ubx, further highlighting the role of Ubx in determining the size, shape, and cellular properties of the haltere. Note: Although *Ubx*-GAL4 is a null allele of *Ubx*, we do not find any significant difference in their cellular size, shape or in actomyosin levels compared to the wild type.

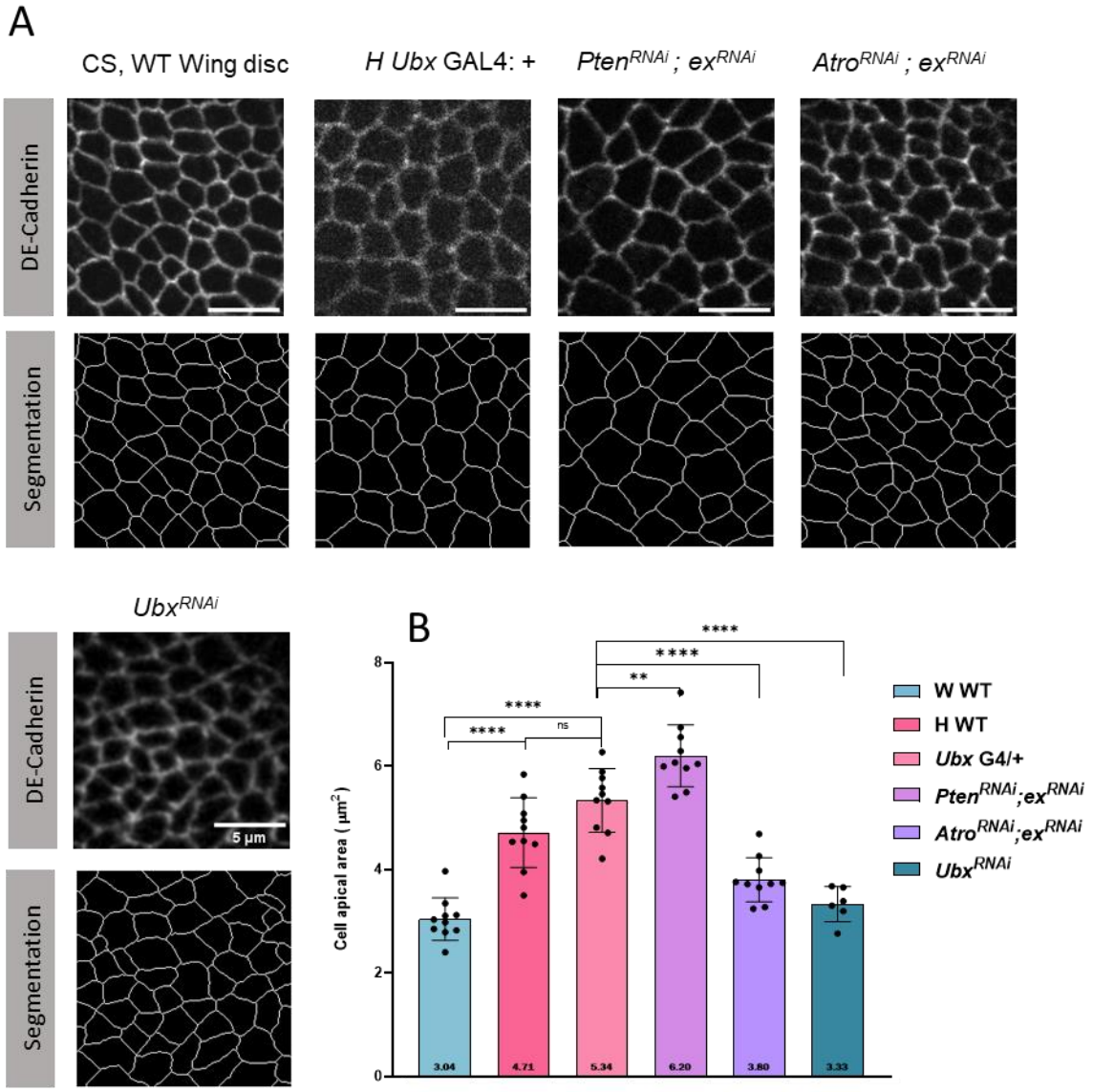

Figure 4.1 A. Wildtype wing (left) and, haltere cells with indicated genotypes expressing DE cadherin to visualise the apical cell membranes. The segmentation panel (below) shows the corresponding cell segmentation achieved. Apical constriction was observed in the *Atro*^{RNAi}; *ex*^{RNAi} and *Ubx*^{RNAi} haltere cells. Scale bar, 5 µm.

B. Quantification of the cell apical area with respect to the control wing and haltere discs. Mean, s.d and individual values are represented, n=10 discs for each genotype except for *Ubx*^{RNAi} (n=6). H denotes haltere.

4.2.2 Atro, Pten and Ex mutant combinations show increased growth, cell apical constriction and changes in cellular morphology of haltere discs

In order to extend our findings and to determine the effect of cell morphology and mechanical properties determining the wing vs. haltere shape, we studied the haltere disc cells of induced mutants, which gave partial homeotic transformations (from Chapter 3). We had identified Atrophin (Grunge), Pten, and Expanded as enhancers of haltere growth during the screening process. Bringing Expanded together with Atrophin and Pten enhanced their respective phenotypes (Chapter 3 Fig 3.6).

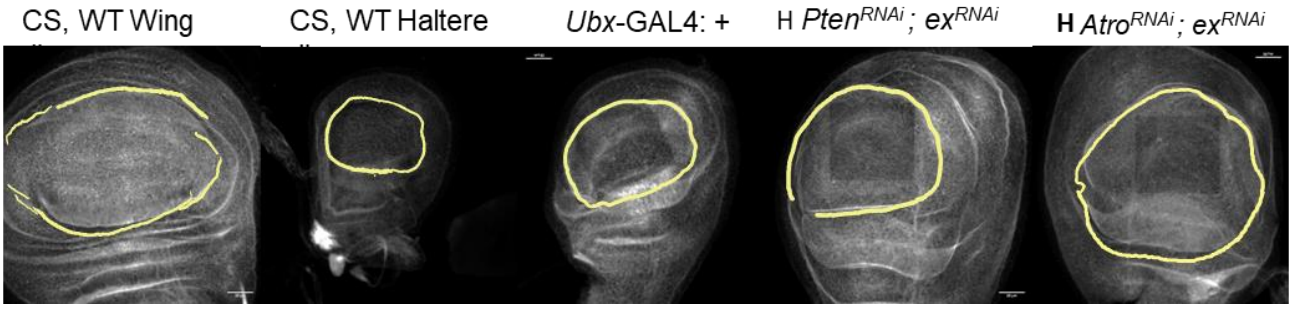

Figure 4.2 The third instar larval wing and haltere discs in indicated genotypes showing their respective sizes. *Atro*^{RNAi}*; ex*^{RNAi} and *Pten*^{RNAi}*; ex*^{RNAi} haltere imaginal discs were significantly bigger compared to the control haltere disc.Thw yellow lines marks the pouch area Scale bar, 25 μm (images were rotated for better comparison).

Cell size:

The *Atro*^{RNAi}*; ex*^{RNAi} and *Pten*^{RNAi}*; ex*^{RNAi} (with *Ubx*-GAL4 driver) haltere imaginal discs were significantly larger compared to the control haltere discs (Fig 4.2). Hippo pathway regulators such as Yki and Ex (lof) are known to regulate growth via increasing cell proliferation, thereby increasing the cell number. Loss of Pten is known to increase cell growth and cell area (De las Heras et al., 2018). The role of Atrophin in determining organ growth or regulating cell size is not clear. In order to understand the effect of *Atro*^{RNAi}*; ex*^{RNAi} and *Pten*^{RNAi}*; ex*^{RNAi} on cell morphologies, we measured their cellular apical area and lateral

height. The discs were stained with an anti-Rat DE cadherin antibody to visualise cell apical boundaries. Interestingly, while the cells of the $Atro^{RNAi}$; ex^{RNAi}, showed a decrease in the cell apical area compared to the control haltere disc, $Pten^{RNAi}$; ex^{RNAi} showed an increase in the apical cell surface area (Fig 4.1).

Cell height:

Next, we measured the lateral cell height of the DP cells in these mutant halteres. The cells were stained with phalloidin. We observed an increase in cell height in both the $Atro^{RNAi}$; ex^{RNAi} and $Pten^{RNAi}$; ex^{RNAi} mutants (Fig 4.3 A, B). The cells were significantly elongated compared to the control haltere and were comparable to the wild-type wing disc. Some $Pten^{RNAi}$; ex^{RNAi} halteres went up to approximately 55 microns in length, much higher than what we normally observe for wild-type wing discs. Taken together, our data suggests that the Atro, Pten and Ex modulate organ growth by regulating the cell size and height and, thus, the overall three-dimensional morphology of the epithelium.

Apical Actomyosin:

To see whether the aforementioned cell shape changes are accompanied by alterations in the actomyosin cytoskeleton, we investigated the actin and myosin levels at the apical cell junctions in the two mutants. Notably, we found that both F-actin and Myosin II (Sqh) were enriched at the apical surfaces of the mutant haltere discs compared to the wildtype haltere discs at L3 (Fig 4.3 A, C, D, E).

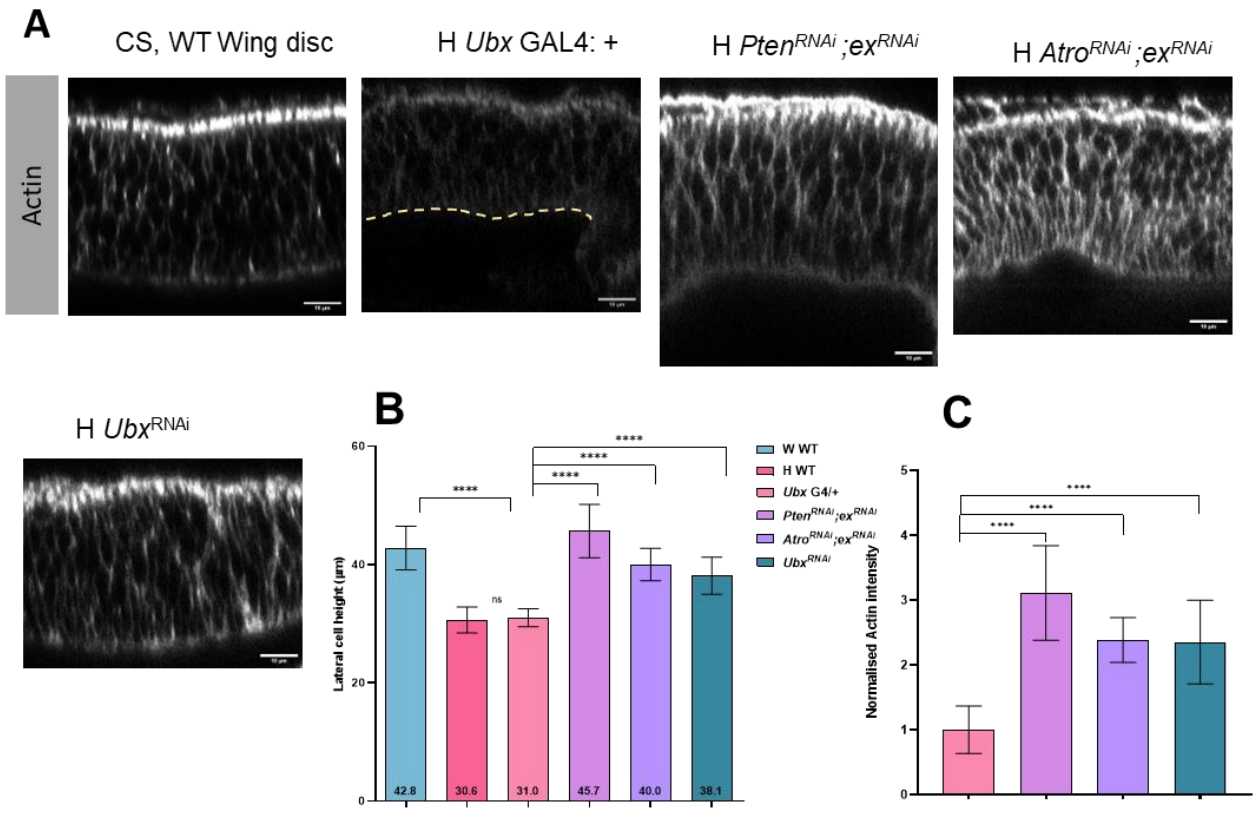
A
CS, WT Wing disc
H Ubx GAL4: +
H Pten^{RNAi};ex^{RNAi}
H Atro^{RNAi};ex^{RNAi}
Actin
H Ubx^{RNAi}
B
C
W WT
H WT
Ubx G4/+
Pten^{RNAi};ex^{RNAi}
Atro^{RNAi};ex^{RNAi}
Ubx^{RNAi}
Lateral cell height (µm)
Normalised Actin intensity
42.8
30.6
31.0
45.7
40.0
38.1
ns
****

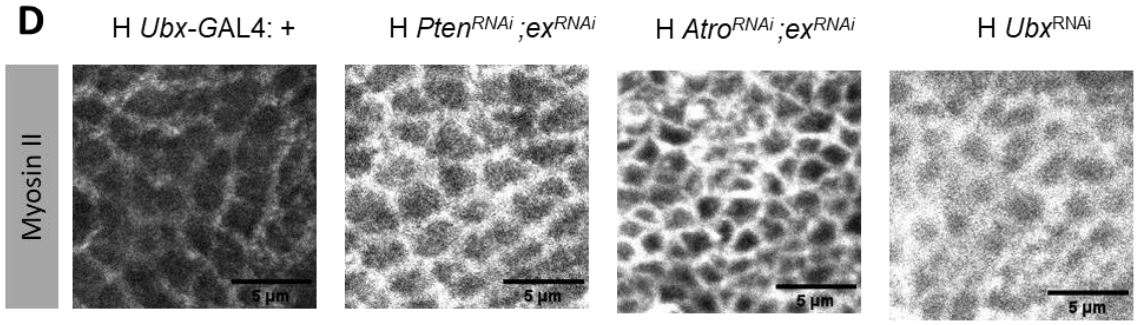
D
H Ubx-GAL4: +
H Pten^{RNAi};ex^{RNAi}
H Atro^{RNAi};ex^{RNAi}
H Ubx^{RNAi}
Myosin II
5 µm

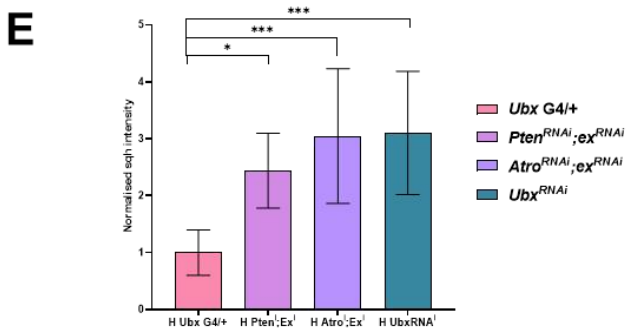
E
Normalised sqh intensity
Ubx G4/+
Pten^{RNAi};ex^{RNAi}
Atro^{RNAi};ex^{RNAi}
Ubx^{RNAi}
H Ubx G4/+
H Pten;Ex
H Atro;Ex
H UbxRNA
***
*

Figure 4.3 Increased cell height and apical actomyosin accumulation in *Atro^{RNAi}; ex^{RNAi}* *Atro^{RNAi}; ex^{RNAi}*, *Pten^{RNAi}; ex^{RNAi}* and *Ubx^{RNAi}* haltere discs. A. Cross-section of wildtype wing and haltere discs of indicated genotypes stained with actin showing the respective cell height (pouch).Yellow dotted line in the *Ubx*-GAL4 control indicate the basal boundary of the cross-section. Scale bar, 10 μm, H-indicates haltere discs B. Quantification of the lateral cell height, n≥7 discs, mean value is shown in the bottom of the bars, mean and s.d are plotted, one-way ANOVA. C. Quantification of mean apical Actin fluorescence intensity, normalised with control halteres, n≥7. D. Sum of slices-apical intensity projection of haltere disc DP cells stained for anti-squash myosin at L3. Scale bar, 5 μm. E Quantification of mean apical sqh-myosin II fluorescence intensity, normalised with control haltere. Mean and s.d plotted, n=8,6,7,10 respectively. One-way ANOVA.

Laser ablation

The alterations in cell morphology and the heightened accumulation of actomyosin at the apical belt potentially signify changes in cellular and tissue tension in the mutants (Heer & Martin, 2017; Murrell et al., 2015). To explore this possibility, we employed laser ablation to measure apical cell contractility in DP cells (Farhadifar et al., 2007). Our findings indicate that the mutant haltere discs exhibit higher mean displacement and recoil velocity compared to the control, suggesting an increased tension at the apical belt of columnar cells (Fig 4.4). These results suggest that the *Atro^{RNAi}; ex^{RNAi}* and *Pten^{RNAi}; ex^{RNAi}* halteres undergo homeotic transformations at the cellular level during the L3 stage, albeit to varying extends. The cells exhibit greater elongation, increased actomyosin levels, and heightened cell junctional tension. While *Atro^{RNAi}; ex^{RNAi}* cells showed higher apical constriction, *Pten^{RNAi}; ex^{RNAi} cells* lacked such apical constriction as they had slightly increased apical area compared to the control halteres.

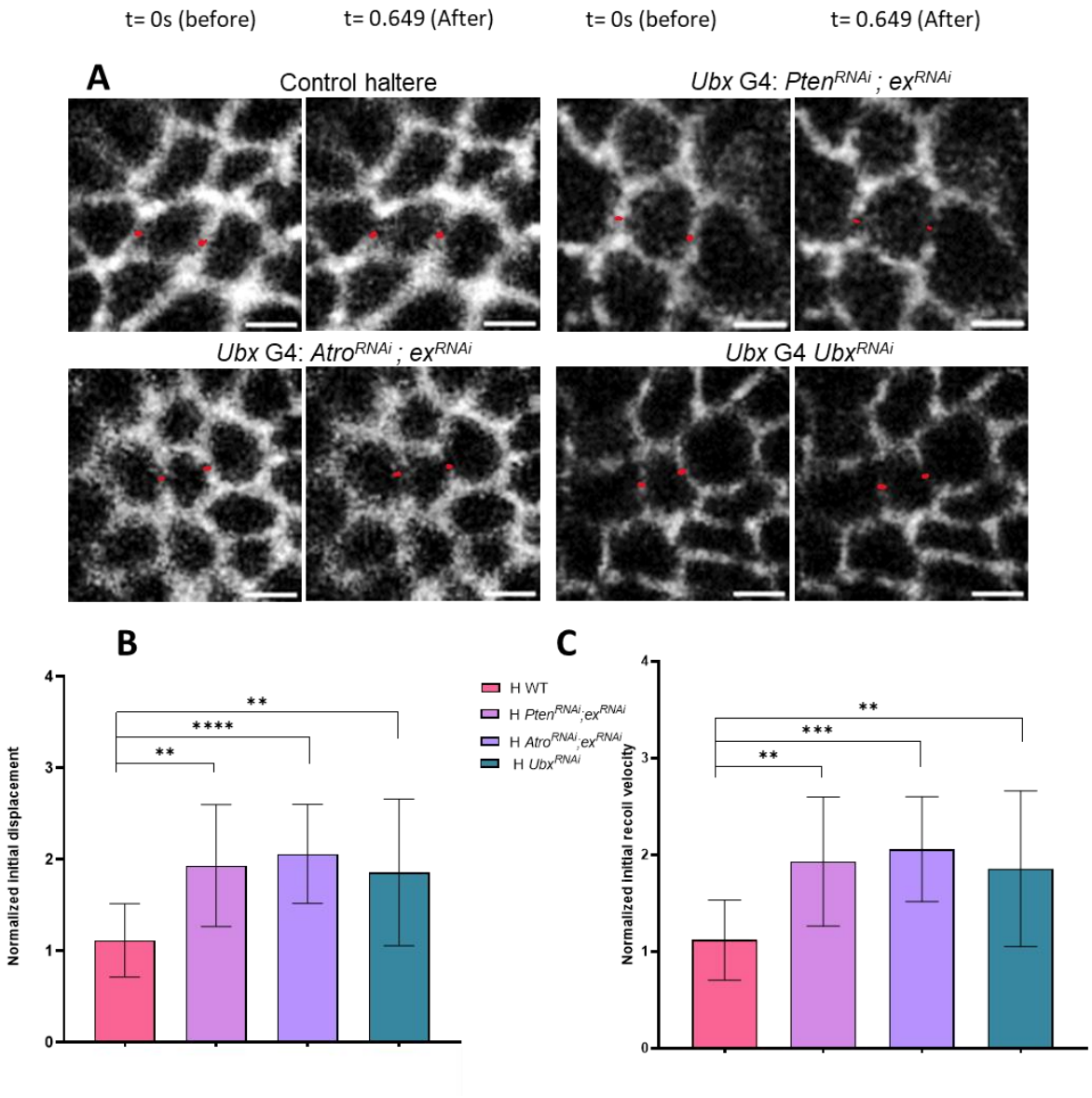

Figure 4.4 Increased bond tension at apical cell junctions in *Atro*^{RNAi}*; ex*^{RNAi}, *Pten*^{RNAi}*; ex*^{RNAi} and *Ubx*^{RNAi} haltere discs. Haltere disc cells expressing endo E cadherin GFP before (t=0s) and after (t= 0.649s) the laser cut is shown. The red spots indicate the site of ablation. Scale bar, 2 μm. B, C Quantification of initial displacement (B) and initial recoil velocities (C) normalised with control haltere disc after 0.649 s of ablation. n= 17,18,20,19 cuts, one-way ANOVA.

4.2.3 De-repression of Wg expression in mutant halteres

Ubx is known to regulate the wingless signalling in haltere, where Wg is expressed only in the anterior (A) compartment of the haltere disc. However, in the wing disc, Wg is expressed in both the anterior and posterior (P) compartments. Upon staining with the wg antibody, we observed an extended wingless (wg) signalling in the posterior compartment (P) of the mutant halteres (Fig 4.5 A). At this point, it remains somewhat unclear whether the observed expression of Wg is a consequence of extended growth in the anterior compartment, considering that the posterior compartment is notably diminutive to begin with and, also, as *Ubx*-GAL4 is predominantly expressed in the A compartment. However, the staining with engrailed (expressed in the P compartment) suggests that, indeed, there might be a de-repression of Wg expression in the P compartment of $Atro^{RNAi}$; ex^{RNAi} and $Pten^{RNAi}$; ex^{RNAi} halteres (Fig 4.5 A, B). We were unable to perform co-staining for Wg and En, as both of their antibodies were raised in mice.

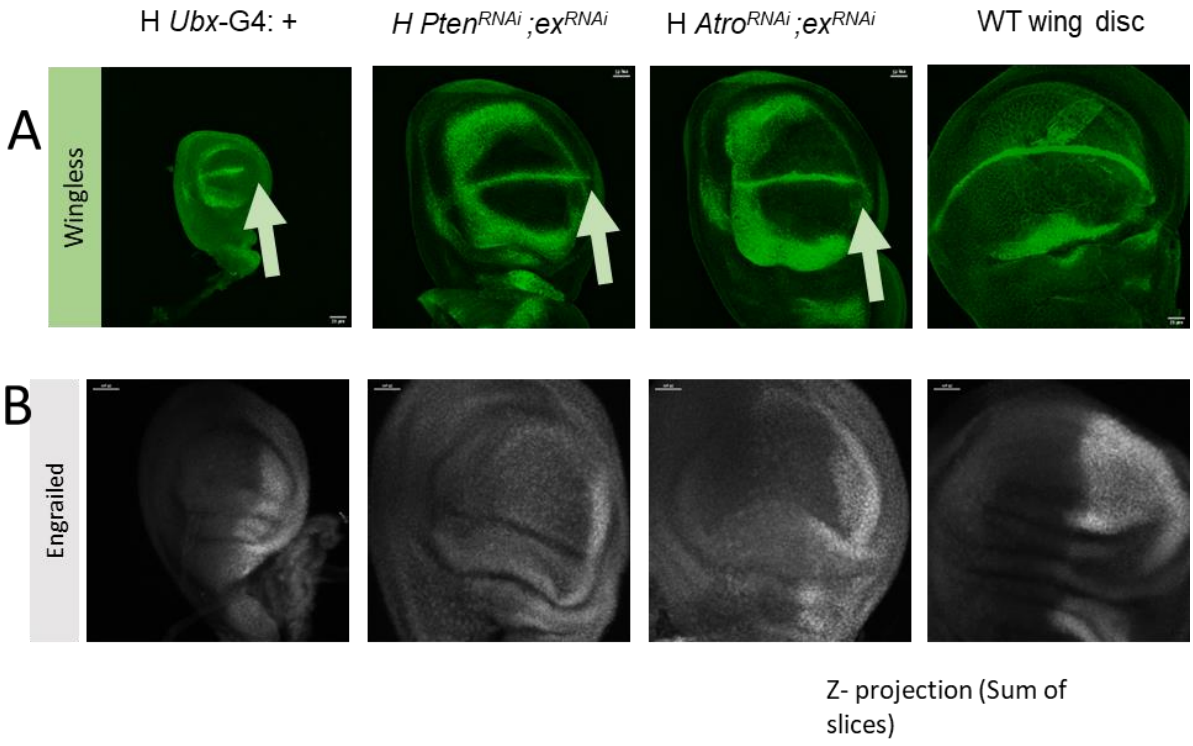

Figure 4.5 Extended wingless expression in $Atro^{RNAi}$; ex^{RNAi} and $Pten^{RNAi}$; ex^{RNAi} halteres discs. A. wing (right most) and haltere discs with the respective genotypes showing Wg expression (Green) in the P compartment (arrows). B. The imaginal discs expressing engrailed in the P compartment. Z-projection images are represented, scale bar, 25 μm.

4.2.4 Atrophin, Expanded, and Pten regulate haltere size and shapes downstream of Ubx.

To investigate whether the observed phenotypes of *Pten*^{RNAi}*; ex*^{RNAi} and *Atro*^{RNAi}*; ex*^{RNAi} were attributed to a decline in Ubx levels, we stained the discs for Ubx. The anti-N-ter *Ubx* antibody was used to visualise the Ubx protein. We did not detect any noteworthy decrease in Ubx levels in these 'partially transformed haltere discs' (Fig 4.6), indicating that Atrophin, Expanded, and Pten act downstream of Ubx.

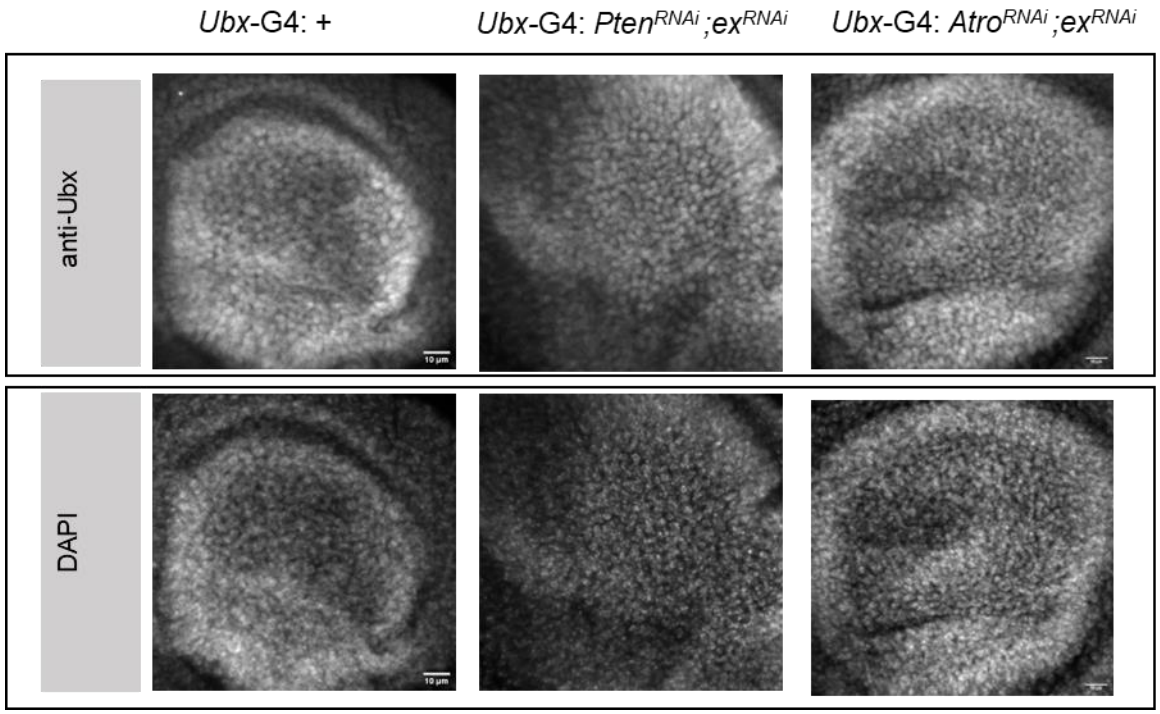

Figure 4.6 Haltere discs stained for Ubx in *Pten*^{RNAi}*; ex*^{RNAi} and *Atro*^{RNAi}*; ex*^{RNAi} mutants. No significant reduction in Ubx expression levels were observed within these haltere discs. DAPI staining was used as an internal control, Scale bar, 10 μm.

4.3 Discussion

Organ growth and shape control is a highly complex process governed by a combination of genetic, cellular, hormonal, environmental and mechanical factors. We are now beginning to explore and integrate these factors towards a better understanding of organogenesis. The development of wing and haltere provides a powerful niche to track events and factors that are involved in cellular and organ growth and shape changes. The wing and halteres start indistinguishably during early development and become progressively different from each other, ultimately forming two different size and shaped organs. This also opens ways for studying force dynamics in two closely related systems capable of forming two different shapes. In light of the differences identified between wing and haltere disc cells in Chapter 3, we aimed to delve deeper into the cellular features of the partial homeotic mutants identified in Chapter 2, in addition to the *Ubx* ^{RNAi}.

We observed a reduction in cellular apical area in *Ubx RNAi* and *Atro*^{RNAi}*; ex*^{RNAi} L3 haltere discs. However, the cells of *Pten RNAi; Ex RNAi*, showed an inverse trend; the cells were slightly larger compared to the control haltere discs. It's worth noting that components of the Hippo pathway, such as Yki and Ex, primarily regulate growth through cell proliferation rather than cell size. Previous research has indicated that the downregulation of Ex leads to increased growth by promoting proliferation without significant changes in cell size. On the other hand, Pten influences growth by modulating cell size (Gao et al., 2000). Interestingly, *Atro*^{RNAi}*; ex*^{RNAi}, *Pten*^{RNAi}*; ex*^{RNAi} and *Ubx*^{RNAi} haltere discs also showed an increase in the lateral cell height, indicating their role in changing the three-dimensional shape of the cells.
Actomyosin contractility is a major player in governing cell and tissue shape; it maintains structural integrity and responds to mechanical cues, all of which are crucial for generating and preserving the intricate shapes of organs in multicellular organisms (Heisenberg & Bellaïche, 2013; Vasquez et al., 2014). Non-muscle Myosin II (motor protein), plays a crucial role by bringing together two actin filaments, which results in the generation of contractile forces (Lecuit et al., 2011). This tension produced by the actin-myosin network has been shown to promote apical constriction during various morphogenetic events. We observed an increase in both F-actin and Myosin II abundance at the cell apical junctions of all the three mutant backgrounds tested in this study, indicating an increased apical contractility. This was further verified by performing laser-mediated cell bond ablation experiments. We observed

that, there is an increased cell junctional tension in the mutant discs compared to the wildtype haltere discs at L3. Changes in cell contractility and tension are reported to not only drive two-dimensional shape deformation; they also impact cell division and proliferation (e.g., via the Hippo pathway), collectively influencing organ size in a three-dimensional context(Liu et al., 2022).

CHAPTER 5

ECM Dynamics, 3D Shape Changes, and DV Zippering: Keys to Morphological Variation

ECM Dynamics, 3D Shape Changes, and DV Zippering: Keys to Morphological Variation

5.1 Introduction

In previous chapters, our focus primarily centered on the apical-intracellular components of the cell. These individual cells interact with their neighbours through cell-cell adhesion, and they are also enveloped apically and basally by apical and basal extracellular matrix (ECM). The basal ECM comprises four main components: collagen IV, laminin, nidogen, and perlecan. Laminin and collagen IV are heterotrimeric proteins that form network (Fibrous) structures (Pastor-Pareja & Xu, 2011). Collagen IV is more abundant in the basement membrane and is conserved across the animal kingdom. In *Drosophila*, collagen IV is encoded by the *viking (vkg)* and *Collagen at 25C (Cg25C)* genes. At the third instar larval stage, the basal ECM can be observed at the base of peripodial membrane (PM) cells and the base of disc proper (DP) cells (Le Parco et al., 1986; Natzle et al., 1982; Yasothornsrikul et al., 1997). The ZP-domain containing protein Dumpy is a relatively well-characterized apical ECM component in the *Drosophila* wing disc. This large extracellular protein plays a role in mediating the connection between the epidermis and the cuticle. When dysregulated, it results in wider wings with a notch at the end.

The extracellular matrix (ECM) is a highly dynamic structure that undergoes constant remodelling, involving processes such as deposition, degradation, and modification of ECM components. These ECM dynamics are essential for reshaping tissue architecture; for instance, gain- or loss-of-function alleles of *MMP*s or *Timp*s in mice result in defects in branched organs, indicating that ECM dynamics play a role in epithelial branching morphogenesis (Page-McCaw et al., 2007).

During *Drosophila* wing morphogenesis, apical and basal ECM degradation seems to be an important step in flattening the individual cells and tissue of the wing discs at pupal stages. However, the complete picture of the *Drosophila* appendage morphogenesis is still an enigma. During the development of wing discs, it undergoes two rounds of apposition, i.e. there is an apposition at 6-9hr APF, and after that, the tissue separates and reapposes again in the wing disc intervein regions (Fristrom et al., 1993; Fristrom & Fristrom, 1975;

Waddington, 1939). It is still unclear of the developmental purpose and significance of this. Haltere discs must resist these appositions to maintain the globular shape.

Integrins on the surface of wing epithelial cells are known to bind to laminins in the basal membrane, facilitating the attachment of these two tissue layers (Sun et al., 2021). This interaction could also play a critical role in dorsoventral apposition and the structural integrity of the wing.

In this chapter, we re-investigate the ECM dynamics and three-dimensional structural changes between the wing and haltere discs during the early pupal stages. Subsequently, we draw comparisons between these findings and the two mutant combinations identified in the previous chapter.

5.2 Results

5.2.1 Ubx prevents extracellular matrix degradation in halteres at early pupal stages

Until the late third instar larval stages, both the dorsal (D) and ventral (V) cell layers in the wing and haltere discs lie in the same plane. Towards the end of late L3, these discs start to undergo eversion, resulting in the formation of a bilayer of columnar dorsal-ventral (DV) cells, where the D and V layer cells face each other basally, with a lumen inside.

Previous studies have reported that by 7-9h APF, the apical and basal ECM remodelling is complete, the cells transform from columnar to cuboidal shape, and there is an overall cell and tissue expansion in the presumptive wing "blade". The tight zippering between the basal layers of DV cells leads to the apposition and, subsequently, a flat wing (De las Heras et al., 2018; Diaz-de-la-Loza et al., 2020; Fristrom et al., 1993, 1994). In contrast, halteres do not undergo ECM remodelling during this process, and their cells remain columnar. There is no zippering observed between the DV layers of haltere cells. Ubx represses the expression of matrix metalloproteinases (MMPs) and other proteases like Np and Sb in the halteres (targets of Ubx ChIP, Chapter 3).

In line with these studies, we also observed a clear retention of bECM in the haltere discs compared to the wing discs at 4-6hAPF (Fig 4.7 A, B, C). This was visualised using actin, to see the overall tissue architecture and Viking (Vkg) GFP, a major component of the basal membrane (Collagen IV α2-subunit), to visualise the bECM. Note that the wing disc cells are zippered with very little lumen filled with ECM (cyan).

5.2.2 Wing and haltere disc undergo differential three-dimensional tissue deformation at 4-6 h APF

The wing and haltere disc shapes are very dynamic during the initial stages of pupal development. The eversion creates complex morphologies that are challenging to understand in 3D because of the limited knowledge of the system. However, we observed that the haltere disc epithelia exhibit a more circular two-dimensional shape, while the wing disc epithelia appear to be more elliptical in cross-sections (Fig 5. A, B).

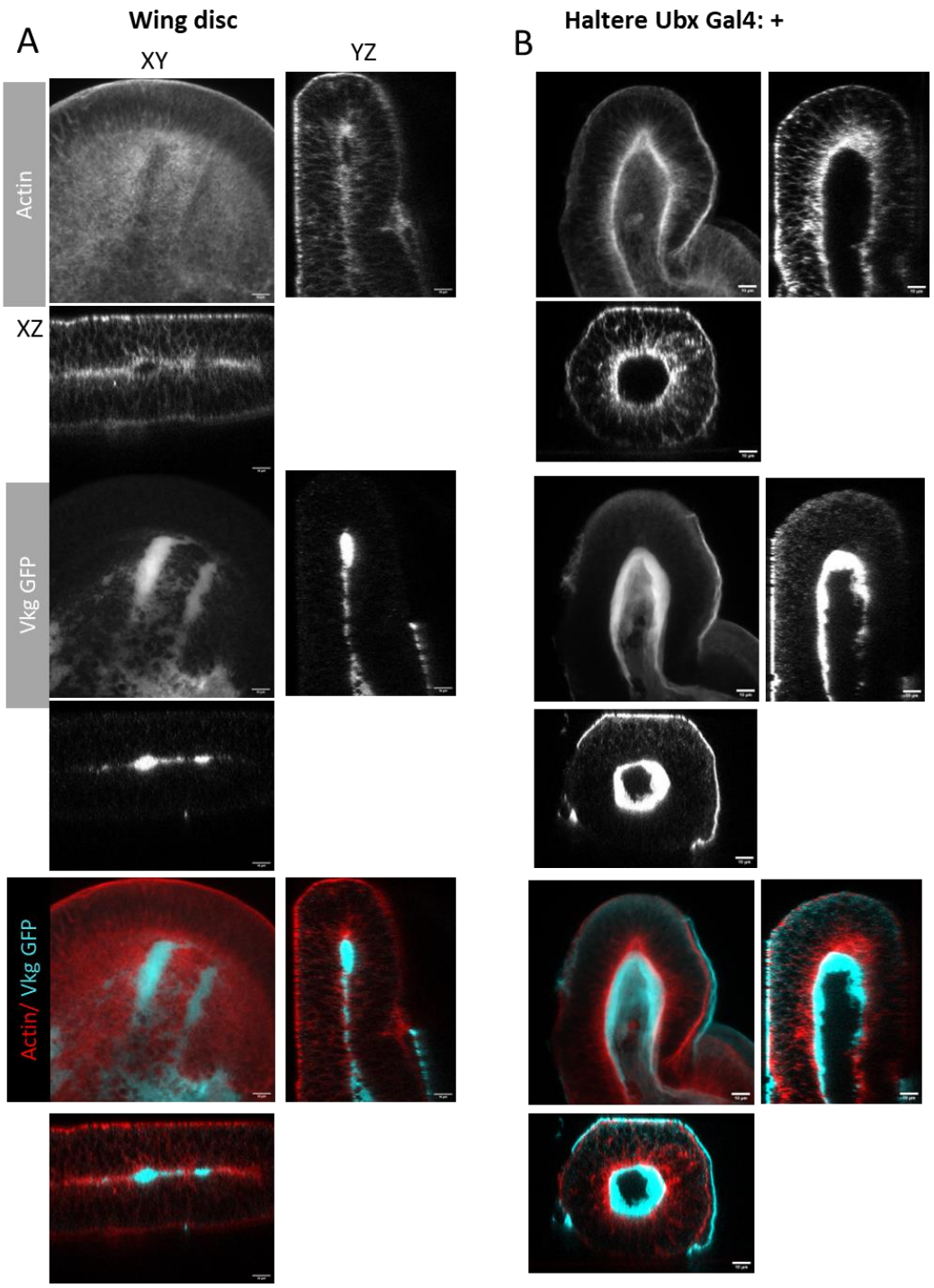

Figure 5.1 Differential Basal ECM remodelling and tissue flattening between wing and haltere discs (4-6h APF). A. Wing disc and B. haltere discs showing basal ECM visualised through Vkg GFP (cyan) and Actin cytoskeleton (red). Individual channels are shown in greyscale, with their respective cross-sections. The haltere discs display a substantial lumen lined with Vkg. Notably, there are noticeable differences in the 3D shapes of the two discs. Scale bar, 10 μm.

5.2.3 Atrophin and Expanded double knockdown induce DV apposition and ECM remodelling

In the previous chapter (Chapter 3), we observed that *Atro^{RNAi}; ex^{RNAi}* halteres were larger and flattened with partial apposition of the D and V layer (Fig 3.6, 5.2 E). This might indicate alterations in the basal ECM remodelling- as, clearing ECM in halteres, either by using mutants of Ubx or inducing the expression of MMPs, resulted in the flattening of the organ. Interestingly, it was also noted that the remodelling of bECM is more critical compared to the aECM for the DV apposition and organ flattening (Diaz-de-la-Loza et al., 2020). Thus, we hypothesised that the ECM degradation and/or the 3-dimensional architecture in *Atro^{RNAi}; ex^{RNAi}* halteres at early stages of puparium formation might be altered. To investigate this, we generated fly lines expressing Vkg GFP with *Atro^{RNAi}; ex^{RNAi} and Pten RNAi; Ex RNAi.* The respective imaginal discs were stained with the bECM marker- Vkg and Actin. Extreme care was taken to minimise any flattening of the tissue while processing for staining and imaging. The discs were imaged using long coverslips (22x60mm) instead of traditional slides (only one sample at a time-minimises the sample drying), thus avoiding the need for a coverslip on an inverted microscope. Alternatively, proper spacers with appropriate thickness were also used to prevent squishing of the sample; this is crucial to assess the apposition and 3D structure.

Interestingly, at 4-6h APF, we observed that some of the *Atro^{RNAi}; ex^{RNAi}* halteres exhibited areas of basal ECM degradation and apposition, evidenced by the absence of Vkg GFP signal and the lack of a distinct lumen between the DV layers (Fig 4.7 A, B, C). The overall morphology of these tissues was flatter compared to the more circular wildtype haltere tissues at the same stage of development. We also see variations in the overall 3D morphology amongst *Atro^{RNAi}; ex^{RNAi}* individuals (Fig 4.7 D). This could be due to the presence of inherent noise in the system, which may or may not be cleared in the later stages of development and cannot be fully explained at this point.

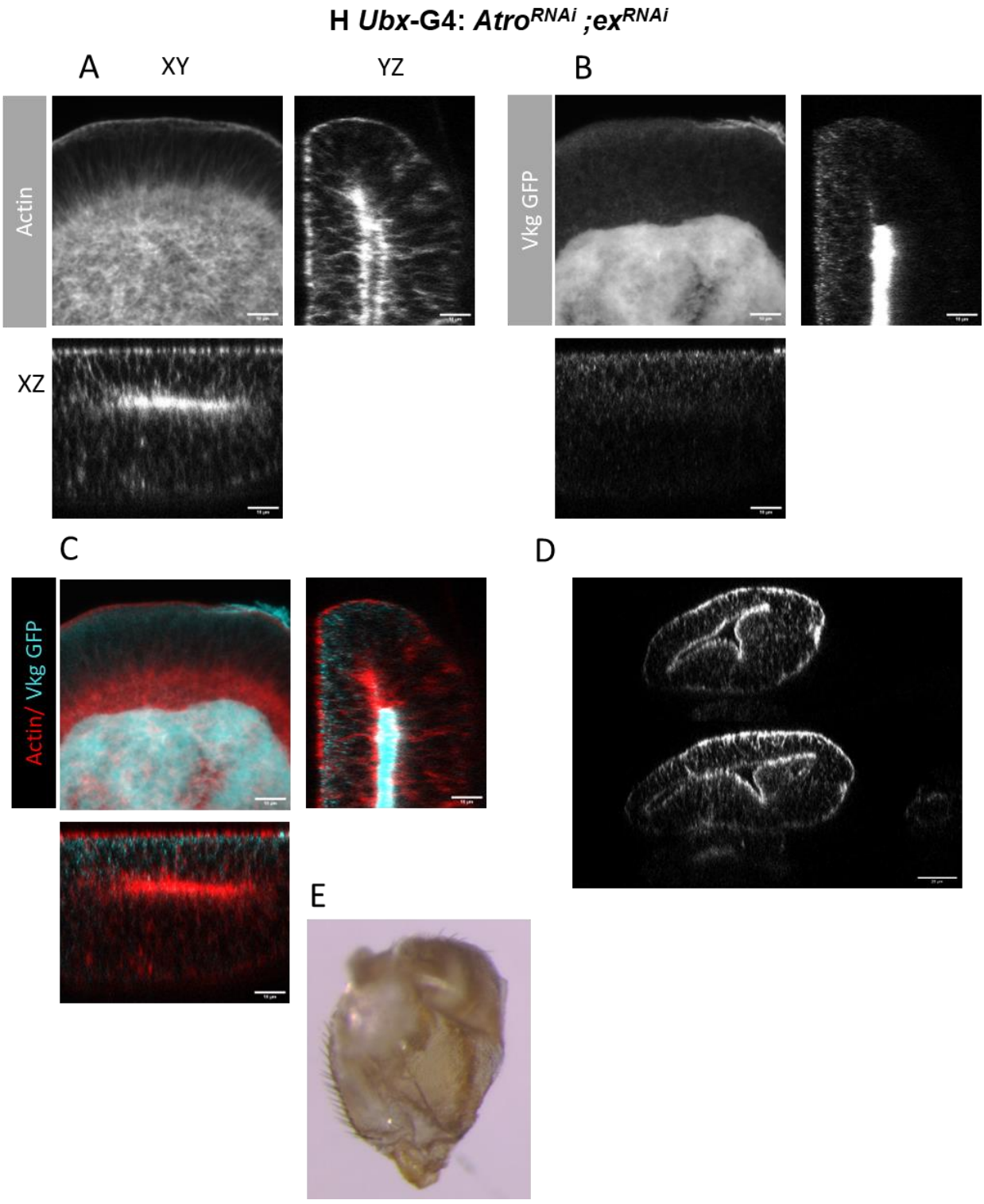

Figure 5.2 Basal ECM remodelling and 3D tissue shape deformations in partially transformed *Atro*^{RNAi}*; ex*^{RNAi} haltere discs at 4-6hAPF.

A, B: Haltere discs stained for F-actin and Vkg GFP, respectively, with a Z-projection of the pouch (a sum of slices spanning the bECM). The corresponding cross-sections are presented

alongside the individual images. Note the pronounced actin accumulation at the basal surface of the cells.

C: Shows the merged images displaying bECM (cyan) and actin cytoskeleton (red). The discs show areas of the absence of ECM signal, and the presence of zippering, evidenced from lack of lumen and ECM.

D: Cross sections of $Atro^{RNAi}$; ex^{RNAi} halteres stained for actin, revealing variations in their 3D architecture. Notice the pronounced actin accumulation at the basal surface and the presence of "apposition" at some areas. Scale bar, 25 μm.

E. Adult $Atro^{RNAi}$; ex^{RNAi} haltere showing partial apposition and "blistered" phenotype. (For size related quantifications, refer to chapter 3, fig 3.6). Scale bar, 10 μm. H denotes haltere.

5.2.4 $Pten^{RNAi}$; ex^{RNAi} haltere discs retain basal ECM

In $Pten^{RNAi}$; ex^{RNAi} flies, the halteres exhibited a bulbous and significantly enlarged appearance. During the third instar larval stage (L3), these halteres displayed elevated actomyosin levels and increased junctional tension. Although there was a marginal increase in cell height compared to wing discs, the apical cell area was also larger (even more than haltere). These cellular characteristics appeared to be intermediate between those of the wing and haltere.

Therefore, in this Chapter, we explored the disc architecture and the bECM dynamics at 4-6hAPF. $Pten^{RNAi}$; ex^{RNAi} discs do not show bECM clearance. The Vkg signal was consistently detected in all sections and across all the tested discs. However, an overall 3D deformation and flattening of the tissue geometry was seen in some discs.

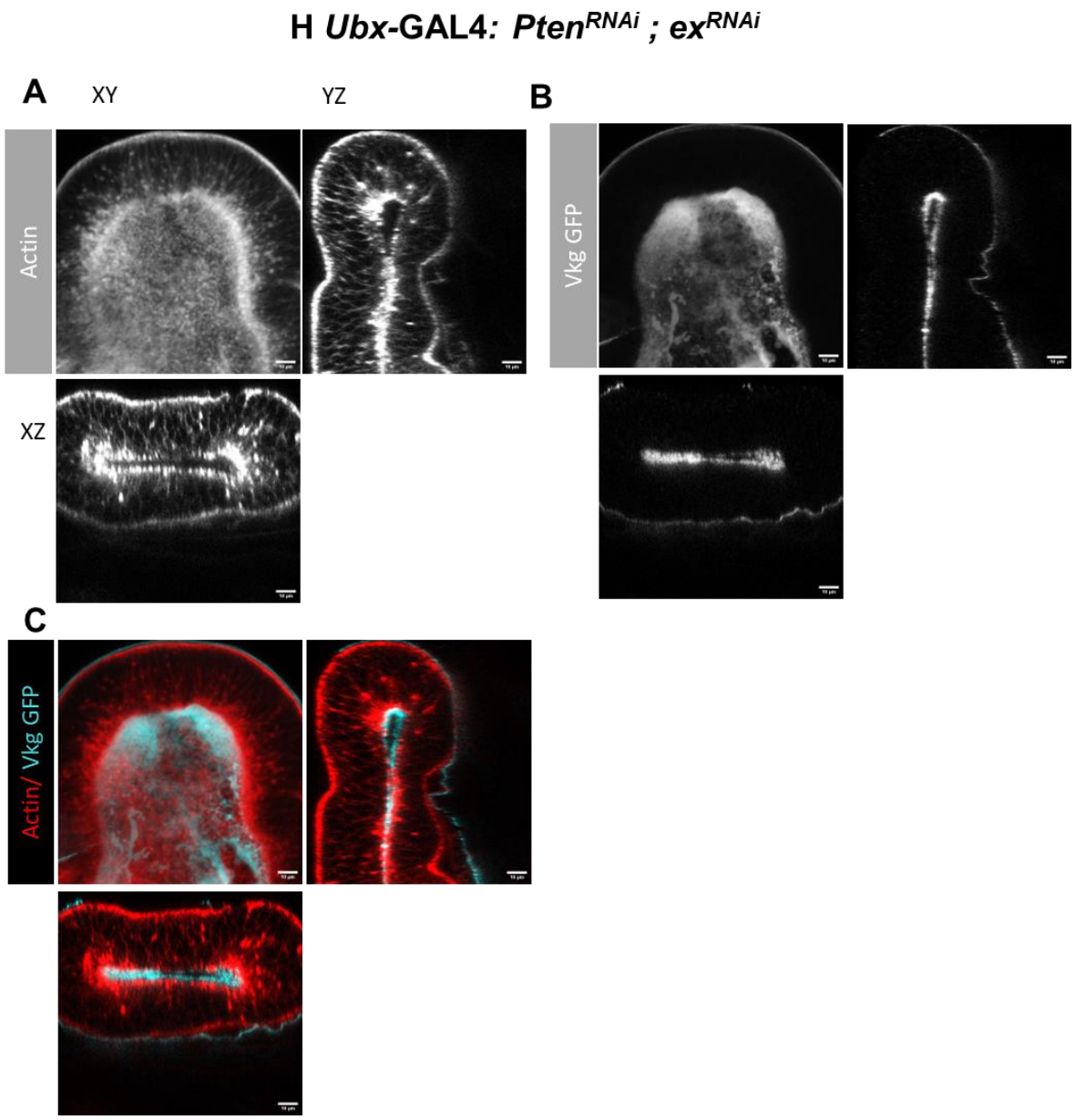

Figure 5.3 *Pten*^{RNAi}*; ex*^{RNAi} haltere discs retain the basal ECM at 4-6hAPF.

A, B: Haltere discs stained for F-actin and Vkg GFP, respectively, with a Z-projection of the pouch (a sum of slices spanning the bECM). The corresponding cross-sections are presented alongside the individual images. Note that the cross-sections of the discs appeared less rounded, indicating a 3D deformation towards a flatter geometry. Additionally, in some discs, an increased lumen was observed, thus, making the overall structure more globular.

C: Shows the merged images displaying bECM (cyan) and actin cytoskeleton (red). The Viking GFP signal was intact throughout all the optical sections. Scale bar, 10 μm. H denotes haltere.

5.3 Discussion

Recent studies have shown that the presence of ECM, accompanied by cell shape changes at 4-9hAPF, is an important determinant of wing vs. haltere shape, as the presence of ECM (esp basal) inhibits tight zippering of the D and V layers. Ubx represses MMP1 and other proteases like Sb and Np in halteres, inhibiting ECM remodelling and cell shape changes(De las Heras et al., 2018; Diaz-de-la-Loza et al., 2020a). Thus, the loss of Ubx activity in the haltere disc led to ECM degradation and tissue expansion (De las Heras et al., 2018). Akin to this, we also observed signs of ECM clearance and changes in the three-dimensional structure of the tissue in $Atro^{RNAi}$; ex^{RNAi} mutants. The overall shape of the tissue appeared flattened, indicating that the changes in the actomyosin cytoskeleton, cell shape, size, and tension observed during the larval stage may indeed influence the three-dimensional structure of the tissue. It is worth emphasising here that the adult $Atro^{RNAi}$; ex^{RNAi} halteres showed flattened morphology, and areas of DV apposition, and blistering.

In the case of $Pten^{RNAi}$; ex^{RNAi} pupal haltere discs, we observed a 3D shape deformation, but the existence of bECM hindered the DV zippering process. As a result, this space was eventually filled with hemolymph, leading to the bulbous haltere shape.

Taken together, our study emphasises the significance of cell shape, mechanical forces (Actin myosin contractility) and ECM in driving wing and haltere epithelial tissue deformations, which in turn play a crucial role in determining organ size and shape. In the next chapter, we further dissect these individual factors to understand their plausible role in cell and tissue shape generation using simple vertex models.

Apart from the role of ECM in determining the flat vs globular shape of the haltere, the components that mediate apposition could also play an important role. We observed an increased accumulation of F-actin at the basal surface of the cells, including in the halteres. Notably, F-actin projections were visible at these surfaces, extending towards the lumen or even reaching the adjacent cell through the lumen, tempting to think that these cytoskeletal projections might be involved in the zippering of the basal sides of the two D and V cells. Recently, in the wing discs, it was observed that atypical laminin spots and the pull generated by microtubule-actin projections mediate the adhesion (Sun et al., 2021). Thus, there could be a differential regulation of integrins and other adhesion proteins mediated by Ubx between wing and halteres that further inhibits this process.

CHAPTER 6

Modelling Cell shape transitions and Organ Morphogenesis

Modelling Cell shape transitions and Organ morphogenesis

6.1 Introduction

Mathematical models serve as valuable tools to unveil mechanisms that may be challenging to explore experimentally. The comprehension of the intricate processes driving tissue folding has greatly advanced through the application of various computational models. For instance, 2D vertex models focusing on the cross-section have illustrated that active apical constriction, while maintaining volume conservation of cells and exerting greater tensile forces on the lateral sides compared to the basal side, can effectively replicate the geometries of ventral furrows in both healthy and mutant tissues (Conte et al., 2012; Polyakov et al., 2014).

Our study on the differential development of organ shapes with wing and haltere suggests that cell shape, cell size and height, apical and basal ECM, and actomyosin contractility – all at the disc or very early stages of pupal development - are some of the major correlates of organ size and shape. During the initial hours of puparium formation, wing discs undergo: 1. Apical and basal ECM remodelling, 2. Apical to lateral localisation of myosin II, 3. Columnar to cuboidal cell shape transition and, 4. Achieves tissue flattening. Halteres, on the other hand, resists all these changes, rendering it a globular geometry in the early pupal stages (De las Heras et al., 2018; Diaz-de-la-Loza et al., 2018, 2020) (detailed in section 1.7 and Chapter 5).

The experimental study presented in the earlier chapters demonstrated that the initial shape difference between the wing and haltere pupal discs is potentially due to the differences in heights, surface area, and contractility between the individual cells of the wing and haltere. Moreover, we also find that, starting from this initial state, different experimental conditions involving cell growth, ECM degradation, cellular contractilities, etc., lead to different overall organ shapes in haltere and wing. However, we lack direct experimental evidence beyond 6-8hAPF, specifically for developing haltere, regarding the underlying physical factors involved in these morphological differences- ultimately leading to the adult wing and haltere morphology, as they are challenging to explore experimentally. Hence, with the help of Prof. Mandar. M. Inamdar (IIT Mumbai), we made an attempt to understand the relationship from the initial to these final stages of morphogenesis using simple theoretical consideration.

Specifically, we used lateral section 2D vertex model to qualitatively understand how the interplay between adhesivity at different locations (apical, basal, and lateral), extracellular matrix (ECM) degradation, and lumen dynamics modulate the shape of individual cells and the overall tissue shape.

Vertex Model Formulation

A 2D vertex model is typically used to model the physics of the planar apical surface of an epithelial monolayer. However, in the current case, we use this framework to describe the lateral cross-section of the 3D epithelial tissue of the wing and haltere. In a 2D cross-section (Fig 6.1), we effectively expose all the key elements that are predicted to be involved in the *Drosophila* wing and haltere morphogenesis.

As shown in Figure 6.1, in the lateral vertex model, we represent each of the cells as a quadrilateral with four vertices and four edges. The apical edge of the cell with line tension of λ_a is exposed to the surrounding environment. The bottom or the basal edge of any cell is in contact with the central lumen and has a contractility of λ_b. Any cell has two lateral edges with contractility λ_l such that each lateral edge is shared between the neighbouring cells. The cells are forced to maintain the effective area A_0 using quadratic energy penalty. The apical and basal ECM are modelled using linear springs of stiffness k_a and k_b, respectively. The rest length of the spring corresponds to the initial length of the corresponding edge. The ECM corresponding to the linear springs resists changes in apical and basal lengths. The central lumen is provided with bulk stiffness of K_l (or K_{lum}, Fig 6.1) and preferred area A_{l0} which together control the lumen pressure and size. In our model we dynamically modulate A_{l0} as a surrogate for cytoplasmic deposition from the cells into the lumen or fluid exchanges between the lumen and the exterior.

The overall dynamics of these factors dictate the shape of individual cells and the overall organ geometry in our model. The associated mathematical equations are given in Materials and Methods.

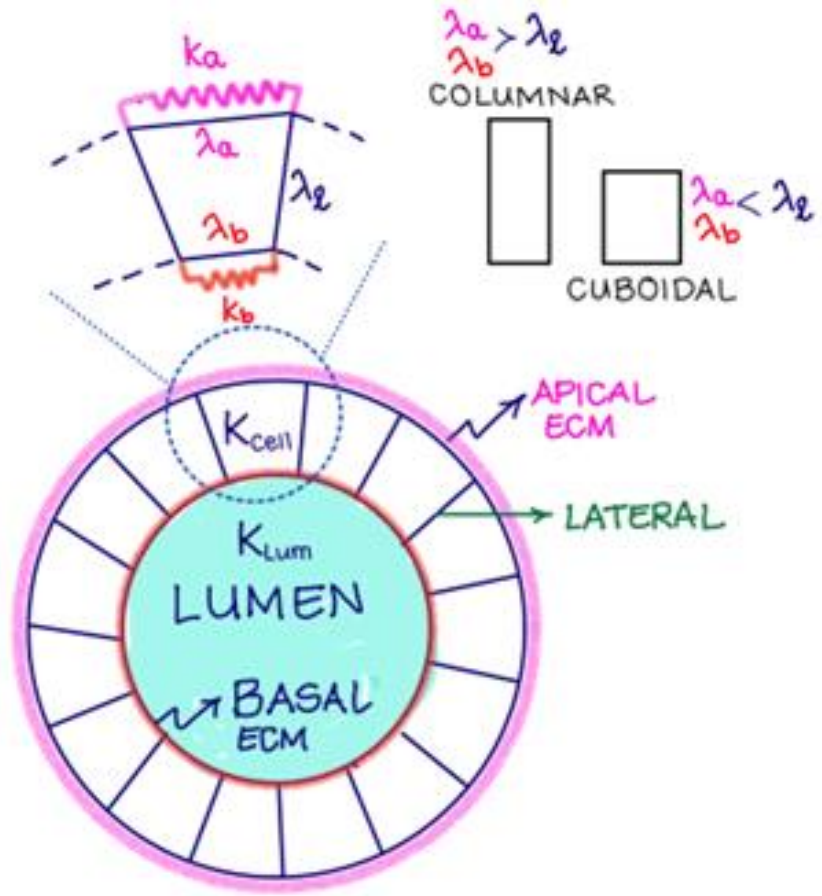

Figure 6.1: The schematic showing different components of a lateral cut haltere model with a spherical geometry. Various components of the model are discussed in the text. The apical, basal, and lateral contractilities are λ_a, λ_b, and λ_l, respectively. Individual cell has bulk stiffness of K and preferred area A_0. The apical and basal ECM are represented as linear springs of stiffnesses k_a and k_b, respectively. The central lumen is provided a preferred area A_{l0} and bulk stiffness K_l. For the columnar cells, $\lambda_a, \lambda_b > \lambda_l$, whereas for cuboidal cells we have $\lambda_l > \lambda_b, \lambda_a$.

6.2 Results

Complex morphogenesis, including in the wing and haltere, is thought to be partly driven by individual cell shape changes in the epithelia (Diaz-de-la-Loza et al., 2018b; Widmann & Dahmann, 2009b, 2009a). Wing discs undergo a cell shape transition from columnar to cuboidal in the early hours of puparium formation, while haltere cells retain the columnar morphology. Using a simple monolayer vertex model with identical columnar cells, we first demonstrate the cell shape changes of a homogeneous sheet, representing an epithelial cross-section. We considered a freely deformable sheet without mechanical constraints and no cell division. By changing parameters such as apical (λ_a), basal (λ_b) cell contractility and lateral cell contractility (λ_l), we observed cell shape changes from columnar to cuboidal. We find that the columnar to cuboidal cell shape transition, along with the overall flattening of the geometry, is promoted by increasing the lateral contractility more than apical and basal contractility ($\lambda_l > \lambda_a, \lambda_b$).

We next incorporated ECM parameters, as they are mechanically coupled to the cells and are controlled to achieve cell and tissue shape changes. Apical and basal ECM were modelled as springs with resistances- ka and kb, respectively. Increasing the lateral contractility and removing apical and basal ECM ($\lambda l > \lambda a, \lambda b$; $ka = kb = 0$) also resulted in columnar to cuboidal cell shape transition, along with the monolayer flattening and bending (Fig 6.2).

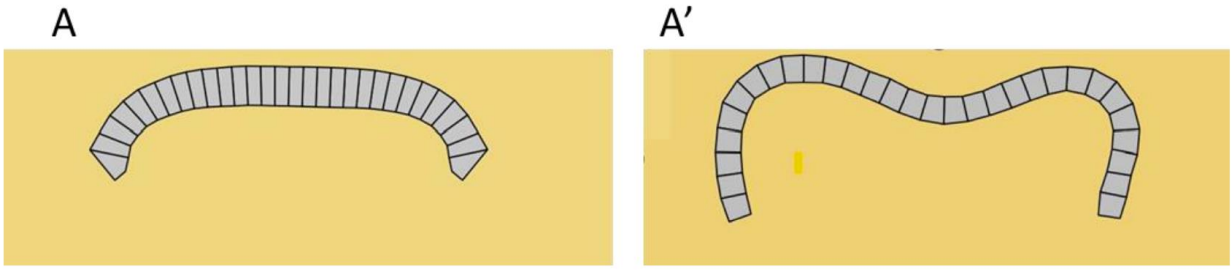

Figure 6.2 Transformation from columnar (A) to cuboidal cell shape (A') upon increasing lateral tension and removing apical and basal ECM.

We now take a look at the model findings across different experimental conditions presented in previous chapters, starting from the widtype wing and haltere.

6.2.1 Wildtype Wing shape

We started with the wing-disc geometry at 4-6APF in which two layers of columnar cells are apposed and zippered to each other (Fig. 5.1A; 6.3a). As reported earlier, the ECM degradation at the basal layer of the wing is important for the zippering of these two layers (De las Heras et al., 2018; Diaz-de-la-Loza et al., 2018, 2020). As mentioned earlier, when $\lambda_a, \lambda_b > \lambda_l$, i.e., the lateral contractility of the cells is smaller when compared with their basal and apical counterparts, each of the individual cells will be columnar, in other words, their lateral dimensions would be larger when compared to their apical and basal sizes (Fig 6.3a, left). When, due to localization of myosin to the lateral side (as reported in Diaz-de-la-Loza et al., 2018), the lateral contractility becomes larger as compared to the apical and basal side, i.e., $\lambda_l > \lambda_a, \lambda_b$, the cells change their shape from columnar to cuboidal when, simultaneously, the apical and basal ECM is also degraded ($k_a = k_b = 0$), thus facilitating changes in individual cell morphologies. However, since the cells in the top and the bottom layer (or D and V layers) are connected to each other with the help integrins (Domínguez-Giménez et al., 2007; Sun et al., 2021) , this leads to flattening and expansion of the overall wing geometry along with the transformation of the individual cells from columnar to cuboidal (Fig 6.3a).

6.2.2 Wildtype haltere

Our observations along with previously published reports suggest that the cross-section of haltere pouch at 4-6hAPF has a globular overall geometry (Fig 5.1B) (De las Heras et al., 2018). Thus, we modelled haltere with an initial globular geometry as depicted in Figure 6.1b. Although there is relatively less actin-myosin in the apical cortex and apical tension, qualitatively, the observed columnar shape of individual haltere cells at larval stages would still be due to $\lambda_a, \lambda_b > \lambda_l$. As reported earlier and observed here, at 4-6h APF, in the absence of ECM degradation, the dorsal and ventral layers are not connected to each other and thereby leading to the formation of pronounced lumen (De las Heras et al., 2018). The morphogenesis of two layers are decoupled.

The presence of lumen provides an initial globular geometry to the haltere. However, for such geometries, the overall shape of the tissue is strongly coupled with the basal and apical areas of individual cells. Consequently, the size of lumen and morphology of individual cells are

related to each other. If in the simulations, the cells are made to undergo rapid transition from columnar to cuboidal shapes, there isn't enough area left of the modified surface of the cells to still maintain the overall rounded morphology of the haltere thus resulting in a highly deformed or wiggly overall geometry. However, if consider delayed decay of ECM (as observed experimentally) and similar slow pace in the increase in the lumen size, then the increased surface area of individual cells due to modifications in lateral contractility($\lambda_l > \lambda_a, \lambda_b$) can be accommodated thus resulting in more spherical shape as is observed experimentally. Interestingly, the technical modifications required to be done in the simulations for this purpose requires a longer time when compared with the wing counterpart and could possibly explain the observed developmental time between wing and the haltere cells to undergo columnar to cuboidal transitions. The dynamical evolution of the model haltere from its initial morphology to the final organ shape is shown in Figure 6.3 b.

6.2.3 *Pten^{RNAi}; ex^{RNAi}* haltere

Pten^{RNAi}; ex^{RNAi} larval haltere cells are similar to wing cells in lateral height, the levels of apical acto-myosin complex and the apical contractility (Fig 4.3, 4.4). During 4-6h APF, although we did not observe ECM degradation, the cross-section of discs were flatter compared to the wildtype haltere discs (Fig 5.1B, 5.3). However, there was a presence of small lumen keeping the dorsal and the ventral layers separate from each other.

Interestingly, the outcome of the simulation for these mutant discs was a geometry very similar to that of wildtype haltere discs (Fig 6.3 c). *Pten^{RNAi}; ex^{RNAi}* adult halteres too showed overall globular morphology (Fig 3.6). This suggests due to the lack of coupling between the dorsal and the ventral layer, increase in the size of the lumen is not resisted resulting in the overall globular geometry.

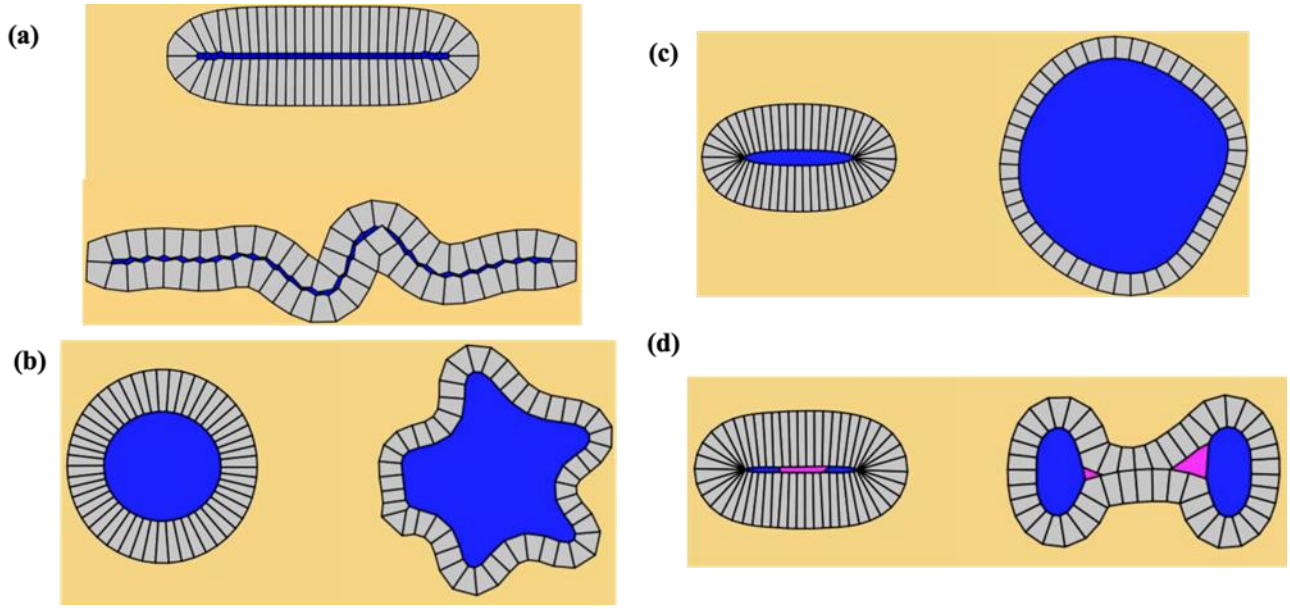

Figure 6.3 The dynamical evolution haltere and wing from the initial state (3-4 hAPF).

(a) At the 4-6h APF, the wing has two apposed layers of columnar cells that are adhered to each other by a layer of integrins (blue layer of cells). A reduction in apico-basal contractilities and increase in lateral contractility along with ECM degradation results in the columnar to cuboidal cell transition. Because of the lack of central lumen and adhesion between the top and bottom cell layers, unlike haltere, the wing retains flat morphology. (b) For WT haltere, the initial condition corresponds to columnar cells surrounding a central lumen (blue). A reduction in apico-basal contractilities and increase in lateral contractility while accompanied with a continuous lumen increase and ECM degradation results in the maintenance of the final globular haltere shape (right) that is now lined with cuboidal cells. (c) In the $Pten^{RNAi}$; ex^{RNAi} haltere mutant, the initial condition is very similar to that of the wing. However, the top and the bottom layers do not adhere to each other and there is a small central lumen. Consequently, any increase in lumen size due to material exchange ultimately results in a globular haltere. As in the WT haltere case, the final geometry of the individual cells can undergo a columnar to cuboidal transition if modifications in contractilities happen (d) The $Atro^{RNAi}$; ex^{RNAi} haltere mutant, as the $Pten^{RNAi}$; ex^{RNAi} mutant, has a wing-like flat initial arrangement of columnar cells. However, the top and the bottom layers are partly adhered to each other (pink connection) while encompassing a small lumen (blue). The adhesion of the central layer in this case, while the growth of the lumen results in a final shape that is partly adhered like wing while partly being globular like haltere.

6.2.4 *Atro^{RNAi}; ex^{RNAi}* haltere

Atro^{RNAi}; ex^{RNAi} larval haltere cells are also similar to wing cells in lateral height, the levels of apical acto-myosin complex, apical constriction and the apical contractility (Fig 4.1, 4.3, 4.4). During early pupal stages (4-6hAPF), the discs were flatter compared wildtype haltere discs (Fig 5.2). However, unlike *Pten^{RNAi}; ex^{RNAi}*, we did observe ECM degradation. The dorsal and the ventral layers were closely opposed to each other, although heterogeneously (Fig 5.2).

With this starting point, the outcome of the simulation for these mutant discs was flat wing-like geometry at the locations wherever the dorsal and the ventral layers are coupled (Fig 6.3 d). In other locations, wherever this coupling was absent, we observed globular geometry giving an overall blistered appearance as observed experimentally (Fig 6.3d, right).

6.3 Discussion

In line with D'Arcy Thompson's original concept proposing that biological form emerges from the amalgamation of physical processes and mechanical forces (Thompson, 1917), recent work in the past decades has underscored the pivotal role of mechanical forces and tissue mechanics in governing epithelial cell behaviour and the dynamic transformations that underlie tissue morphogenesis. Epithelial geometry is determined by the balance of biomechanical properties of the individual cells comprising the tissue (Diaz de la Loza & Thompson, 2017). The acquired shape of the tissue or its constituent cells is an outcome of the actomyosin levels, which determines membrane contractility cell-intrinsically and three-dimensional cell-cell adhesion, cell-ECM interactions cell extrinsically.

Throughout development, epithelial tissues undergo extensive two- and three-dimensional transformations, collectively known as morphogenesis. These morphogenetic processes are orchestrated by the temporal and spatial coordination of cellular behaviours, notably including alterations in cell shape and size, collective cell migration, cell-cell intercalation, cell division, and delamination events (Etournay et al., 2015; Gilmour et al., 2017; Heisenberg & Bellaïche, 2013; Miller & Davidson, 2013).During the *Drosophila* wing and haltere morphogenesis, the two tissues attain distinct structures both at the cellular and tissue levels by the end of 7-9hAPF. We show that these differences in the cell and tissue morphology can be attained by tweaking the cellular biomechanical properties, such as cell contractilities, ECM, and adhesion, along with initial cell constraints.

One of the key propositions from our computer modelling presented here is that in addition to starting with a flat geometry, it is essential that the two layers (D and V) of the tissue be zippered to each other. Degradation of ECM in wing discs not only facilitate the columnar to cuboidal transition of the cells, but also ensures the zippering of the layers (De las Heras et al., 2018; Diaz-de-la-Loza et al., 2018, 2020). Ubx plays a crucial role in maintaining the ECM in halteres. In fact, the ectopic expression of Ubx in wings, results in non-zippering of the two layers which ultimately results in haltere like morphology (Pavlopoulos & Akam, 2011). Another key finding of the model is the role of lumen or fluid exchange in retaining the morphology of the haltere. Any mechanism that could drain out the lumen from a haltere could also aid in the creating wing-like morphology starting from a haltere. Overall, the

findings of the computer simulations are qualitative and not counterintuitive. However, the modelling utility lies in the fact that they directly demonstrate that while different signalling processes can lead to expression of various genes and signalling molecules, it ultimately results in modification of a few key physical parameters that ultimately govern the shape of individual cells and the overall tissue geometry as was demonstrated with our $Pten^{RNAi}$; ex^{RNAi} and $Atro^{RNAi}$; ex^{RNAi} mutants. A combinatorial control of these physical parameters can lead, in a manner of speaking, to a conversion between haltere-to-wing and wing-to-haltere.

These observations underscore the sensitivity of tissue morphology to the interplay of adhesion dynamics and mechanical forces, revealing the critical role of zippering and initial geometry constraints in shaping the final tissue configuration. A recent study shows that reducing myosin levels in wing discs affects the overall tissue curvature and eversion process, resulting a globular wing disc after eversion- in other words, the discs fail to flatten by 4-6hAPF (Fuhrmann et al., 2024) . Thus, further supporting our observations that differences in the initial geometry may arise from the differences in the cellular biomechanical properties between wing and haltere discs prior to eversion.

CHAPTER 7

Discussion and Future Perspectives

Discussion

Organ size and shape determination is by no means a simple biological process. Rather, it is a series of complex events governed by a combination of genetic, cellular, hormonal, environmental and mechanical factors. We are now beginning to integrate these factors towards a better understanding of organogenesis. The development of the *Drosophila* wing and haltere offers a unique paradigm to investigate the events and elements that govern cellular and organ growth, as these two organs originate from remarkably similar progenitor cells but, ultimately, differentiate into distinct functional structures. The wing is large and flat, while halteres are smaller and globular in shape. Moreover, alterations in a single gene, Ubx, is capable of interchanging their wing vs. haltere identity, with wings being the default fate. As the loss of function of Ubx activity in halteres leads to a complete haltere to wing homeotic transformation (Lewis, 1978).

The wing and haltere progenitors are specified during the early embryonic stages, and Ubx is thought to regulate the number of cells of the haltere primordium. Up until the third instar larval stages, aside from the difference in cell number and, consequently, tissue size, the wing and haltere disc cells were generally regarded as indistinguishable in terms of their individual cell size, shape, and polarity (Makhijani et al., 2007; Roch & Akam, 2000; Singh et al., 2015). The role of Ubx in modulating various growth and patterning pathways has been extensively studied (Agrawal et al., 2011; Crickmore & Mann, 2006; Khan et al., 2020; Makhijani et al., 2007; Mohit et al., 2006; Pallavi et al., 2006; Pavlopoulos & Akam, 2011; Prasad et al., 2003; Shashidhara et al., 1999; Weatherbee et al., 1998). Nevertheless, to form such distinct structures, the various signalling networks and cues from the external environment must converge at the level of altering the individual cell behaviours such as cell shape, size and mechanical properties- dictating the overall tissue geometry. This convergence is essential since the adult organs and their cells exhibit distinct morphologies: the wing is flat with squamous cells, while the haltere is globular, comprised of cuboidal cells. However, our understanding of the mechanisms responsible for shaping organs and how Ubx specifies the globular shape of the haltere remains limited.

In this study, we present novel findings regarding distinctions in cell characteristics, including size, shape, and contractility, between the third instar wing and haltere disc cells. At L3, wing and haltere discs are made up of pseudostratified columnar cells. Examination of

wing and haltere discs during the third instar larval stage revealed that wing cells were more laterally elongated with a narrower apical surface compared to haltere cells. Additionally, we observed higher levels of apical actin and myosin II, key regulators of cell tension and contractility, in wing discs. Quantification of their relative contractility using laser ablation, further supported the notion of increased cell contractility in wing discs as compared to haltere discs.

Reducing the Ubx levels using Ubx^{RNAi} in halteres led to an increase in the actomyosin abundance and cell contractility at the apical cell surface compared to the control haltere cells. The cells were apically constricted and laterally elongated, contrasting with the control halteres. This observation indicated a transformation in cell characteristics towards a more wing-like phenotype. The resultant adult morphology is flatter 'winglets' in place of globular halteres, albeit smaller in size (compared to wings), with a sparser trichome arrangement. This suggests a previously unrecognised role of Ubx in altering the cellular mechanical properties of haltere cells as early as the third instar larval stage.

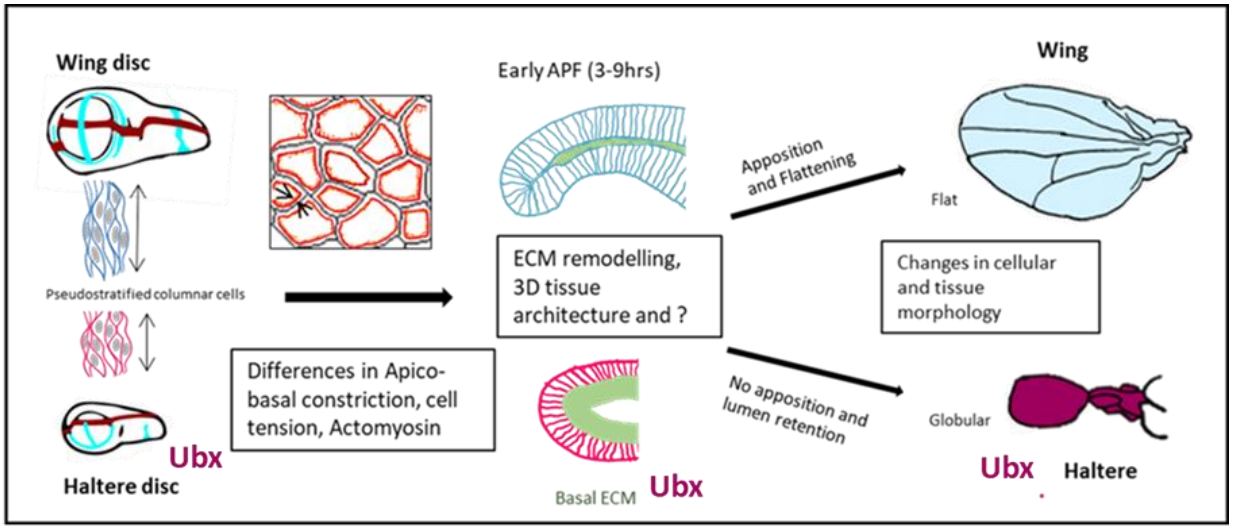

Figure 7.1.1 Schematic showing the summary of the factors influencing the cell and organ morphology between wing and haltere.

Wing and haltere cells, like other epithelial cells, display apicobasal polarity, and the mechanical properties of these cells differ across their intracellular domains. Modifying the properties of these domains has the potential to alter cell shape and, consequently, the overall tissue architecture. For instance, at the subcellular level, differential actomyosin

accumulation-induced constriction drives tissue bending (Heer & Martin, 2017; Heisenberg & Bellaïche, 2013). Furthermore, cells are mechanically coupled to their neighbours through adherent junctions, coordinating the forces generated by individual cells to be integrated across the tissue. Our simple vertex models suggest that the transition between squamous (flat) and cuboidal cell shapes can be facilitated by adjusting cell contractilities. Specifically, modifying parameters such as apical, basal and lateral cell contractility allows us to shift cell shapes from a columnar to a cuboidal morphology and vice versa. Cuboidal cell shapes emerge when lateral cell contractility exceeds both apical and basal contractility, and this process involves tissue deformation, in this case, flattening. Tissue deformations result from the coordinated cell shapes within individual cells.

Additionally, cells are surrounded by ECM at apical and basal surfaces, which also acts as a controllable mechanical constraint for morphogenesis (Harmansa et al., 2023). Previous studies have shown that wing discs undergo columnar to cuboidal cell shape at early pupal stages, which correlates with ECM remodelling. Halteres, on the other hand, does not undergo cell shape transition or ECM remodelling. A compromised Ubx level in halteres using Ubx^{RNAi}, induces ECM degradation and an overall flatter geometry (De las Heras et al., 2018; Diaz-de-la-Loza et al., 2018, 2020). Incorporating ECM in our computational models predicts that clearance of ECM is necessary to change from columnar to cuboidal cell shape.

Taken together, our results suggest that the dynamics of ECM and actomyosin complexes, along with adhesion molecules which impart cell contractilities, are important in determining the cell and tissue architecture. The alterations in these can have a profound impact on organ development. Hence, the signalling pathways that activate actomyosin contractility, such as Hippo and ECM, are fine-tuned by a balance of both positive and negative regulation by Ubx.

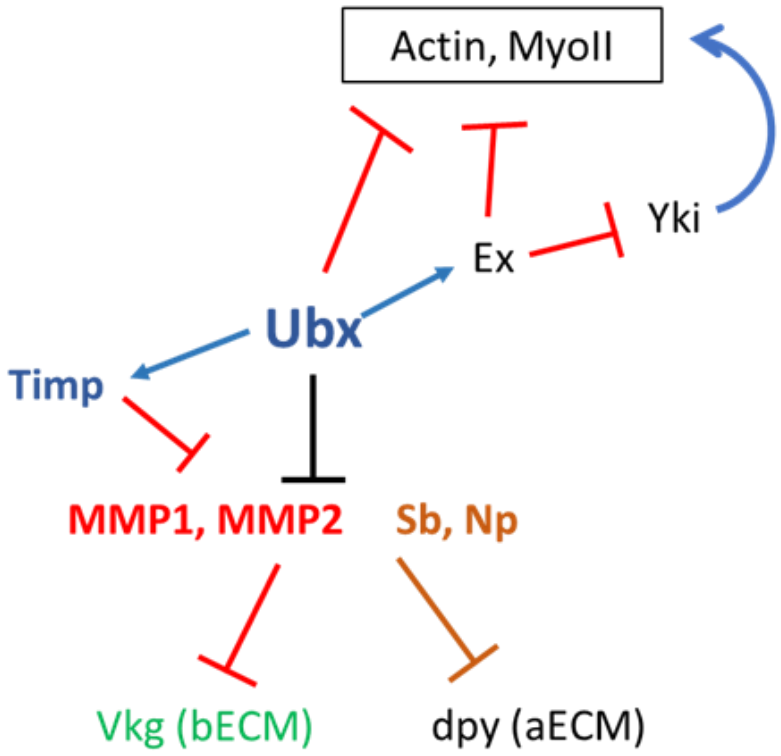

Figure 7.1.2 Ubx regulates the cell tension and ECM dynamics by modulating multiple genes and pathways.

We also identified additional mutant combinations that exhibited varying degrees of haltere-to-wing transformation. In the $Atro^{RNAi}$; ex^{RNAi} halteres, during the larval stage (L3), we observed that the cells had transitioned towards a more wing-like appearance, exhibiting increased apical constriction, cell height and actomyosin levels, as well as cell junctional tension. At 4-6 APF, we detected signs of heterogenous basal extracellular matrix (ECM) clearance, as indicated by the absence of Vkg GFP signals. Remarkably, in the regions where ECM clearance occurred, we observed tight zippering of the dorsal and ventral layers, alongside an overall flattening of tissue geometry. The $Atro^{RNAi}$; ex^{RNAi} halteres, after eclosion, displayed areas of partial apposition and small blistered phenotypes. The halteres were significantly enlarged, with a flatter morphology, resembling "wing-like" (smaller than wildtype wing), complete with marginal bristles and a reduced trichome density.

$Pten^{RNAi}$; ex^{RNAi} flies also exhibited enlarged halteres, with the presence of wing marginal bristles and a sparser arrangement of trichomes but, retained the bulbous shape. We noted an overall increase in the apical cell size within the $Pten^{RNAi}$; ex^{RNAi} haltere discs. The cells were elongated with heightened levels of actomyosin complexes at the cell cortex, indicative of

enhanced cell contractility. This increased contractility was subsequently confirmed through contractility experiments. During the early pupal stages (3-6 APF, we monitored), clearance of the ECM was not observed, but there was an overall 3D shape deformation of the tissue towards flatter geometry.

The arrangement of trichomes and their density can serve as an indirect indicator of cell size and polarity. In the adult wing, each cell typically bears only one trichome, and the cells are larger; hence, the trichomes appear to be sparsely arranged on the cell surface. In contrast, haltere cells are smaller, and they may have more than one trichome per cell. As a result, the trichomes on haltere cells appear denser. Thus, the reduced trichome density observed in the Ubx^{RNAi}, $Atro^{RNAi}$; ex^{RNAi}, and $Pten^{RNAi}$; ex^{RNAi} halteres may suggest an increase in the cell size.

The shape of the haltere is highly resistant to changes as evidenced by our screen and previous literature. Apart from Ubx, only a limited number of genes or combinations of genes have been identified with the potential to induce a flatter morphology in the haltere. In the case of the $Pten^{RNAi}$; ex^{RNAi} mutant, despite undergoing a partial homeotic transformation at the cellular level during the larval and adult stages and exhibiting a somewhat flat geometry at early APF, the organ remained globular. A plausible explanation is that due to the absence of basal ECM degradation and dorsoventral zippering, the lumen was retained, eventually filling with hemolymph, resulting in the adult globular geometry as also evidenced from the modelling. This observation also implies that the flattening observed in the wings cannot solely be attributed to differences in cell numbers between the wing and haltere. Even if the disc is significantly larger in size (higher cell number), it can still exhibit a globular morphology, highlighting the importance of other factors influencing tissue shape beyond cell numbers.

An interesting enigma arises when considering the influence of extracellular matrix (ECM) degradation on wing and haltere shape generation. In the case of wing discs, preventing basal ECM degradation is sufficient to hinder the apposition of dorsal and ventral layers and render the organ globular. Conversely, inducing ECM degradation by overexpressing MMP1 or reducing Timp expression does not suffice to flatten the halteres completely. For instance, when MMP1 expression is induced in halteres during the mid-late larval stage, it clears the basal ECM and alters individual cell morphology to a cuboidal shape. However, The D and V layers remain separated with an increased lumen size, resulting in adult globular halteres with

no apposition or expansion (De las Heras et al., 2018). This uncouples ECM degradation and cell shape transition from dorsal-ventral zippering and 3D flattening of tissue. This, again, emphasises the multi-level control of haltere fate by Ubx, rendering the halteres highly resistant to shape changes, unlike the wing. Organ flattening is only observed when MMP1 expression is induced during the early L3 stage (De las Heras et al., 2018).

Similarly, reducing Ubx levels in halteres using Ubx^{RNAi} leads to the de-repression of ECM (Vkg) degradation, resulting in flatter cells and tissue, ultimately giving rise to an adult organ with a flat 'winglet' morphology. However, the timing of Ubx expression appears to correlate with appendage development and attaining its characteristic shape. Early downregulation of *Ubx* results in large, flat appendages (small wings), while late downregulation (late L3 onwards) leads to smaller appendages that are globular in shape (De las Heras et al., 2018). These observations emphasise that modifications to the halteres must be initiated at least by early to mid-larval stages to substantially impact the organ's shape. Therefore, this further supports our findings that the variances in cellular mechanical characteristics achieved by the haltere in late L3 may represent an additional factor in determining the shape of the haltere.

Organ size and shape determination is a complex biological process. Here, we add to the knowledge of key factors that might influence the size and morphology of an organ, starting from its constituent cells. It's becoming increasingly clear that major force changes within and between cells are happening during morphogenesis to drive various events. The *Drosophila* wing and haltere seem to be no exception. By the late third instar larvae, the discs are prepared to undergo complex folding patterns observed in eversion followed by dramatic changes in the 3D morphology. Thus, it seems like there are some mechanical initial constraints attained by individual organs, to drive their respective morphogenesis. Our study suggests that the cellular biophysical properties at these stages are critical. We conclude that, there are multiple factors starting from individual cell properties to nutrition and environmental factors, that integrate to determine an organ's specific size and shape. Ubx, in halteres, is a master regulator, specifying all the aspects of haltere fate at multiple levels, increasing the system's resistance to small changes. Towards this, Ubx also alters the mechanical environment within and between cells at L3 and pupal stages to bring about the globular shape of the haltere.

Future Directions:

1. The cells at the dorsoventral (DV) boundary within the wing discs exhibit intriguing mechanical characteristics, displaying elevated levels of actin, myosin, and E-cadherin accumulation, forming a distinctive layer. This suggests notable differences in the mechanical properties of these cells compared to their neighbouring cells. Interestingly, such a distinction is not observed in the haltere discs. In tissues, boundaries between regions with varying mechanical properties can potentially give rise to mechanical conflicts. These localised conflicts can lead to anisotropic deformations, potentially resulting in tissue folding and buckling. Our preliminary observations suggest that there are distinctions in the eversion processes between wing and haltere discs. Notably, the initial folding during eversion appears to be asymmetrical in halteres, with the P compartment leading the way. Thus, it would be important to understand the differences in eversion, if any, and its implication on achieving the final size. Furthermore, it is worth investigating whether the varying properties of the DV boundary cells contribute to the initiation of these differences in the eversion process and play a role in shaping the three-dimensional structure that emerges during the initial hours of pupation. Interestingly, we observe the appearance of faint actin rich boundary cells in the mutants (Fig 7.2.1).

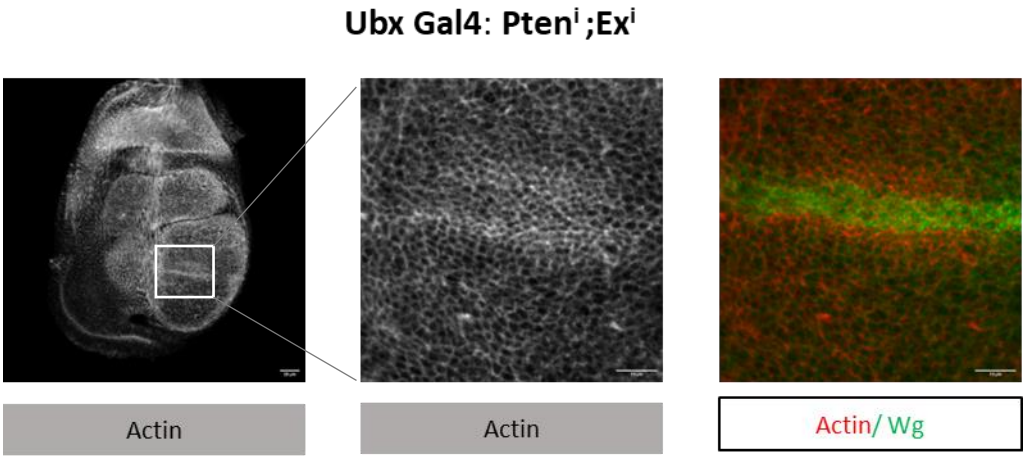

Figure 7.2.1 F-Actin accumulation is seen in the DV boundary cells of *the Pten^{RNAi}; ex^{RNAi}* halteres. Scale bars, 25,10,10 microns, respectively.

2. Our study primarily focused on characterising cell properties at the apical cell membrane in the L3 stage between wing and haltere, yet it is essential to consider the mechanical properties of the basal cell membranes. Cell shape alterations and tissue organisation are also influenced by interactions between the cell plasma membrane and the basal extracellular matrix (ECM). For instance, the convex dome-shaped topology of the discs requires increased basal constriction. Therefore, exploring the properties and distinctions within the basal cell surface between the wing and haltere at L3 is important. Given the mechanical differences we have uncovered between wing and haltere cells in this study, when coupled with the basal properties of the cells, it is plausible that these distinctions could extend to their three-dimensional architectural differences even at the late L3 stage. Which, in turn, may have the potential to influence their respective eversion processes.

3. Our understanding of the events that transpire beyond 7-9 hours after puparium formation in halteres remains limited. Notably, while halteres exhibit resistance to transitioning from columnar to cuboidal cell shapes at 7-9 hours APF, adult halters eventually possess cuboidal cells. The wing discs undergo another round of apposition, i.e., a separation of the DV layer followed by a reapposition around 40 hours APF. Halteres might undergo cell shape changes at this time. Studying the haltere pupal discs and their cell shapes at these hours can give us insights into what drives the cell shape transition of columnar to cuboidal in halteres.

4. We have conducted an extensive characterisation of the cellular and mechanical traits associated with Pten, Ex, and Atro knockdown. However, the precise molecular mechanisms underlying their capacity to induce these changes remain unclear. It is possible that the simultaneous knockdown of these genes may trigger the activation of growth-regulating pathways such as Insulin and EGFR, in addition to inhibiting the Hippo pathway. Furthermore, these genetic perturbations may lead to modifications in cell adhesion properties (which, in turn, changes the mechanical properties observed), mediated by fat/dachsous/four-jointed, given the known interactions between Atrophin and Expanded with these molecules. Our data also hint at potential implications for wingless signalling in haltere development. Therefore, it is imperative to elucidate the downstream events and the molecular mechanisms orchestrated by Atrophin and Expanded that influence extracellular matrix (ECM) dynamics and overall organ growth, as well as their impact on wingless signalling.

5. We observed that inducing Timp expression using a UAS *Timp* line with pouch-specific *nubbin*-GAL4 or downregulating one of the components of the beta subunit of integrins *Inflated (If)* resulted in blistered wings. These inflated wings clearly lacked dorsoventral apposition, and were filled with fluid after eclosion. Retaining ECM by inducing Timp expression can also affect cell morphology at L3, as reported in (LeBlanc et al., 2021) Thus, it would be interesting to study the effect of these genotypes on cellular mechanical properties at L3 wing in bringing these shape changes.

6. The role of ecdysone reception, developmental delay in halteres.

Ecdysone is a steroid hormone synthesised in a series of pulses dictating various developmental transitions in insects, including *Drosophila*. There is a higher titre pulse of ecdysone (20E) towards the end of larval development, marking the onset of metamorphosis. Studies have shown that ecdysone signalling induces growth in imaginal discs, and inhibition of the same results in decreased cell size and cell number in the L3 wing disc (Herboso et al., 2015). Our work (RNAseq, ChIP, and qPCR) from our lab shows that some of the Ecdysone-

responsive genes are not only targets of Ubx, but are differentially expressed between wing and haltere (Soumen and Simran). Thor, which is a negative regulator of growth and under the control of both ecdysone and Insulin pathways, is upregulated in the haltere. Whereas, Hr46 and Usp, which are essential for ecdysone-mediated growth of wing discs, are downregulated in the haltere. Also, another interesting study shows that ecdysone and juvenile hormone induces the expression of MMPs and inhibits Timp in fat bodies during early pupal hours (Jia and Liu, 2017). Taken together, we hypothesise, that during the late third instar larval stage, the cells of the haltere disc might become less sensitive to ecdysone. As, Thor which is repressed by ecdysone and Hr46, which is activated by it, start showing such differential expression patterns. Overall, this might contribute to the delay in ECM remodelling in halteres, thus resisting the cell shape changes in haltere compared to that in the wing.

7. Simulations using a 3D vertex model for wing and haltere eversions can provide better insights into the constraints of eversion and organ shape changes.

Materials and Methods

Materials and methods

2.1 Fly stocks and maintenance.

The required fly stocks for crosses were grown on standard cornmeal agar media and were maintained at 25^{o}C. The wild-type strain used during the study is Canton-S. All the crosses were set up at a temperature of 25^{o}C, unless stated otherwise. To ensure optimal conditions and to avoid overcrowding for comparative analysis of organ and cell sizes, the number of male and female flies was maintained constant within each set of experiments. Following a two-day mating period, the flies were transferred to fresh vials for egg laying over a duration of two additional days; thereafter, adult parental flies were removed.

Fly lines used in this study: CS, Sqh GFP (BL57145), *endo-DE-cadherin-GFP* (BL60584), *Ubx*-GAL4(Pallavi & Shashidhara, 2003), *vkg*-GFP (BL 98343), UAS *Ubx*^{RNAi} (v37823), UAS *Atro*^{RNAi} (KK107413, BL51414), UAS *ex*^{RNAi} (TRiP.JF03120, KK109281), UAS Pten^{RNAi} (KK101475), Yki driver- w*, *ap*-GAL4, UAS-GFP/CyO; UAS-Yki, tub-Gal80ts/TM6B (Song et al., 2017), *nub* GAL4 (from Chaudhary V, IISER Bhopal), *If*^{RNAi} (BL27544), *Timp*^{RNAi} (BL61294).

2.2 Screen Methodology

2.2.1 Screen 1

The *RNAi* stocks were obtained from Vienna Drosophila RNAi Center (VDRC). For each cross, 5 males from the KK transgenic RNAi stock were crossed separately to 10-15 virgins from w*, *ap*-GAL4, UAS-GFP/CyO; UAS-Yki, tub-Gal80ts/TM6B (Yki driver); and w*; *ap*-GAL4, UAS-GFP/CyO (GAL4 or GFP control). Virgin females were mated to RNAi stock males (day 1), and the crosses were stored at 18°C for four days to provide ample time for mating before starting the screen protocol. Gal80ts was used to allow UAS driven transgene expression after temperature switch from 18°C to 29°C. On the day five, the crosses were transferred into new, freshly yeasted vials for another three days at 18°C for egg laying. On day eight, the adult flies were discarded, and larvae were allowed to develop until day 11 at 18°C. The vials were then moved to 29°C incubators to induce GAL4 activity on day 11.

Crosses were aged at 29°C for another 8-9 days, after which larvae were dissected to assess the wing and haltere disc overgrowth.

2.2.2 Screen 2

The genes that were shortlisted through Screen 1 were subsequently subjected to a crossing scheme, as illustrated below:

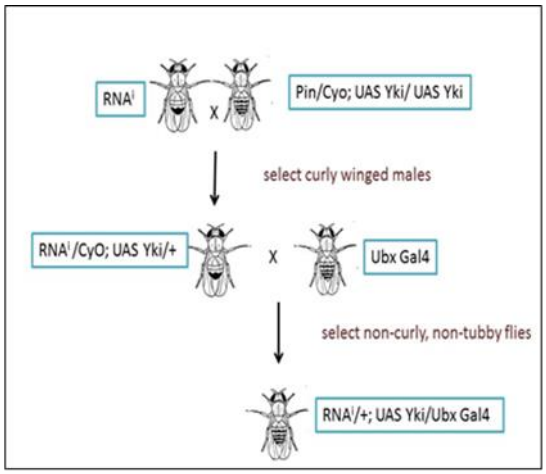

2.3 Immunohistochemistry

Staining of larval discs:

Wandering third instar larvae were collected and were washed with Phosphate buffer saline (PBS, pH7.2 Invitrogen) in a glass cavity block. After giving a posterior cut to remove maximum fat bodies, the anterior part, which contains the discs of interest, was turned inside out. At least 8 such heads were fixed for 20 minutes in 4% Paraformaldehyde. Fixed larval heads were given 2 washes of 0.1% PBTX for 10min each and were blocked with 0.5% BSA for 2hr at room temperature. Larval heads were then incubated with primary antibodies of the desired dilution overnight at 4°C. This was then followed by two washes for 10 min each with 0.1% PBTX and incubation with the secondary antibody (1:1000) in blocking solution for 2 hr at room temperature in the dark. Then larvae were again given two washes of 10 min each with PBTX. A final wash with PBS was given to remove all PBTX. Imaginal disc of interest is obtained by dissecting them from anterior heads in microscopic slides. Imaginal discs were then mounted with anti-fade mountant (Invitrogen) or Vectorshield and double-

sided tape as spacers. All the imaging was done Leica Sp8 confocal microscope using either 40X/1.30NA oil or 63X/1.40NAoil with a magnification of 0.75 or 2.5, respectively.

Reagents

Phosphate buffer saline PBS pH7.4 Sigma Blocking solution: PBS + 0.1% TritonX-100 (sigma) + 0.5% BSA (Sigma). PBTX : PBS + 0.1% TritonX-100 (sigma).

Antibodies Used:

Primary antibodies used in this study are anti-N-terminal Ub*x* 1:1000 dilution (Agrawal *et al.*, 2011), rabbit anti-sqh (1:400) (Vasquez et al., 2014), rat anti-DE Cadherin (DSHB) (1:50), Rhodamine Phalloidin (1:200) Invitrogen, Rabbit anti-GFP (1:750 Invitrogen), rabbit anti-Viking antibody (1:400 a gift from Stéphane Noselli), mouse anti-Wingless (1:200; DSHB), mouse anti-Engrailed 4D9 (1:200; DSHB). All secondary antibody used in this study, Alexa-fluor 568,594,488 and 633 (1:1000) has been obtained from Invitrogen.

2.4 Pupal disc ex-vivo culturing

Schneider's medium from Gibco ThermoFisher 21720024 was supplemented with 15% FBS and 1% penicillin-streptomycin (15140–122; Invitrogen). Ecdysone from Sigma, 20-hydroxyecdysone H5142, was added at a final concentration of 0.5 µg/mL for attached discs. 0hr or 3hr pupae were washed in sterile PBS and disinfected in 70% ethanol again, followed by a wash with 1X PBS. After rinsing in the eversion media, the Pupal case was cut opened in the chilled eversion media. The wing and haltere imaginal disc attached to the pupal walls were then cultured in 48 well dishes at 25˚C incubator. After the completion of the respective developmental time, the tissue was fixed in 4% PFA for 20 minutes, and Immunostaining was performed (modified from Aldaz et al., 2010; De las Heras et al., 2018; Diaz-de-la-Loza et al., 2018)

Schneider's media composition: 15%FBS, 1% pen-strep, 0.14µg/ml Insulin, 20HE (0.1 µg/ml)

2.5 Laser ablation experiment

Endo DE-cad-GFP expressing wing and haltere discs of appropriate genotypes were used to visualise cell membranes. The respective discs were carefully dissected in the filter-sterilized chilled Schneider's media to keep them alive. The discs were mounted in coverslip bottom chambers or on normal slides with appropriate spacers with apical surface facing the coverslip bottom in the same media (Sui et al., 2018). Laser ablation was performed using a Zeiss LSM780 microscope equipped with an 800 nm multiphoton femtosecond pulsed Mai Tai laser under a 63X/1.4 oil immersion objective (3-zoom). A reduced area of 13x13 microns was used for the acquisition, and a linear horizontal ROI of approximately 2.5-3.8 microns spanning one cell was ablated using laser power between 45-50%. Single slice images of apical cell edges were acquired using the GFP channel, and ablation was performed after 3 frames. Imaging was continued for at least 50 frames after ablations, with a frame duration of 0.57 seconds, except for the frame immediately following an ablation event, which had a duration of 0.65 seconds. Care was taken to only ablate the ROI and not to damage the cells.

2.6 Quantification of laser ablation

The vertices of the ablated cell edges in the recorded images were tracked manually using Fiji (ImageJ) (Schindelin et al., 2012). To determine the initial mean displacement, we measured the increase in vertex distance between the time point just before ablation (t=0s) and the first image acquired 0.64 seconds after ablation. The initial recoil velocity was calculated by dividing the initial displacement by 0.65 seconds (Sui et al., 2018). This average recoil velocity serves as an indicator of the relative mechanical tension on the cell edge before ablation.

2.7 Cell height measurement

Respective imaginal discs stained with phalloidin and DAPI were mounted carefully on coverslips without flattening. The discs were acquired with a Leica SP8 confocal system using 63X/1.40 oil objective and 2.5 zoom. Z-stacks of 0.4-microns interval were captured. Cell height of the disc proper epithelial cells was determined using the 'straight line' selection tool in ImageJ on orthogonal projections of the Z-stacks.

2.8 Cell apical area measurement

Discs expressing DE-cadherin GFP or stained with E-cadherin were used to measure the cell apical area. The wing and haltere discs were mounted with an apical side facing the objective. Apical sections of DP cells were acquired with Leica SP8 63x/1.40 Oil, 2.5 zoom and 0.4-micron step size. To analyse the cell apical area, at least three ROIs of 15X15 microns within the pouch region of each disc were analysed. 4 slices were Z-projected to accurately measure the cell size as the pouch has a curvature. For all images, Gaussian blur is set to 0.5, and the background is subtracted to rolling 50, to get clear cell boundaries for segmentation. The cells were then segmented using an ImageJ plugin - Tissue analyzer (Aigouy et al., 2016).

2.9 Measurement of fluorescent intensities

To quantify the apical fluorescent intensities of Actin and Myosin-II in the DP cells of the imaginal wing and haltere discs, at least three ROIs of 5X5 micron square were randomly selected within the pouch region. the first 12 apical confocal z-sections of DP acquired with 0.4-micron interval were carefully selected and projected using the sum of slices function in Fiji (ImageJ). Within the 5x5 ROIs, smaller ROIs of 1-micron squares were placed on cell membranes randomly, and the mean intensity was measured. Fluorescence intensity at these edges were calculated manually using Fiji with an in-house macro. To determine the average fluorescence for each disc, mean intensity values along each disc were normalised relative to the average total intensity fluorescence observed in control haltere discs of the same set.

2.10 Cell volume analysis

Three 15X15 um^2 ROIs were chosen arbitrarily from the pouch region of confocal Z-stacks of both the wing and haltere discs that were stained for F-Actin. The mean cell height of Disc proper epithelial cells of each ROI was obtained by averaging over five measurements taken for each ROI. The number of cells in each ROI was estimated using the Tissue Analyser plugin in Fiji and corrected manually for boundary cells. The mean cell volume of the Disc proper epithelial cells for each ROI was obtained by multiplying the mean cell height of epithelial cells with the area of the ROI (i.e. 225 um^2), to obtain the pouch volume of epithelial cells of the ROI. This product was divided with the number of cells in each ROI to obtain the mean cell volume, which was then averaged over three independent ROIs to report the volume of the disc cells.

2.11 Scanning electron microscopy

Scanning electron microscopy (SEM) was carried out on Carl Zeiss EVO LS10 Scanning Electron Microscope Zeiss using Axiovision 4.8.2 software to operate the microscope and for image analysis. Fresh samples of flies were cleaned with 70% ethanol, flash-freezed and were directly used for imaging.

2.12 Adult cuticle preparation

Female adult flies of specified genotypes were collected and sequentially dehydrated in 10%, 50%, 70%, and 100% ethanol for 1 hour each. The flies were then left in clove oil for overnight. The wing and halteres were dissected and mounted in DPX mountant.

2.13 Measurement of trichome density

Bright field Images of adult haltere cuticles were taken using Zeiss Apotome microscope at 40X magnification. Ten wing blade or haltere capitellum per each genotype were analysed. The number of trichomes in three different ROIs of 30X30 micron square area (of wing blade or capitellum) per sample were manually estimated using Image J software.

2.14 RNA Sequencing sample preparation and analysis:

ap GAL4 driven with GFP and the Yki driver (as previously described) wing and haltere discs were dissected in chilled PBS and transferred immediately to TRIzol. Approximately 350 and 250 haltere discs and 150 and 70 wing discs per genotype per replicate were dissected for the control and Yki driver, respectively. The respective numbers were standardised by isolating the RNA to yield >1µg of total RNA. The Sequencing was performed with four replicates using an Illumina sequencing platform. FASTQC software was used to check the quality of raw sequence data. Raw fastq files were aligned to the dm6 genome using HiSAT2 software, sorted using the samtools software and read counting done using HTSeq software. The edgeR software was used to identify differentially expressed genes between the wing and haltere using a cutoff of Log FC values (fold change) with a 1.5 and a minimum count per million values (CPM) of 1, into upregulated, downregulated, and not differentially regulated.

2.15 STRING analysis

STRING analysis was performed using the online tool https://string-db.org/. For all the analyses performed in this study, we applied a stringent high confidence (0.007) and MCL clustering was applied for generating the STRING network output.

2.17 Mathematical details of the model

The lateral cut vertex model is similar to the standard apical 2D vertex model. Each cell is formed of four vertices that are connected with four edges. There are three types of cell boundaries, apical, lateral and basal, with contractilities or line tensions given by $\lambda_a, \lambda_b, \lambda_l$. In our model, the apical and basal boundaries also have linear springs of stiffness k_a and k_b, respectively, that idealize the mechanical resistance of ECM at these locations — the rest length of these springs l_{0a} and l_{0b} are equal to the corresponding edge lengths at the start of the simulation. The preferred size of individual cell is A_{0c} and the corresponding stiffness is K_c. In the case of the haltere, there is a central lumen that is idealised as a single cell of

stiffness K_l and preferred area A_{0l} (Figure 2b, central blue cell). The work function of the system is given by

$$W = \sum_{\alpha} \frac{1}{2} K_c (A_\alpha - A_{0c})^2 + \sum_{\alpha\beta} \left[\lambda_{\alpha\beta} l_{\alpha\beta} + \frac{1}{2} k_{\alpha\beta} (l_{\alpha\beta} - l_{0\alpha\beta})^2 \right] + \frac{1}{2} K_l (A_l - A_{0l})^2.$$

Here, the index α goes over all over the cells and the index $\alpha\beta$ correspond to an edge that is shared between cells α and β. Note that, as discussed above, lumen is also considered to be a cell. The dynamics of lumen can be controlled by increasing or decreasing the preferred lumen size $A_{0l}(t)$ as a function of time. For the case of wing, a thin layer of cells (Figure 2a, thin blue layer of cells) are interpreted to be the cohesive zone between the top and bottom layers of the wing epithelium. In this case, the addition to the work function above has terms of the form these central layer of cells is given an area modulus

$$\Delta W = \sum_{\gamma} \frac{1}{2} K_{adh} (A - A_{0adh})^2 + \sum_{\gamma\omega} \frac{1}{2} k_{adh} (l - l_{0adh})^2$$

where K_{adh} is the size modulus of the central cells, which k_{adh} is the spring constant of the springs along the vertical edges that resists separation between the top and the bottom layer. This is a pretty crude way of implementing the adhesion between the top and the bottom layer, but it does the job well qualitatively.

2.16 Statistical analysis

Experiments were performed with at least four biological replicas. Statistical analysis of data was performed using the GraphPad Prism 5 software. The average and standard deviation were represented in the graphs. Unpaired t-tests were used to determine whether distribution means are significantly different between wing and haltere experiments in normally distributed data. One way ANOVA was used to determine the significance when more than two samples were analysed. Mann-Whitney test and Kruskal-Wallis test were used in case of not normally distributed data. All the tests were done using GraphPad Prism 8.4.3 software. ns, not significant, *p < 0.05, **p < 0.01, ***p < 0.001, ****p < 0.0001.

ANNEXURE

Transcriptome analysis of Yki overexpressing halteres

We conducted a transcriptome analysis to identify genes that are differentially expressed between wing and haltere third instar larval imaginal discs upon upregulation of Yki. We used ap-UAS GFP expressing WT wing and haltere discs as a baseline for genes expression. The respective wing and haltere discs were dissected in 4˚C, transferred immediately to the TRIzol solution and then frozen. Three biological replicates for the control and Yki overexpressing wings are a part of the previously published study in our lab (Nagarkar et al., 2020). Four independent biological replicates were used for the control and the Yki halteres. Both the samples were prepared together and sequenced using Illumina platform. The raw fastq reads were aligned to the *Drosophila* genome (dm6), and the edgeR software was employed to detect genes with differential expression between the two tissue types upon Yki overexpression.

We compared the gene expression between control and Yki overexpressing wings (also referred to as Yki wing) to the differentially expressed genes of the control and Yki overexpressing halteres. In other words, we compared the genes that were upregulated and downregulated in Yki wings (relative to the *ap*-GAL4 control) with the set of genes that were upregulated or downregulated in the Yki halteres (relative to the *ap*-GAL4 control). We have categorized the genes based on their Log FC values (fold change) with a 1.5 cut-off and a minimum count per million values (CPM) of 1, into upregulated, downregulated, and not differentially regulated.

Genes up and downregulated in Yki halteres compared to Yki wing (all w.r.t to control)

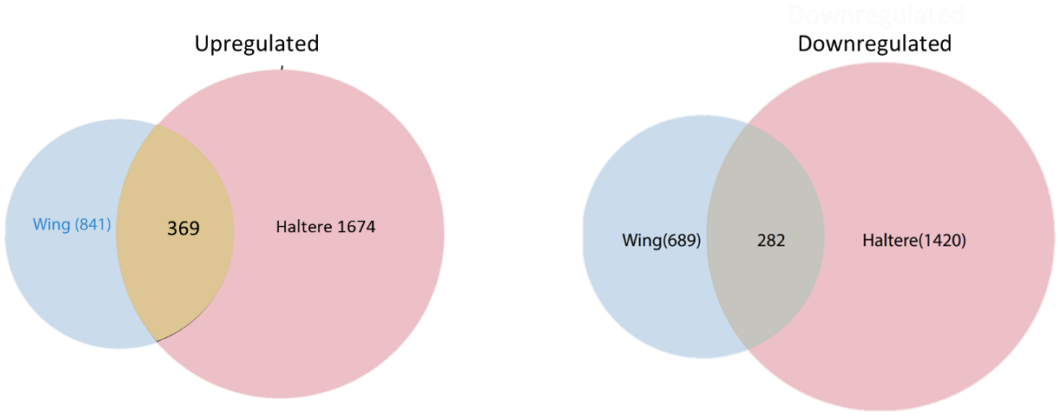

Figure 8.1 Comparison of genes differentially expressed in Yki overexpressing wing and haltere tissues. Venn diagram showing the up (left) and downregulated (right) genes in Yki expressing wing and halteres. The total number of transcripts identified and the genes common between the two organs are depicted in the respective areas of the Venn diagram.

We compared the up and downregulated genes between the Yki overexpressing wing and halteres. A total of 841 and 1674 genes were upregulated in the Yki wing and Yki halteres, respectively. Out of which, 369 genes were upregulated in both wing and haltere (Fig 8.1 Venn diagram). Hippo pathway components and Yki responsive genes such as *ex, kibra* and upd's are upregulated. Upon The STRING analysis of these commonly upregulated genes, Hippo pathway components, Double-strand break repair via non-homologous end joining, and Ku70:Ku80 complex & RNA ligase related KEGG pathway and Go terms got enriched (Fig 8.2). It is notable that genes such *as thor, wg, dorsal, ilp8, dorsal interacting protein (dip), tiggrin &Ndg* (components of ECM), *dia* (actin polymerase*), lamC, dif, elf4a* were upregulated in both Yki overexpressing wing and haltere discs. Furthermore, *Ex, dia, dl, thor and ilp8* are direct targets of Yki according to the Yki ChIP data (Oh et al., 2013).

Commonly upregulated 369 genes

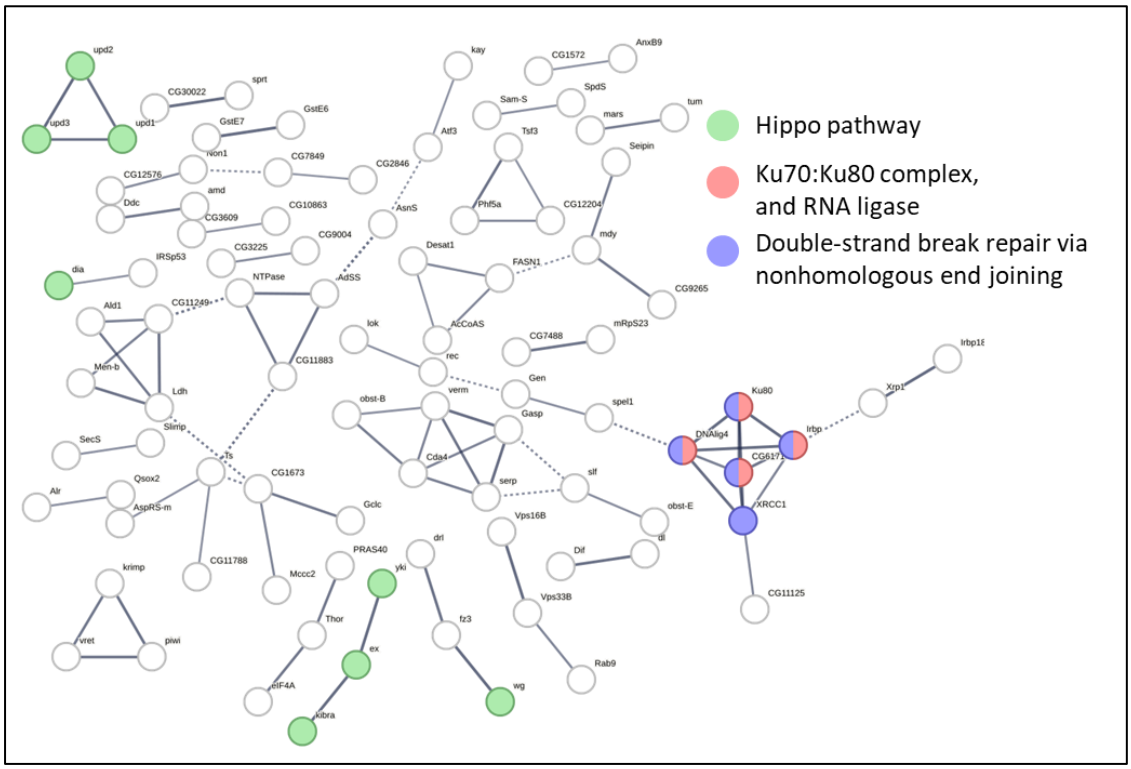

Figure 8.2 STRING map of commonly upregulated genes in Yki expressing wing and haltere discs. For the simplicity, only some of the enriched genes and pathways are highlighted in the above map.

Common downregulated 282

Similarly 282 genes were downregulated in both Yki overexpressing wing and haltere discs compared to the control. We did not observe any particular pathway enrichment in these set of genes with KEGG or DAVID analysis. However, GO terms like RNA polymerase II core promoter proximal region sequence-specific DAN Binding and contractile fiber were picked up. It is interesting to note that twinstar (tsr) which is known to depolymerise actin filaments is downregulated upon Yki expression while dia (role in actin polymerisation) is upregulated. Some of the other genes that are downregulated in Yki wing and haltere are *Np, MMP2, Mp, Sb* (ECM components, except for Mp, they have protease activity); *hr4, hr78 (*ecdysone-related*), nmo, tsr,dac, wnt2, tsh***.**

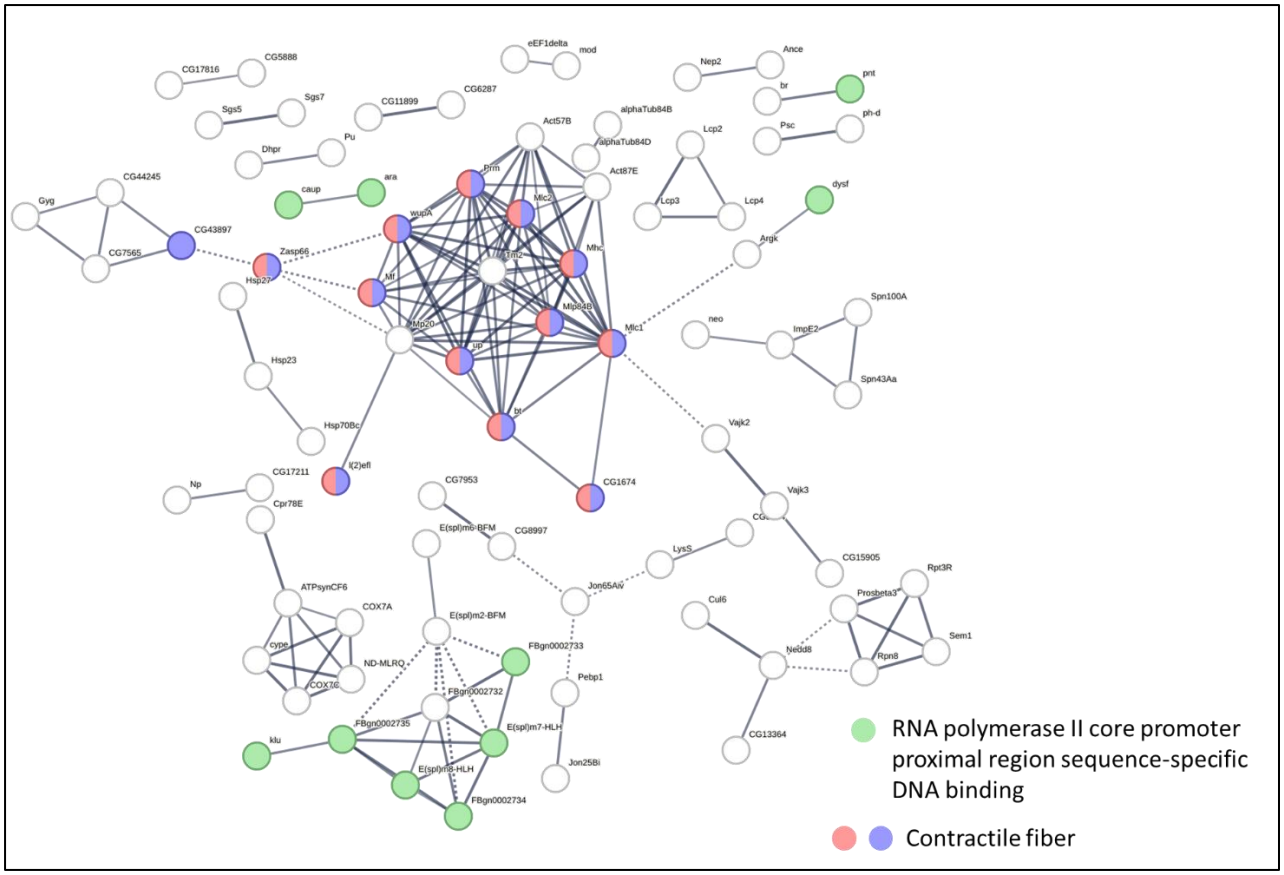

Figure 8.3 STRING map of commonly downregulated genes in Yki expressing wing and haltere discs. No specific pathway enrichment was observed. A subset of the enriched GO terms are colour coded in the above map.

Genes downregulated in Yki haltere and upregulated in Yki wing

Within these datasets, a distinct subset of genes displayed an interesting pattern of upregulation in halteres but downregulation in wings, or vice versa. A total of 98 genes demonstrated differential upregulation in halteres while exhibiting downregulation in wings. While no specific enrichments were observed in terms of KEGG or other pathways, certain enrichments did emerge. Among these, there was enrichment related to processes like the Sulphur compound metabolic process and Cellular amide metabolic process within the GO processes category. Furthermore, in the GO cellular component category, enrichment was observed for Cytosolic ribosomes (Fig 8.4).

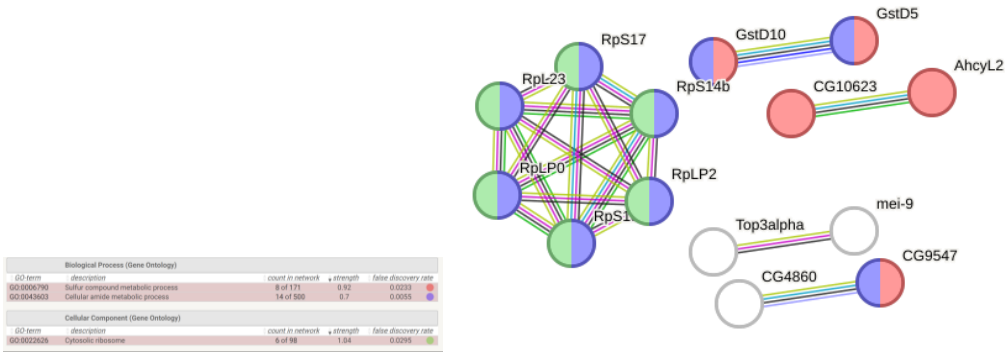

FIGURE 8.4 STRING network of connected genes that are downregulated in haltere and upregulated in Yki wing.

Genes upregulated in Yki haltere and downregulated in Yki wing

81 gene transcripts showed downregulation in Yki halteres, while they were conversely upregulated in Yki wings. Although no distinct biological pathway enrichment was evident, enrichment was observed in functions/terms such as histone acetyltransferase and zinc finger domain, with notable significance. Enrichment extended to terms like the H4 histone acetyl transferase complex, albeit with a less stringent cut-off. Among the candidate genes that emerged from this analysis are *Pten*, *Fas2*, and *Polycomb (pc)*.

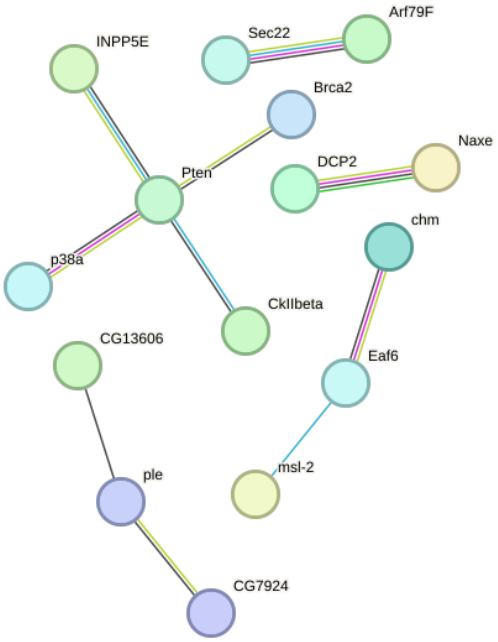

Figure 8.5 STRING network of connected genes that are upregulated in haltere and downregulated in Yki wing. No specific pathways were enriched.

Next, we compared the genes that are exclusively up or downregulated in the halteres and not in wings to the Ubx ChIP targets. There were 97 genes each common between the Ubx ChIP targets and both the upregulated and downregulated transcripts in halteres. We then performed the string analysis on both of these sets separately (Fig 8.6). The functions and pathways enriched are listed in Fig 8.6 A,B. . A Subset of Ubx target genes linked to Wnt signalling and negative regulation of MAP kinase were upregulated in halteres upon Yki overexpression. However, no notable enrichment in terms of biological pathways was observed in the downregulated subset. Expectedly, both categories displayed an enrichment in transcription regulation/activity, a trivial role of hox genes such as Ubx. Note: the string pathways shown here contain only the genes with an enriched hub, and disconnected nodes are hidden from the map for simplicity.

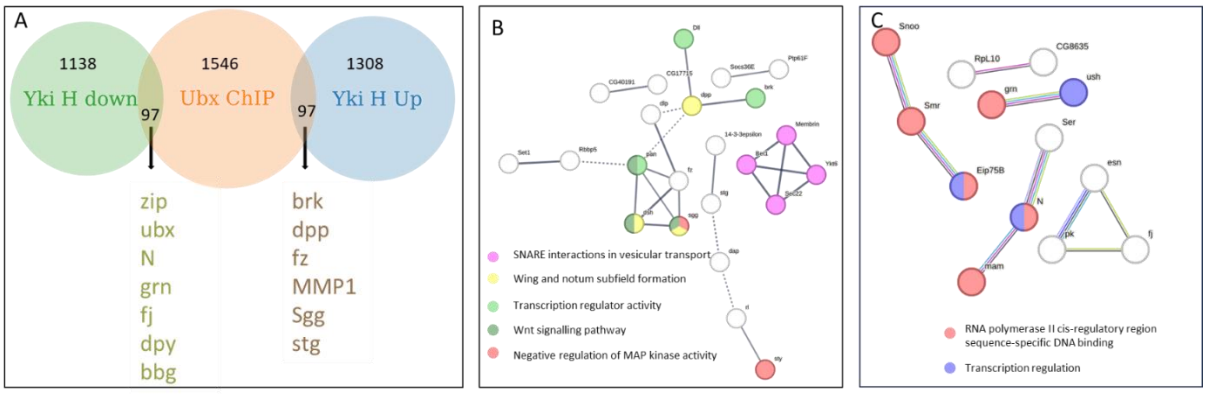

Figure 8.6 A. A Venn diagram showing the comparison of genes differentially expressed exclusively in Yki overexpressing halteres with the Ubx ChIP. The total number of transcripts identified and the genes common between the groups are depicted in the respective areas of the Venn diagram. B, C String map of the genes that are upregulated (B) and downregulated (C) targets of Ubx, respectively.

APPENDIX

Table 1: List of genes that are potential direct targets of both Yki and Ubx

zfh2	H
z	GV1
wun	gukh
wts	Gug
Wnt4	GstS1
Wnt2	GstE12
wdp	grp
vvl	grn
vri	grh
Vha16-1	Gprk1
Vha100-2	goe
vg	GEFmeso
vers	GCS2alpha
ush	galectin
upSET	fz2
unc-13	fz
uif	Fur1
Ugt302C1	ftz-f1
Ubx	fs(1)h
twz	fru
tws	fra
twin	foxo
tun	FoxK
Tsp42Ea	for
Tsp3A	fng
Tsp	fj
tsl	firl
tsh	FER
trx	fax
trh	Fatp3
z	
trc	eyg
tou	ex
Tollo	Ets98B
toe	en
toc	ems
tna	emp
tkv	Eip75B
tio	Eip74EF
tinc	Eip63E
Tg	Egfr
tey	eg
Tep4	edl
tara	ed

Tango8	EcR
T48	ec
Syp	E2f1
sty	E(spl)mbeta-HLH
stg	E(spl)malpha-BFM
ss	E(spl)m2-BFM
Spt20	Dys
spri	Dyrk2
Spn43Aa	dve
Spn100A	Dtg
spin	dsx
spi	drpr
spen	drl
SoxN	Dr
Sox15	dpy
Sox14	dpp
Socs36E	Dp
so	dor
Snoo	DOR
sn	dnt
SMSr	dnc
Smox	Dmtn
Slmap	dlp
sky	Dl
SKIP	dl
siz	Diap1
simj	Deaf1
shot	dco
shn	dap
shg	dan
shf	Dad
sgg	DAAM
serp	Cyp310a1
Ser	CycB
Sema1b	cv-2
Sema1a	cue
sd	ctrip
Scr	CtBP
Scp1	crp
SCaMC	crol
sca	corto
sba	corn
Sb	comm2
Samuel	ckn
salm	Cklalpha

S	cic
Rx	Cht5
rux	chn
rut	CHKov1
rpr	chinmo
RpL15	CHES-1-like
RpL13	CG9932
robo2	CG9896
rl	CG9674
RhoU	CG9596
RhoGAP18B	CG9331
Rho1	CG9328
rgn	CG9205
raw	CG8635
ras	CG8306
Raf	CG8170
Rac2	CG7741
qsm	CG7720
pyd	CG7702
pxb	CG7011
px	CG6966
pum	CG6959
Pu	CG6891
Ptp99A	CG6739
Ptp10D	CG6465
ptc	CG6163
Psc	CG6145
Psa	CG6051
ps	CG6006
pros	CG5953
Ppn	CG5888
Ppa	CG5521
Poxm	CG5346
pot	CG5001
pnt	CG4914
PNPase	CG4766
Pli	CG42797
plh	CG42788
pk	CG42673
Pits	CG42336
Pisd	CG42306
ph-p	CG41099
ph-d	CG4080
Pgant9	CG3919
Pgant6	CG3842

Pepck2	CG3726
Pep	CG34398
pdm3	CG34347
Pdk1	CG3328
pdgy	CG32982
Pde11	CG32365
pan	CG32264
Paics	CG31869
osa	CG31612
Orct2	CG31495
Optix	CG30103
olf413	CG30089
ogre	CG30069
oc	CG2528
numb	CG2003
nub	CG18766
Ntan1	CG18508
Ns1	CG17834
nrv1	CG17715
Notum	CG17691
noc	CG17544
nmo	CG16721
nkd	CG14830
ND-AGGG	CG14505
Ncc69	CG14502
nab	CG14478
N	CG14434
Myo61F	CG14304
mthl8	CG13252
mtgo	CG13204
mtd	CG11905
Msp300	CG11883
msi	CG1146
Mrtf	CG11247
mol	CG11170
modSP	CG10939
mnd	CG10428
Mmp2	CenG1A
Mkp3	CD98hc
mirr	caup
mid	Calr
MFS14	CAHbeta
mey	C1GalTA
mew	bun
MEP-1	Btk29A

melt	bs
Mekk1	brk
Marf1	brat
mam	bowl
magu	boi
lwr	blow
LpR2	blot
lncRNA:CR34052	Blimp-1
lncRNA:CR34006	bif
lncRNA:CR31647	bib
lncRNA:CR13130	bi
Lmpt	B-H2
lbl	beat-IIIc
LanA	BEAF-32
Lac	bbg
l(3)L1231	bab2
l(2)09851	bab1
kuz	ATbp
kst	ASPP
ko	Art4
knrl	Arpc2
klar	Arl8
kibra	ara
kek5	apt
kek1	aos
Kdm2	aop
kay	Antp
Kank	alt
Kal1	alpha-Man-Ia
jim	al
JIL-1	Akap200
jar	AGO3
inv	Adf1
IntS6	14-3-3epsilon
Inos	
ImpL2	
hth	
Hs6st	
hng3	
Hnf4	
HmgZ	
hh	
heph	
hdc	
HDAC4	

Haspin	
H15	
h	

REFERENCES

Agrawal, P., Habib, F., Yelagandula, R., & Shashidhara, L. S. (2011). Genome-level identification of targets of Hox protein Ultrabithorax in Drosophila: novel mechanisms for target selection. *Scientific Reports*, *1*(1), 205. https://doi.org/10.1038/srep00205

Aigouy, B., Umetsu, D., & Eaton, S. (2016). Segmentation and Quantitative Analysis of Epithelial Tissues. *Methods in Molecular Biology (Clifton, N.J.)*, *1478*, 227–239. https://doi.org/10.1007/978-1-4939-6371-3_13

Akam, M. (1998). Hox genes: From master genes to micromanagers. *Current Biology*, *8*(19), R676–R678. https://doi.org/10.1016/S0960-9822(98)70433-6

Aldaz, S., Escudero, L. M., & Freeman, M. (2010). Live imaging of *Drosophila* imaginal disc development. *Proceedings of the National Academy of Sciences*, *107*(32), 14217–14222. https://doi.org/10.1073/pnas.1008623107

Aza-Blanc, P. (1999). Ci: a complex transducer of the Hedgehog signal. *Trends in Genetics*, *15*(11), 458–462. https://doi.org/10.1016/S0168-9525(99)01869-7

Bardet, P.-L., Guirao, B., Paoletti, C., Serman, F., Léopold, V., Bosveld, F., Goya, Y., Mirouse, V., Graner, F., & Bellaïche, Y. (2013). PTEN Controls Junction Lengthening and Stability during Cell Rearrangement in Epithelial Tissue. *Developmental Cell*, *25*(5), 534–546. https://doi.org/10.1016/j.devcel.2013.04.020

Beira, J. V., & Paro, R. (2016). The legacy of Drosophila imaginal discs. *Chromosoma*, *125*(4), 573–592. https://doi.org/10.1007/s00412-016-0595-4

Bennett, F. C., & Harvey, K. F. (2006). Fat Cadherin Modulates Organ Size in Drosophila via the Salvador/Warts/Hippo Signaling Pathway. *Current Biology*, *16*(21), 2101–2110. https://doi.org/10.1016/j.cub.2006.09.045

Brook, W. J., Diaz-Benjumea, F. J., & Cohen, S. M. (1996). ORGANIZING SPATIAL PATTERN IN LIMB DEVELOPMENT. *Annual Review of Cell and Developmental Biology*, *12*(1), 161–180. https://doi.org/10.1146/annurev.cellbio.12.1.161

Cabrera, C. V., Botas, J., & Garcia-Bellido, A. (1985). Distribution of Ultrabithorax proteins in mutants of Drosophila bithorax complex and its transregulatory genes. *Nature*, *318*(6046), 569–571. https://doi.org/10.1038/318569a0

Carroll, S. B. (1995). Homeotic genes and the evolution of arthropods and chordates. *Nature*, *376*(6540), 479–485. https://doi.org/10.1038/376479a0

Castelli-Gair, J. E., Micol, J. L., & García-Bellido, A. (1990). Transvection in the Drosophila Ultrabithorax gene: a Cbx1 mutant allele induces ectopic expression of a normal allele in trans. *Genetics*, *126*(1), 177–184. https://doi.org/10.1093/genetics/126.1.177

Chan, C. J., Heisenberg, C.-P., & Hiiragi, T. (2017). Coordination of Morphogenesis and Cell-Fate Specification in Development. *Current Biology*, *27*(18), R1024–R1035. https://doi.org/https://doi.org/10.1016/j.cub.2017.07.010

Charroux, B., Freeman, M., Kerridge, S., & Baonza, A. (2006). Atrophin contributes to the negative regulation of epidermal growth factor receptor signaling in Drosophila. *Developmental Biology*, *291*(2), 278–290. https://doi.org/10.1016/j.ydbio.2005.12.012

Chen, C.-Y., Chen, J., He, L., & Stiles, B. L. (2018). PTEN: Tumor Suppressor and Metabolic Regulator. *Frontiers in Endocrinology*, *9*. https://doi.org/10.3389/fendo.2018.00338

Conte, V., Ulrich, F., Baum, B., Muñoz, J., Veldhuis, J., Brodland, W., & Miodownik, M. (2012). A Biomechanical Analysis of Ventral Furrow Formation in the Drosophila Melanogaster Embryo. *PLoS ONE*, *7*(4), e34473. https://doi.org/10.1371/journal.pone.0034473

Crickmore, M. A., & Mann, R. S. (2006). Hox Control of Organ Size by Regulation of Morphogen Production and Mobility. *Science*, *313*(5783), 63–68. https://doi.org/10.1126/science.1128650

Crickmore, M. A., & Mann, R. S. (2007). Hox control of morphogen mobility and organ development through regulation of glypican expression. *Development*, *134*(2), 327–334. https://doi.org/10.1242/dev.02737

Crossman, S. H., Streichan, S. J., & Vincent, J.-P. (2018). EGFR signaling coordinates patterning with cell survival during Drosophila epidermal development. *PLOS Biology*, *16*(10), e3000027. https://doi.org/10.1371/journal.pbio.3000027

De las Heras, J. M., García-Cortés, C., Foronda, D., Pastor-Pareja, J. C., Shashidhara, L. S., & Sánchez-Herrero, E. (2018). The Drosophila Hox gene Ultrabithorax controls appendage shape by regulating extracellular matrix dynamics. *Development*, *145*(13). https://doi.org/10.1242/dev.161844

de Navas, L. F., Garaulet, D. L., & Sánchez-Herrero, E. (2006). The Ultrabithorax Hox gene of Drosophila controls haltere size by regulating the Dpp pathway. *Development*, *133*(22), 4495–4506. https://doi.org/10.1242/dev.02609

Diaz de la Loza, M. C., & Thompson, B. J. (2017). Forces shaping the Drosophila wing. *Mechanisms of Development*, *144*, 23–32. https://doi.org/10.1016/j.mod.2016.10.003

Diaz-Benjumea, F. (1993). Interaction between dorsal and ventral cells in the imaginal disc directs wing development in Drosophila. *Cell*, *75*(4), 741–752. https://doi.org/10.1016/0092-8674(93)90494-B

Diaz-de-la-Loza, M.-C., Loker, R., Mann, R. S., & Thompson, B. J. (2020). Control of tissue morphogenesis by the HOX gene *Ultrabithorax*. *Development*, *147*(5). https://doi.org/10.1242/dev.184564

Diaz-de-la-Loza, M.-C., Ray, R. P., Ganguly, P. S., Alt, S., Davis, J. R., Hoppe, A., Tapon, N., Salbreux, G., & Thompson, B. J. (2018). Apical and Basal Matrix Remodeling Control Epithelial Morphogenesis. *Developmental Cell*, *46*(1), 23-39.e5. https://doi.org/10.1016/j.devcel.2018.06.006

Díaz-de-la-Loza, M.-C., & Stramer, B. M. (2024). The extracellular matrix in tissue morphogenesis: No longer a backseat driver. *Cells & Development*, *177*, 203883. https://doi.org/10.1016/j.cdev.2023.203883

Domínguez-Giménez, P., Brown, N. H., & Martín-Bermudo, M. D. (2007). Integrin-ECM interactions regulate the changes in cell shape driving the morphogenesis of the *Drosophila* wing epithelium. *Journal of Cell Science*, *120*(6), 1061–1071. https://doi.org/10.1242/jcs.03404

Erkner, A., Roure, A., Charroux, B., Delaage, M., Holway, N., Coré, N., Vola, C., Angelats, C., Pagès, F., Fasano, L., & Kerridge, S. (2002). Grunge, related to human Atrophin-like proteins, has multiple functions in *Drosophila* development. *Development*, *129*(5), 1119–1129. https://doi.org/10.1242/dev.129.5.1119

Etournay, R., Popović, M., Merkel, M., Nandi, A., Blasse, C., Aigouy, B., Brandl, H., Myers, G., Salbreux, G., Jülicher, F., & Eaton, S. (2015). Interplay of cell dynamics and epithelial tension during morphogenesis of the Drosophila pupal wing. *ELife*, *4*. https://doi.org/10.7554/eLife.07090

Farhadifar, R., Röper, J.-C., Aigouy, B., Eaton, S., & Jülicher, F. (2007). The Influence of Cell Mechanics, Cell-Cell Interactions, and Proliferation on Epithelial Packing. *Current Biology*, *17*(24), 2095–2104. https://doi.org/10.1016/j.cub.2007.11.049

Fernández, B. G., Gaspar, P., Brás-Pereira, C., Jezowska, B., Rebelo, S. R., & Janody, F. (2011a). Actin-Capping Protein and the Hippo pathway regulate F-actin and tissue growth in Drosophila. *Development*, *138*(11), 2337–2346. https://doi.org/10.1242/dev.063545

Fernandez-Gonzalez, R., Simoes, S. de M., Röper, J.-C., Eaton, S., & Zallen, J. A. (2009). Myosin II Dynamics Are Regulated by Tension in Intercalating Cells. *Developmental Cell*, *17*(5), 736–743. https://doi.org/10.1016/j.devcel.2009.09.003

Fristrom, D., & Fristrom, J. W. (1975). The mechanism of evagination of imaginal discs of Drosophila melanogaster. *Developmental Biology*, *43*(1), 1–23. https://doi.org/10.1016/0012-1606(75)90127-X

Fristrom, D., Gotwals, P., Eaton, S., Kornberg, T. B., Sturtevant, M., Bier, E., & Fristrom, J. W. (1994). *blistered* : a gene required for vein/intervein formation in wings of *Drosophila*. *Development*, *120*(9), 2661–2671. https://doi.org/10.1242/dev.120.9.2661

Fristrom, D., Wilcox, M., & Fristrom, J. (1993a). The distribution of PS integrins, laminin A and F-actin during key stages in *Drosophila* wing development. *Development*, *117*(2), 509–523. https://doi.org/10.1242/dev.117.2.509

Fuhrmann, J. F., Krishna, A., Paijmans, J., Duclut, C., Eaton, S., Popović, M., Jülicher, F., Modes, C. D., & Dye, N. A. (2024). Active shape programming drives Drosophila wing disc eversion. *BioRxiv*, 2023.12.23.573034. https://doi.org/10.1101/2023.12.23.573034

Fulford, A. D., Enderle, L., Rusch, J., Hodzic, D., Holder, M. V., Earl, A., Oh, R. H., Tapon, N., & McNeill, H. (2023). Expanded directly binds conserved regions of Fat to restrain growth via the Hippo pathway. *Journal of Cell Biology*, *222*(5). https://doi.org/10.1083/jcb.202204059

Fulford, A. D., Holder, M. V, Frith, D., Snijders, A. P., Tapon, N., & Ribeiro, P. S. (2019). Casein kinase 1 family proteins promote Slimb-dependent Expanded degradation. *ELife*, *8*. https://doi.org/10.7554/eLife.46592

Galant, R., Walsh, C. M., & Carroll, S. B. (2002). Hox repression of a target gene: extradenticle-independent, additive action through multiple monomer binding sites. *Development*, *129*(13), 3115–3126. https://doi.org/10.1242/dev.129.13.3115

Gao, X., Neufeld, T. P., & Pan, D. (2000). Drosophila PTEN Regulates Cell Growth and Proliferation through PI3K-Dependent and -Independent Pathways. *Dev Biol*, *221*(2), 404–418. https://doi.org/https://doi.org/10.1006/dbio.2000.9680

Gilmour, D., Rembold, M., & Leptin, M. (2017). From morphogen to morphogenesis and back. *Nature*, *541*(7637), 311–320. https://doi.org/10.1038/nature21348

Gjorevski, N., & Nelson, C. M. (2010). The mechanics of development: Models and methods for tissue morphogenesis. *Birth Defects Research Part C: Embryo Today: Reviews*, *90*(3), 193–202. https://doi.org/10.1002/bdrc.20185

Goberdhan, D. C. I., Paricio, N., Goodman, E. C., Mlodzik, M., & Wilson, C. (1999). Drosophila tumor suppressor PTEN controls cell size and number by antagonizing the Chico/PI3-kinase signaling pathway. *Genes & Development*, *13*(24), 3244–3258. https://doi.org/10.1101/gad.13.24.3244

Gokhale, R. H., & Shingleton, A. W. (2015). Size control: the developmental physiology of body and organ size regulation. *WIREs Developmental Biology*, *4*(4), 335–356. https://doi.org/10.1002/wdev.181

Goodman, F., & Scambler, P. (2001). Human *HOX* gene mutations. *Clinical Genetics*, *59*(1), 1–11. https://doi.org/10.1034/j.1399-0004.2001.590101.x

Groth, C., Vaid, P., Khatpe, A., Prashali, N., Ahiya, A., Andrejeva, D., Chakladar, M., Nagarkar, S., Paul, R., Kelkar, D., Eichenlaub, T., Herranz, H., Sridhar, T. S., Cohen, S. M., & Shashidhara, L. S. (2020). Genome-Wide Screen for Context-Dependent Tumor Suppressors Identified Using in Vivo Models for Neoplasia in Drosophila. *G3 (Bethesda)*, *10*(9), 2999–3008. https://doi.org/10.1534/g3.120.401545

Hariharan, I. K. (2015). Organ Size Control: Lessons from Drosophila. *Developmental Cell*, *34*(3), 255–265. https://doi.org/10.1016/j.devcel.2015.07.012

Harmansa, S., Erlich, A., Eloy, C., Zurlo, G., & Lecuit, T. (2023). Growth anisotropy of the extracellular matrix shapes a developing organ. *Nature Communications*, *14*(1), 1220. https://doi.org/10.1038/s41467-023-36739-y

Heer, N. C., & Martin, A. C. (2017). Tension, contraction and tissue morphogenesis. *Development*, *144*(23), 4249–4260. https://doi.org/10.1242/dev.151282

Heisenberg, C.-P., & Bellaïche, Y. (2013). Forces in Tissue Morphogenesis and Patterning. *Cell*, *153*(5), 948–962. https://doi.org/10.1016/j.cell.2013.05.008

Hersh, B. M., & Carroll, S. B. (2005). Direct regulation of knot gene expression by Ultrabithorax and the evolution of cis-regulatory elements in *Drosophila*. *Development*, *132*(7), 1567–1577. https://doi.org/10.1242/dev.01737

Hueber, S. D., Weiller, G. F., Djordjevic, M. A., & Frickey, T. (2010). Improving Hox Protein Classification across the Major Model Organisms. *PLOS ONE*, *5*(5), e10820-. https://doi.org/10.1371/journal.pone.0010820

Hughes, C. L., & Kaufman, T. C. (2002). Hox genes and the evolution of the arthropod body plan. *Evolution and Development*, *4*(6), 459–499. https://doi.org/10.1046/j.1525-142X.2002.02034.x

Ingham, P. W., & McMahon, A. P. (2001). Hedgehog signaling in animal development: paradigms and principles. *Genes & Development*, *15*(23), 3059–3087. https://doi.org/10.1101/gad.938601

Irvine, K. D., & Harvey, K. F. (2015). Control of Organ Growth by Patterning and Hippo Signaling in *Drosophila*. *Cold Spring Harbor Perspectives in Biology*, *7*(6), a019224. https://doi.org/10.1101/cshperspect.a019224

J. Durston, A., Wacker, S., Bardine, N., & J. Jansen, H. (2012). Time Space Translation: A Hox Mechanism for Vertebrate A-P Patterning. *Current Genomics*, *13*(4), 300–307. https://doi.org/10.2174/138920212800793375

Jia, J., Zhang, W., Wang, B., Trinko, R., & Jiang, J. (2003). The *Drosophila* Ste20 family kinase dMST functions as a tumor suppressor by restricting cell proliferation and promoting apoptosis. *Genes & Development*, *17*(20), 2514–2519. https://doi.org/10.1101/gad.1134003

Khan, S., Dilsha, C., & Shashidhara, L. S. (2020). Haltere development in D. melanogaster: implications for the evolution of appendage size, shape and function. *Int J Dev Biol*, *64*(1-2–3), 159–165. https://doi.org/10.1387/ijdb.190133LS

Khan, S., Pradhan, S. J., Giraud, G., Bleicher, F., Paul, R., Merabet, S., & Shashidhara, L. S. (2023). A Micro-evolutionary Change in Target Binding Sites as a Key Determinant of Ultrabithorax Function in Drosophila. *Journal of Molecular Evolution*. https://doi.org/10.1007/s00239-023-10123-2

Kozyrina, A. N., Piskova, T., & Di Russo, J. (2020). Mechanobiology of Epithelia From the Perspective of Extracellular Matrix Heterogeneity. *Frontiers in Bioengineering and Biotechnology*, *8*. https://doi.org/10.3389/fbioe.2020.596599

Lai, Z.-C., Wei, X., Shimizu, T., Ramos, E., Rohrbaugh, M., Nikolaidis, N., Ho, L.-L., & Li, Y. (2005). Control of Cell Proliferation and Apoptosis by Mob as Tumor Suppressor, Mats. *Cell*, *120*(5), 675–685. https://doi.org/10.1016/j.cell.2004.12.036

Le Parco, Y., Knibiehler, B., Cecchini, J. P., & Mirre, C. (1986). Stage and tissue-specific expression of a collagen gene during Drosophila melanogaster development. *Experimental Cell Research*, *163*(2), 405–412. https://doi.org/10.1016/0014-4827(86)90071-6

LeBlanc, L., Ramirez, N., & Kim, J. (2021). Context-dependent roles of YAP/TAZ in stem cell fates and cancer. *Cellular and Molecular Life Sciences*, *78*(9), 4201–4219. https://doi.org/10.1007/s00018-021-03781-2

Lewis, E. B. (1978). A Gene Complex Controlling Segmentation in Drosophila. In *Genes, Development, and Cancer* (pp. 229–242). Springer Netherlands. https://doi.org/10.1007/978-1-4020-6345-9_10

Ling, C., Zheng, Y., Yin, F., Yu, J., Huang, J., Hong, Y., Wu, S., & Pan, D. (2010). The apical transmembrane protein Crumbs functions as a tumor suppressor that regulates Hippo signaling by binding to Expanded. *Proceedings of the National Academy of Sciences*, *107*(23), 10532–10537. https://doi.org/10.1073/pnas.1004279107

Liu, P., Guo, Y., Xu, W., Song, S., Li, X., Wang, X., Lu, J., Guo, X., Richardson, H. E., & Ma, X. (2022). Ptp61F integrates Hippo, TOR, and actomyosin pathways to control three-dimensional organ size. *Cell Reports*, *41*(7), 111640. https://doi.org/10.1016/j.celrep.2022.111640

Luciano, M., Versaevel, M., Vercruysse, E., Procès, A., Kalukula, Y., Remson, A., Deridoux, A., & Gabriele, S. (2022). Appreciating the role of cell shape changes in the mechanobiology of epithelial tissues. *Biophysics Reviews*, *3*(1). https://doi.org/10.1063/5.0074317

Makhijani, K., Kalyani, C., Srividya, T., & Shashidhara, L. S. (2007). Modulation of Decapentaplegic gradient during haltere specification in Drosophila. *Dev Biol*, *302*(1), 243–255. https://doi.org/10.1016/j.ydbio.2006.09.029

Mammoto, A., Mammoto, T., & Ingber, D. E. (2012). Mechanosensitive mechanisms in transcriptional regulation. *Journal of Cell Science*, *125*(13), 3061–3073. https://doi.org/10.1242/jcs.093005

Martin, A. C., & Goldstein, B. (2014). Apical constriction: themes and variations on a cellular mechanism driving morphogenesis. *Development*, *141*(10), 1987–1998. https://doi.org/10.1242/dev.102228

Miao, H., & Blankenship, J. T. (2020). The pulse of morphogenesis: actomyosin dynamics and regulation in epithelia. *Development*, *147*(17). https://doi.org/10.1242/dev.186502

Michael Akam. (1995). Hox genes and the evolution of diverse body plans. *Philosophical Transactions of the Royal Society of London. Series B: Biological Sciences*, *349*(1329), 313–319. https://doi.org/10.1098/rstb.1995.0119

Miller, C. J., & Davidson, L. A. (2013). The interplay between cell signalling and mechanics in developmental processes. *Nature Reviews Genetics*, *14*(10), 733–744. https://doi.org/10.1038/nrg3513

Mohit, P., Makhijani, K., Madhavi, M. B., Bharathi, V., Lal, A., Sirdesai, G., Reddy, V. R., Ramesh, P., Kannan, R., Dhawan, J., & Shashidhara, L. S. (2006a). Modulation of AP and DV signaling pathways by the homeotic gene Ultrabithorax during haltere development in Drosophila. *Dev Biol*, *291*(2), 356–367. https://doi.org/10.1016/j.ydbio.2005.12.022

Mohit, P., Makhijani, K., Madhavi, M. B., Bharathi, V., Lal, A., Sirdesai, G., Reddy, V. R., Ramesh, P., Kannan, R., Dhawan, J., & Shashidhara, L. S. (2006b). Modulation of AP and DV signaling pathways by the homeotic gene Ultrabithorax during haltere development in Drosophila. *Developmental Biology*, *291*(2), 356–367. https://doi.org/10.1016/j.ydbio.2005.12.022

Murrell, M., Oakes, P. W., Lenz, M., & Gardel, M. L. (2015). Forcing cells into shape: the mechanics of actomyosin contractility. *Nature Reviews Molecular Cell Biology*, *16*(8), 486–498. https://doi.org/10.1038/nrm4012

Nagarkar, S., Wasnik, R., Govada, P., Cohen, S., & Shashidhara, L. S. (2020). Promoter Proximal Pausing Limits Tumorous Growth Induced by the Yki Transcription Factor in *Drosophila*. *Genetics*, *216*(1), 67–77. https://doi.org/10.1534/genetics.120.303419

Natzle, J. E., Monson, J. M., & McCarthy, B. J. (1982). Cytogenetic location and expression of collagen-like genes in Drosophila. *Nature*, *296*(5855), 368–371. https://doi.org/10.1038/296368a0

Nelson, C. M., & Gleghorn, J. P. (2012). Sculpting Organs: Mechanical Regulation of Tissue Development. *Annual Review of Biomedical Engineering*, *14*(1), 129–154. https://doi.org/10.1146/annurev-bioeng-071811-150043

Neufeld, T. P., de la Cruz, A. F. A., Johnston, L. A., & Edgar, B. A. (1998). Coordination of Growth and Cell Division in the Drosophila Wing. *Cell*, *93*(7), 1183–1193. https://doi.org/10.1016/S0092-8674(00)81462-2

Oh, H., Slattery, M., Ma, L., Crofts, A., White, K. P., Mann, R. S., & Irvine, K. D. (2013). Genome-wide Association of Yorkie with Chromatin and Chromatin-Remodeling Complexes. *Cell Reports*, *3*(2), 309–318. https://doi.org/10.1016/j.celrep.2013.01.008

Page-McCaw, A., Ewald, A. J., & Werb, Z. (2007). Matrix metalloproteinases and the regulation of tissue remodelling. *Nature Reviews Molecular Cell Biology*, *8*(3), 221–233. https://doi.org/10.1038/nrm2125

Pallavi, S. K., Kannan, R., & Shashidhara, L. S. (2006). Negative regulation of Egfr/Ras pathway by Ultrabithorax during haltere development in Drosophila. *Dev Biol*, *296*(2), 340–352. https://doi.org/10.1016/j.ydbio.2006.05.035

Pallavi, S. K., & Shashidhara, L. S. (2003). Egfr/Ras pathway mediates interactions between peripodial and disc proper cells in Drosophila wing discs. *Development*, *130*(20), 4931–4941. https://doi.org/10.1242/dev.00719

Pan, D. (2010). The Hippo Signaling Pathway in Development and Cancer. *Developmental Cell*, *19*(4), 491–505. https://doi.org/10.1016/j.devcel.2010.09.011

Pastor-Pareja, J. C., & Xu, T. (2011). Shaping Cells and Organs in Drosophila by Opposing Roles of Fat Body-Secreted Collagen IV and Perlecan. *Developmental Cell*, *21*(2), 245–256. https://doi.org/10.1016/j.devcel.2011.06.026

Pavlopoulos, A., & Akam, M. (2011). Hox gene *Ultrabithorax* regulates distinct sets of target genes at successive stages of *Drosophila* haltere morphogenesis. *Proceedings of the*

National Academy of Sciences, *108*(7), 2855–2860. https://doi.org/10.1073/pnas.1015077108

Pearson, J. C., Lemons, D., & McGinnis, W. (2005). Modulating Hox gene functions during animal body patterning. *Nature Reviews Genetics*, *6*(12), 893–904. https://doi.org/10.1038/nrg1726

Polyakov, O., He, B., Swan, M., Shaevitz, J. W., Kaschube, M., & Wieschaus, E. (2014). Passive Mechanical Forces Control Cell-Shape Change during Drosophila Ventral Furrow Formation. *Biophysical Journal*, *107*(4), 998–1010. https://doi.org/10.1016/j.bpj.2014.07.013

Prasad, M., Bajpai, R., & Shashidhara, L. S. (2003). Regulation of Wingless and Vestigial expression in wing and haltere discs of *Drosophila*. *Development*, *130*(8), 1537–1547. https://doi.org/10.1242/dev.00393

Ribeiro, P., Holder, M., Frith, D., Snijders, A. P., & Tapon, N. (2014). Crumbs promotes expanded recognition and degradation by the SCF $^{Slimb/\beta\text{-}TrCP}$ ubiquitin ligase. *Proceedings of the National Academy of Sciences*, *111*(19). https://doi.org/10.1073/pnas.1315508111

Roch, F., & Akam, M. (2000). Ultrabithorax and the control of cell morphology in Drosophila halteres. *Development*, *127*(1), 97–107. https://doi.org/10.1242/dev.127.1.97

Roffay, C., Chan, C. J., Guirao, B., Hiiragi, T., & Graner, F. (2021). Inferring cell junction tension and pressure from cell geometry. *Development*, *148*(18), dev192773. https://doi.org/10.1242/dev.192773

Rogulja, D., & Irvine, K. D. (2005). Regulation of Cell Proliferation by a Morphogen Gradient. *Cell*, *123*(3), 449–461. https://doi.org/10.1016/j.cell.2005.08.030

Ruiz-Losada, M., Blom-Dahl, D., Córdoba, S., & Estella, C. (2018). Specification and Patterning of Drosophila Appendages. *Journal of Developmental Biology*, *6*(3), 17. https://doi.org/10.3390/jdb6030017

Sánchez-Herrero, E. (2013). Hox Targets and Cellular Functions. *Scientifica*, *2013*, 1–26. https://doi.org/10.1155/2013/738257

Sansores-Garcia, L., Bossuyt, W., Wada, K.-I., Yonemura, S., Tao, C., Sasaki, H., & Halder, G. (2011). Modulating F-actin organization induces organ growth by affecting the Hippo pathway. *The EMBO Journal*, *30*(12), 2325–2335. https://doi.org/https://doi.org/10.1038/emboj.2011.157

Schindelin, J., Arganda-Carreras, I., Frise, E., Kaynig, V., Longair, M., Pietzsch, T., Preibisch, S., Rueden, C., Saalfeld, S., Schmid, B., Tinevez, J.-Y., White, D. J., Hartenstein, V., Eliceiri, K., Tomancak, P., & Cardona, A. (2012). Fiji: an open-source platform for biological-image analysis. *Nature Methods*, *9*(7), 676–682. https://doi.org/10.1038/nmeth.2019

Schnepp, B., Grumbling, G., Donaldson, T., & Simcox, A. (1996). Vein is a novel component in the Drosophila epidermal growth factor receptor pathway with similarity to the

neuregulins. *Genes & Development*, *10*(18), 2302–2313. https://doi.org/10.1101/gad.10.18.2302

Schneuwly, S., Klemenz, R., & Gehring, W. J. (1987). Redesigning the body plan of Drosophila by ectopic expression of the homoeotic gene Antennapedia. *Nature*, *325*(6107), 816–818. https://doi.org/10.1038/325816a0

Shashidhara, L. S., Agrawal, N., Bajpai, R., Bharathi, V., & Sinha, P. (1999a). Negative regulation of dorsoventral signaling by the homeotic gene Ultrabithorax during haltere development in Drosophila. *Dev Biol*, *212*(2), 491–502. https://doi.org/10.1006/dbio.1999.9341

Shilo, B.-Z. (2005). Regulating the dynamics of EGF receptor signaling in space and time. *Development*, *132*(18), 4017–4027. https://doi.org/10.1242/dev.02006

Shingleton, A. W. (2010). The regulation of organ size in Drosophila. *Organogenesis*, *6*(2), 76–87. https://doi.org/10.4161/org.6.2.10375

Silva, E., Tsatskis, Y., Gardano, L., Tapon, N., & McNeill, H. (2006). The Tumor-Suppressor Gene fat Controls Tissue Growth Upstream of Expanded in the Hippo Signaling Pathway. *Current Biology*, *16*(21), 2081–2089. https://doi.org/10.1016/j.cub.2006.09.004

Singh, S., Sanchez-Herrero, E., & Shashidhara, L. S. (2015). Critical role for Fat/Hippo and IIS/Akt pathways downstream of Ultrabithorax during haltere specification in Drosophila. *Mech Dev*, *138 Pt 2*, 198–209. https://doi.org/10.1016/j.mod.2015.07.017

Slattery, M., Ma, L., Négre, N., White, K. P., & Mann, R. S. (2011). Genome-wide tissue-specific occupancy of the Hox protein Ultrabithorax and Hox cofactor Homothorax in Drosophila. *PloS One*, *6*(4), e14686. https://doi.org/10.1371/journal.pone.0014686

Song, S., Herranz, H., & Cohen, S. M. (2017). The chromatin remodeling BAP complex limits tumor promoting activity of the Hippo pathway effector Yki to prevent neoplastic transformation in *Drosophila* epithelia. *Disease Models & Mechanisms*. https://doi.org/10.1242/dmm.030122

Straßburger, K., Tiebe, M., Pinna, F., Breuhahn, K., & Teleman, A. A. (2012). Insulin/IGF signaling drives cell proliferation in part via Yorkie/YAP. *Developmental Biology*, *367*(2), 187–196. https://doi.org/10.1016/j.ydbio.2012.05.008

Sui, L., Alt, S., Weigert, M., Dye, N., Eaton, S., Jug, F., Myers, E. W., Jülicher, F., Salbreux, G., & Dahmann, C. (2018). Differential lateral and basal tension drive folding of Drosophila wing discs through two distinct mechanisms. *Nature Communications*, *9*(1), 4620. https://doi.org/10.1038/s41467-018-06497-3

Sun, T., Song, Y., Teng, D., Chen, Y., Dai, J., Ma, M., Zhang, W., & Pastor-Pareja, J. C. (2021). Atypical laminin spots and pull-generated microtubule-actin projections mediate Drosophila wing adhesion. *Cell Reports*, *36*(10), 109667. https://doi.org/10.1016/j.celrep.2021.109667

Tapon, N., Harvey, K. F., Bell, D. W., Wahrer, D. C. R., Schiripo, T. A., Haber, D. A., & Hariharan, I. K. (2002). salvador Promotes Both Cell Cycle Exit and Apoptosis in

Drosophila and Is Mutated in Human Cancer Cell Lines. *Cell*, *110*(4), 467–478. https://doi.org/10.1016/S0092-8674(02)00824-3

Thompson, J. A. (1917). On Growth and Form. *Nature*, *100*(2498), 21–22. https://doi.org/10.1038/100021a0

Tomoyasu, Y. (2017). Ultrabithorax and the evolution of insect forewing/hindwing differentiation. *Current Opinion in Insect Science*, *19*, 8–15. https://doi.org/10.1016/j.cois.2016.10.007

Tozluoğlu, M., & Mao, Y. (2020). On folding morphogenesis, a mechanical problem. *Philosophical Transactions of the Royal Society B: Biological Sciences*, *375*(1809), 20190564. https://doi.org/10.1098/rstb.2019.0564

Udan, R. S., Kango-Singh, M., Nolo, R., Tao, C., & Halder, G. (2003). Hippo promotes proliferation arrest and apoptosis in the Salvador/Warts pathway. *Nature Cell Biology*, *5*(10), 914–920. https://doi.org/10.1038/ncb1050

Vasquez, C. G., Tworoger, M., & Martin, A. C. (2014). Dynamic myosin phosphorylation regulates contractile pulses and tissue integrity during epithelial morphogenesis. *Journal of Cell Biology*, *206*(3), 435–450. https://doi.org/10.1083/jcb.201402004

Waddington, C. H. (1939). Preliminary Notes on the Development of the Wings in Normal and Mutant Strains of Drosophila. *Proceedings of the National Academy of Sciences*, *25*(7), 299–307. https://doi.org/10.1073/pnas.25.7.299

Wang, L., Charroux, B., Kerridge, S., & Tsai, C. (2008). Atrophin recruits HDAC1/2 and G9a to modify histone H3K9 and to determine cell fates. *EMBO Reports*, *9*(6), 555–562. https://doi.org/10.1038/embor.2008.67

Wang, L., Rajan, H., Pitman, J. L., McKeown, M., & Tsai, C.-C. (2006). Histone deacetylase-associating Atrophin proteins are nuclear receptor corepressors. *Genes & Development*, *20*(5), 525–530. https://doi.org/10.1101/gad.1393506

Wang, L., & Tsai, C.-C. (2008). Atrophin Proteins: An Overview of a New Class of Nuclear Receptor Corepressors. *Nuclear Receptor Signaling*, *6*(1), nrs.06009. https://doi.org/10.1621/nrs.06009

Wang, X., Zhang, Y., & Blair, S. S. (2019). Fat-regulated adaptor protein Dlish binds the growth suppressor Expanded and controls its stability and ubiquitination. *Proceedings of the National Academy of Sciences*, *116*(4), 1319–1324. https://doi.org/10.1073/pnas.1811891116

Weatherbee, S. D., Halder, G., Kim, J., Hudson, A., & Carroll, S. (1998a). Ultrabithorax regulates genes at several levels of the wing-patterning hierarchy to shape the development of the *Drosophila* haltere. *Genes & Development*, *12*(10), 1474–1482. https://doi.org/10.1101/gad.12.10.1474

White, R. A. H., & Akam, M. E. (1985). Contrabithorax mutations cause inappropriate expression of Ultrabithorax products in Drosophila. *Nature*, *318*(6046), 567–569. https://doi.org/10.1038/318567a0

White, R. A. H., & Wilcox, M. (1985). Regulation of the distribution of Ultrabithorax proteins in Drosophila. *Nature*, *318*(6046), 563–567. https://doi.org/10.1038/318563a0

Widmann, T. J., & Dahmann, C. (2009). Dpp signaling promotes the cuboidal-to-columnar shape transition of Drosophila wing disc epithelia by regulating Rho1. *Journal of Cell Science*, *122*(9), 1362–1373. https://doi.org/10.1242/jcs.044271

Yasothornsrikul, S., Davis, W. J., Cramer, G., Kimbrell, D. A., & Dearolf, C. R. (1997). viking: identification and characterization of a second type IV collagen in Drosophila. *Gene*, *198*(1–2), 17–25. https://doi.org/10.1016/S0378-1119(97)00274-6

Yeung, K., Boija, A., Karlsson, E., Holmqvist, P.-H., Tsatskis, Y., Nisoli, I., Yap, D., Lorzadeh, A., Moksa, M., Hirst, M., Aparicio, S., Fanto, M., Stenberg, P., Mannervik, M., & McNeill, H. (2017). Atrophin controls developmental signaling pathways via interactions with Trithorax-like. *ELife*, *6*. https://doi.org/10.7554/eLife.23084

Zartman, J. J., & Shvartsman, S. Y. (2010). Unit Operations of Tissue Development: Epithelial Folding. *Annual Review of Chemical and Biomolecular Engineering*, *1*(1), 231–246. https://doi.org/10.1146/annurev-chembioeng-073009-100919

Zheng, Y., & Pan, D. (2019). The Hippo Signaling Pathway in Development and Disease. *Developmental Cell*, *50*(3), 264–282. https://doi.org/10.1016/j.devcel.2019.06.003

List of Publications

Khan, S., **Dilsha**, C., & Shashidhara, L. S. (2020). Haltere development in D. melanogaster: implications for the evolution of appendage size, shape and function. *Int J Dev Biol*, *64*(1-2–3), 159–165. https://doi.org/10.1387/ijdb.190133LS

#First author, equal contribution

Dilsha C, Salima Shiju, Neel Ajay Shah, Mandar M. Inamdar, L S Shashidhara (2024).

Differences in Cellular mechanics and ECM dynamics shape differential development of wing and haltere in Drosophila. bioRxiv 2024.04.26.591286; doi: https://doi.org/10.1101/2024.04.26.591286

 # First author # Co-corresponding author